POLITECNICO DI TORINO

Master's degree in

Automotive Engineering

Master's Degree Thesis

Experimental Development of a High Efficiency Engine for PHEV: The PHOENICE Project

Supervisors:

Prof. Federico Millo

Prof. Luciano Rolando

Dr. Giuseppe Castellano

Candidate:

Mario Milite

Academic Year 2024/25

Vindica te tibi,

et tempus quod adhuc

aut auferebatur

aut subripiebatur

aut excidebat

collige et serva.

Abstract

The regulations introduced by the European Commission are becoming increasingly stringent regarding both pollutant and greenhouse gas (GHG) emissions, shifting the focus in the transportation sector toward the development of innovative, environmentally friendly internal combustion engines (ICEs). A plausible short-term solution is represented by plug-in hybrid technology.

In this context, the PHOENICE project aims to demonstrate the potential of a plug-in hybrid vehicle optimized to reduce both fuel consumption and pollutant emissions. The synergistic use of ultra-lean combustion, innovative in-cylinder charge motion, and an electrified turbocharger enables an increase in peak indicated efficiency of up to 47%. Moreover, to ensure compliance with EU7 emission standards, an advanced after-treatment system is implemented, consisting of an electrically heated three-way catalyst (TWC), a gasoline particulate filter (GPF), and a selective catalytic reduction (SCR) system.

This thesis aligns with the experimental development of the PHOENICE project, supporting key stages of steady-state calibration at the Polytechnic of Turin. The research begins with experimental data obtained from the IFP steady-state test campaign and focuses on evaluating the prototype engine's performance and the optimal calibration to maximize the brake thermal efficiency. The study highlights the impact of extensive lean-burn operation and exhaust gas recirculation (EGR), which result in a significant reduction in CO and NOx emissions and an improvement in engine fuel conversion efficiency.

To complement the experimental tests, a transient analysis of engine behaviour is conducted to estimate the effects of ultra-lean combustion and EGR implementation during a real driving cycle, represented by the Worldwide Harmonized Light Vehicle Test Procedure (WLTP). This analysis is carried out using a 0D numerical simulation, based on an interpolation algorithm applied to steady-state engine calibration maps obtained at PoliTo. Additionally, to further investigate the study's findings, an optimized gearshift strategy is implemented using a simple rule-based algorithm, leading to a 5% improvement in fuel consumption and a 47% reduction in carbon monoxide emissions.

To better characterize the key factors of the PHOENICE project that contribute to increased brake thermal efficiency, a GT-Suite engine model is developed. This model

provides a more detailed analysis of the influence of lean-burn combustion, EGR usage, and innovative charge motion turbulence on engine performance. The successful correlation and calibration of the predictive combustion model validate its use as a digital twin of the real engine. Consequently, it serves as a valuable tool in conjunction with experimental research activities to further explore potential advancements and developments within the project.

Table of Contents

Table of Figures

Table of Tables

List of Acronyms

ASC	Ammonia Slip Catalyst
ATS	After-treatment System
BD	Burn Duration
BTE	Brake Thermal Efficiency
BSFC	Brake Specific Fuel Consumption
CAI	Controlled Auto Ignition
CFD	Computational Fluid Dynamics
CPOA	Cylinder Pressure Only Analysis
CoV_{IMEP}	Coefficient of Variation of the IMEP
CR	Compression Ratio
DDCA	Dual Dilution Combustion Approach
EGR	Exhaust Gas Recirculation
ECU	Engine Control Unit
EHC	Electrically Heated Catalyst
FMEP	Friction Mean Effective Pressure
GHG	Greenhouse Gas
HCCI	Homogenous Charge Compression Ignition
HEV	Hybrid Electric Vehicle
ICE	Internal Combustion Engine
IFPEN	Institut Français du Pétrole Energies Nouvelles
IMEP	Indicated Mean Effective Pressure
ITE	Indicated Thermal Efficiency
LIVC	Late Intake Valve Closure
MFB	Mass Fraction Burnt

NOx-Ox	NOx Oxidizer
PHEV	Plug-in Hybrid Electric Vehicle
PHOENICE	
PMEP	Pumping Mean Effective Pressure
PN	Particulate Number
PoliTo	Polytechnic of Turin
RDE	Real Driving Emissions
SA	Spark Advance
SCR	Selective Catalytic Reduction
SI	Spark-Ignition
SPCCI	Spark Controlled Compression Ignition
TWC	Three-way Catalyst
VNT	Variable Nozzle Turbine
VVA	Variable Valve Actuation
WLTC	Worldwide Harmonized Light Vehicles Test Cycle
WLTP	Worldwide Harmonized Light Vehicles Test Procedure
WOT	Wide Open Throttle

1. The Legislative Framework

1.1 Introduction

Today, the growing interest in reducing greenhouse gas emissions and fossil fuel dependency has become a major focus for regulatory authorities. The European Commission (EC) has introduced new regulations to establish more stringent CO_2 emissions standards [1], [2]. In addition, the upcoming Euro7 legislation will further reduce the current limits for air pollutant emissions, while also introducing limits for new species that have not yet been regulated [3], [4].

In this context, hybrid solutions represent the primary short-term response to the challenging targets set by the EC. Consequently, Hybrid Electric Vehicles (HEVs) and Plug-in Hybrid Electric Vehicles (PHEVs) are crucial for the transition to sustainable mobility solutions.

The PHOENICE (PHev towards zerO EmissioNs & ultimate ICE efficiency) project fits into this scenario, aiming to develop a C SUV-class plug-in hybrid vehicle demonstrator that minimizes energy consumption and emissions in real-driving conditions while ensuring optimal vehicle performance and drivability.

1.2 European Commission Proposals

The European Commission recently introduced new regulations both for greenhouse gas and air pollutant emissions to establish more stringer targets.

According to the Fit for 55 package, the CO_2 emissions must be reduced from 95 g/km to 42,8 g/km by 2030, representing a 55% reduction in emissions levels [1]. It is forecast that a 100% reduction in CO_2 emission reduction will be achieved by 2035. However, this regulation cover only CO_2 species, leaving the other greenhouse gas unregulated.

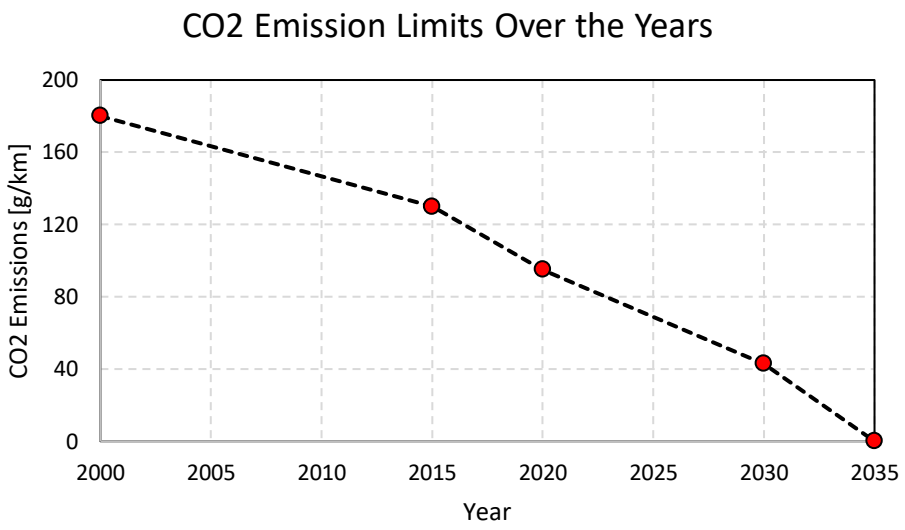

Figure 1 CO_2 Emissions Limits Imposed by the European Commission Over the Years

The upcoming Euro 7 legislation imposes a reduction of 35% for NOx and 13% for particulate matter down to 10 nm compared to the Euro VI. Moreover, regulations for new pollutant species such as NH_3 and CH_4 have been introduced. To bridge the gap between laboratory tests and Real Driving Emissions (RDE), it is also anticipated that the conformity factors will be reduced [4].

Category and class	CO		THC		NMHC		NO_x		THC + NO_x		PM	PN_{10}
	SI	CI	SI	CI	SI	SI	SI	CI	CI	CI	SI & CI	SI & CI
M_1 & N_1 class I	1000	500	100	–	68	–	60	80	–	170	4.5	$6x10^{11}$
N_1 class II	1810	630	130	–	90	–	75	105	–	195	4.5	$6x10^{11}$
N_1 class III	2270	740	160	–	108	–	82	125	–	215	4.5	$6x10^{11}$

Table 1 Euro 7 Tailpipe Emissions Limits for Passenger Cars of Category M_1 and Light-duty Vans of Category N_1 [5]

These ambitious targets, especially for the CO_2 emissions, are simply not feasible in the short term for conventional powertrains. Hybrid vehicles are the only solution to address these challenging reductions in pollutants and greenhouse gases emissions. Anyway, it is expected that a significant portion of PHEVs on the market will continue to use Spark-Ignition (SI) engines in conjunction with electric machines to keep purchase costs as low as possible.

1.3 The Role of the Research

To counteract the increasingly limitations introduced by the European Commission, research activities have become crucial for finding new technological solutions for the transportation sector.

Besides the importance of electrification, innovative solutions for traditional combustion engines are still under study, aiming to improve engine efficiency while maintaining targeted emission levels.

The main technological trends for internal combustion engines (ICEs) are focusing on downsizing and turbocharging. Downsizing involves using smaller combustion engines while maintaining the same power output. This approach shifts the engine's part-load operation to higher loads, ensuring greater efficiency. To accomplish this, downsizing is coupled with turbocharging, which allows more air to be trapped inside the cylinder and enables operation at higher loads. Downsized turbocharged engines are suitable also for hybrid architectures.

Another solution being investigated is cylinder deactivation. This technique involves shutting off some of the engine's cylinders at part-load to effectively increase the load on the remaining active cylinders. This significantly improves part-load efficiency while preserving full engine performance at wide-open throttle (WOT) operation [6]. Cylinder deactivation can also be coupled with HEV architectures, where it is used to minimize cylinder pumping losses and thereby increase recuperation levels.

A widely investigated solution through years is the Homogeneous Charge Compression Ignition (HCCI), also known as Controlled Auto Ignition (CAI). In this mode of operation, the engine relies on the spontaneous ignition of a homogenous mixture - typically extremely lean or with a high level of dilution – thereby improving engine efficiency and producing a cleaner combustion process. These benefits are mainly due to high compression ratios and the elimination of throttling at part-load. Moreover, the use of lean, homogeneous mixtures prevents soot formation, and the low-temperature combustion process reduces NOx emissions. Both gasoline and diesel HCCI engines have been tested in recent years. An example of this solution is the Mazda Spark Controlled Compression Ignition (SPCCI) used in the SkyActiv-X engine, where a spark plug is used to control the compression ignition [7]. A fireball created by the spark plug expands and further compresses the mixture, creating a variable compression ratio and reaching optimal in-cylinder temperature and pressure for compression ignition.

Within this research scenario, the PHOENICE project aims to demonstrate the potential of a high-efficiency, low-emission internal combustion engine. The project focuses on the development of a plug-in hybrid electric vehicle to illustrate the potential of solutions that combine today's major research trends - electrification and innovative ICE - in the pursuit of emission and pollutant reduction.

2. The PHOENICE Project

2.1 Introduction

Environmentally friendly mobility is a primary objective of the European Commission in reducing pollutant and greenhouse gas (GHG) emissions. Innovative technologies, electrified components, and alternative fuels are potential solutions for achieving new powertrain typologies with a low carbon footprint. In this context, the PHOENICE (PHev towards zero EmissioNs & ultimate ICE efficiency) project aims to demonstrate the potential of high-efficiency, low-emission internal combustion engines in mitigating the environmental impact of road transportation.

The project focuses on developing a C-SUV-class plug-in hybrid vehicle, targeting a 10% reduction in fuel consumption compared to the current baseline vehicle. Moreover, compliance with the upcoming EU7 regulations is a necessary requirement to meet the emission standards set by the European Commission. To achieve these ambitious goals, the project integrates homogeneous lean combustion, exhaust gas recirculation (EGR), a high compression ratio, and an aggressive Miller cycle to enhance fuel conversion efficiency and minimize engine-out emissions. These technologies aim to overcome the limitations of other solutions, such as downsizing and turbocharging in spark-ignition engines.

Research supports these approaches: He et al. [8] demonstrated that a stoichiometric engine with a high compression ratio and an aggressive Miller cycle featuring late intake valve closure (LIVC) achieved a 6% reduction in brake specific fuel consumption (BSFC) compared to the baseline engine. Similarly, Osborne et al. [9] examined lean-homogeneous combustion, achieving more than a 10% reduction in BSFC and a peak brake thermal efficiency (BTE) of 42% compared to stoichiometric operation, while maintaining low NOx emissions under real driving conditions. Martinez Boggio et al. [10] demonstrated, using an optical GDI engine, that lean combustion improves fuel conversion efficiency by 10%, with low CO, NOx, and particulate emissions.

Cooled EGR is another widely adopted solution for turbocharged engines, helping to lower combustion temperatures and, consequently, reduce pollutant emissions. Tornatore et al. [11] highlighted the benefits of EGR, particularly in reducing pumping losses at low loads. At high loads, EGR mainly helps decrease NOx

formation. However, mixture dilution combined with the Miller cycle can negatively impact charge motion within the cylinder, reducing flame propagation and combustion efficiency. To address these challenges, an innovative flow motion concept called Swumble™ has been introduced. This approach, which combines tumble and swirl motions, was proposed by Gautrot et al. [12] to enhance turbulent kinetic energy with minimal flow degradation, making it suitable for early and late valve closure strategies in conjunction with mixture dilution and a high compression ratio.

The following sections of this chapter provide a comprehensive overview of the project's fundamentals, detailing the improvements over the baseline engine and their objectives. Additionally, an introduction to the key steps of this thesis is presented, highlighting the core research activities and the support provided for experimental tests at the Polytechnic of Turin.

2.2 The Engine Concept

The baseline engine of the PHOENICE project is a state-of-the-art, 4-cylinder, 1.3L turbocharged direct injection spark-ignition engine [13]. It features a high stroke-to-bore ratio, a compact 4-valve combustion chamber with a side-mounted 200-bar fuel injection system, a MultiAir Variable Valve Actuation (VVA) system [14], and an integrated exhaust manifold.

The PHOENICE project redesigned this engine, upgrading the combustion system to achieve a target peak indicated thermal efficiency (ITE) of 47% by adopting a Dual-Dilution Combustion Approach (DDCA), which combines a homogeneous lean mixture with cooled low-pressure EGR. Due to the challenging operating conditions that slow flame propagation, a high level of turbulence is required. Therefore, the intake ports and piston surface were redesigned to implement the Swumble™ motion, which increases the average turbulent kinetic energy within the spark window.

Moreover, the compression ratio (CR) was increased from the baseline value of 10,5 to 13,6 through a new piston design. This was combined with an aggressive Miller cycle, enabled by the VVA system, to maintain effective knock suppression and reduce pumping work at low loads. To withstand the increased in-cylinder pressure

resulting from the higher CR and DDCA, a new prototype of reinforced connecting rods was implemented.

Boosting is managed by a 48V electrified turbocharger equipped with a Variable Nozzle Turbine (VNT). The specifications of this component were optimized, as stated in [15] and [16], to meet the combustion requirements. The integrated electric machine not only reduces turbo lag but also enables energy recovery when the compressor's energy demand is lower than the turbine's supplied energy.

Finally, the fuel injection system features enhanced pump and injectors, allowing operation at pressures of up to 350 bar.

Table 2 resumes the main features of the PHOENICE prototype engine.

Engine Specifications	
Number of cylinders	4
Displacement	1332 cm^3
Bore x Stroke	70 mm x 86.5 mm
Compression Ratio	13.6:1
Number of valves	16
VVA system	MultiAir III (intake only)
Turbocharging	48 V VNT E-Turbo
Fuel Injection	GDI (up to 350 bar)
Ignition System	Base production
EGR System	Cooled Low Pressure (LP)
Rated Power (target)	100 kw @ 4500 RPM
Rated Torque (target)	218 Nm @ 3500 RPM

Table 2 PHOENICE Engine Specifications

To meet the upcoming Euro 7 emission standards, the After-Treatment System (ATS) consists of two main sections.

The close-coupled section includes an Electrically Heated Catalyst (EHC) and a Three-Way Catalyst (TWC) to control CO, NOx, and HC emissions during cold starts and stoichiometric mixture conditions. This section also features a Gasoline Particulate Filter (GPF) to trap particulate matter. To meet the EU7 particulate number (PN) emission limits, an innovative coating is applied to achieve a significant improvement in filtration efficiency. However, this enhancement comes with an associated penalty in backpressure.

The underfloor section consists of a Selective Catalyst Reducer (SCR) to decrease NOx emissions under lean combustion conditions. To enhance its efficiency at low temperatures, an oxidation catalyst (NOx-Ox) is positioned upstream to convert a portion of NO into NO_2. Additionally, an Ammonia Slip Catalyst (ASC) is integrated downstream to mitigate NH_3 slip, which may result from overdosing or as a by-product of reactions in the upstream components under stoichiometric operating conditions.

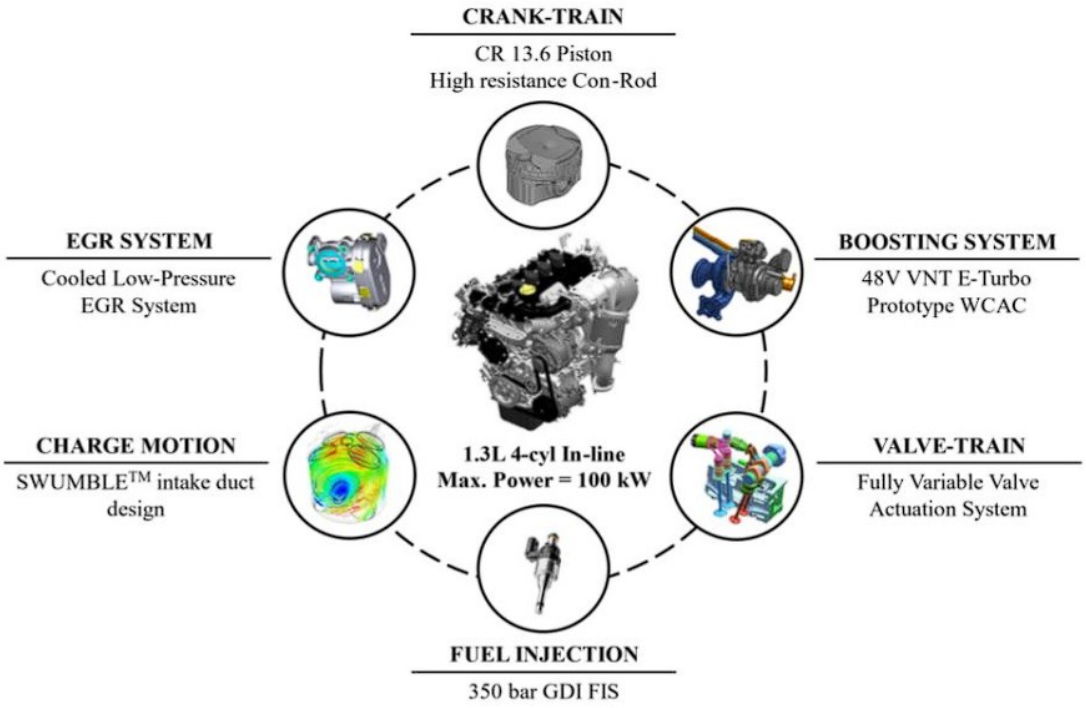

Figure 2 Overview of the PHOENICE Engine Features

2.2 Experimental Setup

The first PHOENICE prototype engine was tested at IFPEN on a multi-cylinder engine dynamometer test bench. To monitor engine behaviour and its key components, thermocouples and low-frequency pressure transducers were installed in the exhaust and intake lines, in the high- and low-temperature cooling systems, and in the EGR loop. Each cylinder was additionally equipped with a piezoelectric high-frequency pressure transducer to enable real-time combustion diagnostics. An exhaust gas analyser was also used to measure gaseous emissions and particulate matter down to a size of 10 nm.

Regarding the exhaust system, only the close-coupled section was installed at the IFPEN test facility due to space constraints. However, to account for the backpressure of the entire exhaust line, as estimated through CFD simulations, an exhaust flap was incorporated.

In addition to the standard Engine Control Unit (ECU) provided by Stellantis, an ETAS ES910 Rapid Control Prototyping (RCP) module was installed to manage the additional actuators on the prototype engine, including the VNT rack, SCR urea injector, EGR valve, and the E-Turbo. Data acquisition was carried out using Osiris from FEV, while combustion analysis was performed with a dedicated in-house tool developed by IFPEN.

The Polytechnic of Turin (PoliTo) utilized a similar test cell setup to IFPEN in terms of engine mounting, instrumentation, and data acquisition programs. However, unlike IFPEN, the exhaust system at PoliTo included both the close-coupled and underfloor sections, allowing for a more accurate backpressure estimation without the need for an exhaust flap.

Another key difference between the two facilities was the type of gasoline used during steady-state tests: E10 at IFPEN and E5 at PoliTo. Different fuels were adopted to state the influence of a production gasoline, normally available at fuel station. However, the difference in the utilised fuel resulted in no substantial influence on the outcomes of the benchmark activities.

2.3 Experimental and Numerical Analyses

This thesis work can be broadly divided into two parts, both aimed at supporting engine calibration during the steady-state tests conducted at the Polytechnic of Turin.

The first part involves analysing experimental data, primarily obtained from the IFPEN test bench, to characterize the engine's operating behaviour resulting from the various implementations introduced in the PHOENICE project. The second part focuses on simulations performed in the GT-Suite environment to calibrate and validate a digital twin of the physical engine. This digital twin must serve as a complementary tool to benchmarking activities, enabling an extended analysis of the project's features potential. Therefore, the foundation of this thesis work is the

experimental data collected from both IFPEN and PoliTo test facilities, from which the entire research activity begins.

2.3.1 Engine Experimental Data

Starting from the analysis of the IFPEN steady-state calibration acquired data, the performance and the combustion indices of the prototype engine are examined in order to understand the capabilities and the influence of the various technological implementations introduced in the PHOENICE project.

The aim of steady-states tests is the fine-tuning of the engine control unit to optimize the engine performance and emissions, ensuring correct operations for the specifications of design and to properly meet the standards requirements.

The IFPEN calibration work was conducted on eleven engine points, representative of a wide range of operating conditions in terms of engine speed and requested load. In Table 3 the tested combinations of speed and BMEP are shown.

IFPEN tested engine points	
Engine speed [RPM]	***BMEP [bar]***
1000	2
1500	2
1500	5,5
1500	11,5
2000	5,5
2000	13,5
2200	20
2600	15
2600	20
3000	7
3000	13

Table 3 IFPEN Tested Engine Points

Figure 3 shows the tested engine points with respect to the full load curve. It is notable that the investigated points emphasize the most adopted operating conditions in normal driving scenarios.

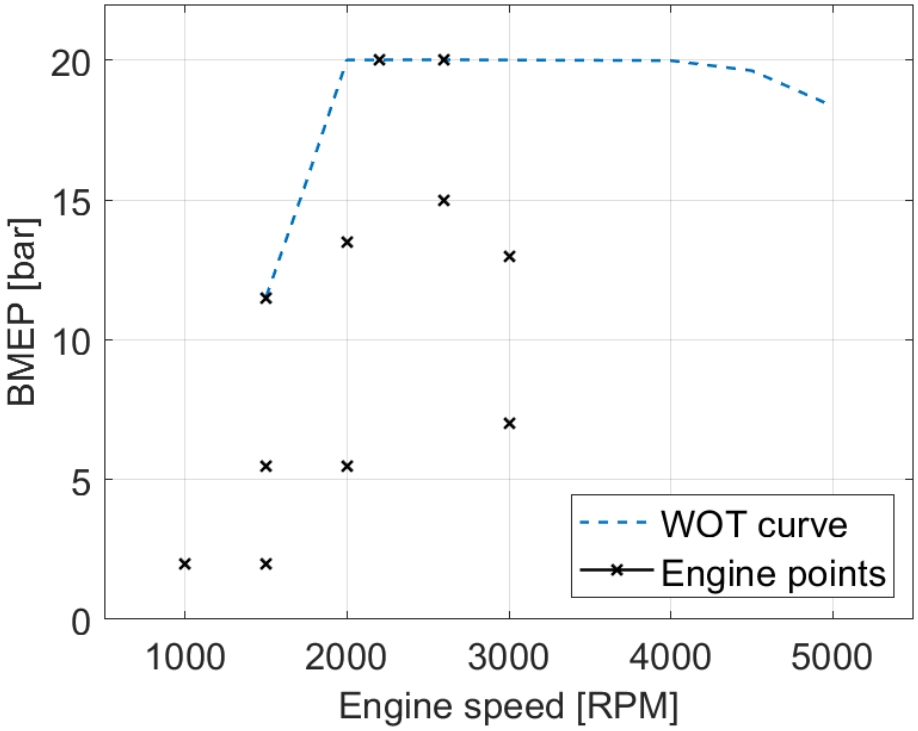

Figure 3 Engine Points and Full Load Curve

To characterize the influence of the dual dilution combustion approach, each engine point was tested at different values of air-fuel ratio (λ) and rates of Exhaust Gas Recirculation. Table 4, Table 5 and Table 6 present three examples of combination of λ and EGR obtained at IFPEN for different engine points, respectively 1500 RPM x 5,5 bar BMEP, 2200 RPM x 20 bar BMEP and 3000 RPM x 7 bar BMEP.

1500 RPM x 5,5 bar BMEP	
Air-fuel ratio [-]	***EGR Rate [%]***
1,00	0,90
	5,20
	10,2
	15,3
	18,9
1,11	0,70
	5,30
	10,3
	15,0
1,25	0,60
	5,10
1,43	0,00

Table 4 1500 RPM x 5,5 bar BMEP λ and EGR sweeps

2200 RPM x 20 bar BMEP	
Air-fuel ratio [-]	***EGR Rate [%]***
1,00	0,60
	5,10
	9,10
	10,0
	11,0
1,11	0,50

Table 5 2200 RPM x 20 bar BMEP λ and EGR sweeps

This research approach enabled a detailed understanding of how the interplay between λ and EGR impacts on the combustion efficiency and stability, as well as on the engine-out emissions. This is a crucial aspect of the PHOENICE project in pursuit of the target peak indicated thermal efficiency of 47%, therefore the completeness of the investigated experimental data set was strictly required.

For each of the possible combination of λ and EGR, data were acquired concerning flow rates, emissions, characteristic pressures and temperatures and combustion process. Specifically, the experimental data used in this research work referred to air flow rate, fuel flow rate, pressure and temperature in the intake plenum, pressure and temperature at the turbine inlet, pressure and temperature at the turbine outlet, brake specific fuel consumption, brake specific CO emissions, brake specific HC emissions, brake specific NOx emissions, turbo group speed and spark advance (SA).

During the IFPEN calibration procedure, pressure traces were acquired for each of the four cylinders with a sampling frequency of one-tenth of crank angle degree, resulting in a total of 7200 points describing the pressure cycle as function of the crank angle. The data provided for this thesis work refer to the mean pressure trace of each cylinder. From the four pressure traces, the average pressure cycle was identified for each engine point and combination of λ and EGR and it was used to characterize the combustion process through a Closed Volume Cylinder Pressure Analysis (CPOA) in GT-Suite. Figure 4 shows an example of the average pressure cycle obtained from the experimental data, specifically for the case 2200 RPM x 2 bar BMEP.

3000 RPM x 7 bar BMEP	
Air-fuel ratio [-]	*EGR Rate [%]*
1,00	0,00 5,20 10,0 15,2 20,6 21,5
1,11	0,00 5,30 9,80 15,1 20,1
1,25	0,00 5,10 10,0 14,4
1,43	0,00 5,20 7,20

Table 6 3000 RPM x 7 bar BMEP λ and EGR sweeps

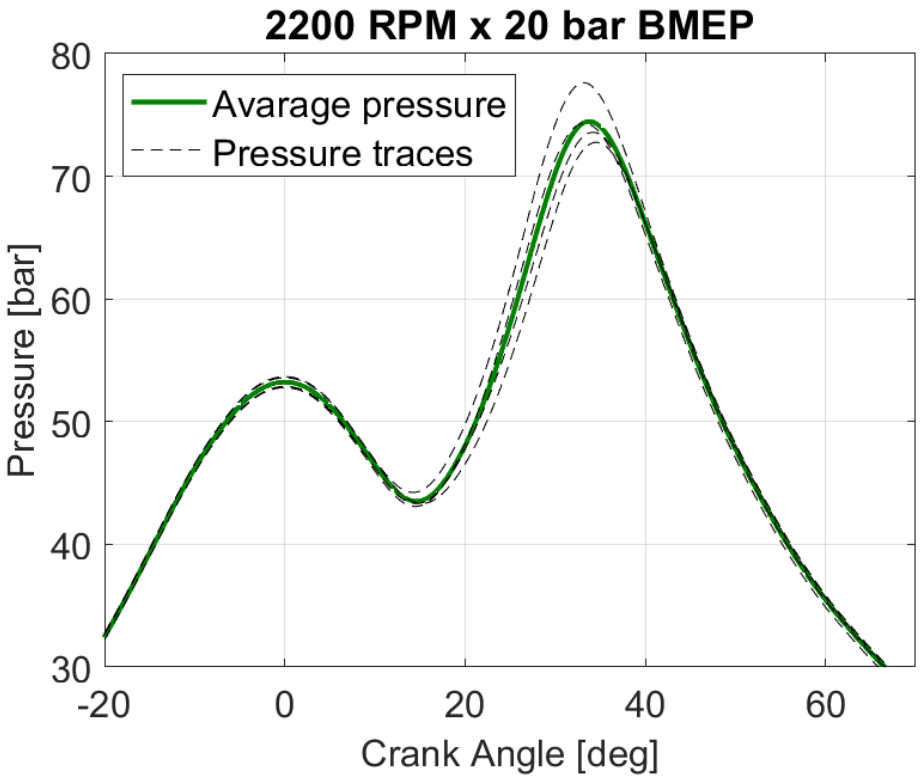

Figure 4 2200 RPM x 20 bar BMEP pressure traces and average cycle

Regarding PoliTo experimental data, they focus on the calibration maps obtained during the steady-state tests. Specifically, the engine maps refer to engine-out emissions (CO, NOx and HC) and fuel consumptions. Figure 5 depicts the Brake Specific Fuel Consumption as function of engine speed and BMEP of the PHOENICE prototype engine as obtained at PoliTo test cell.

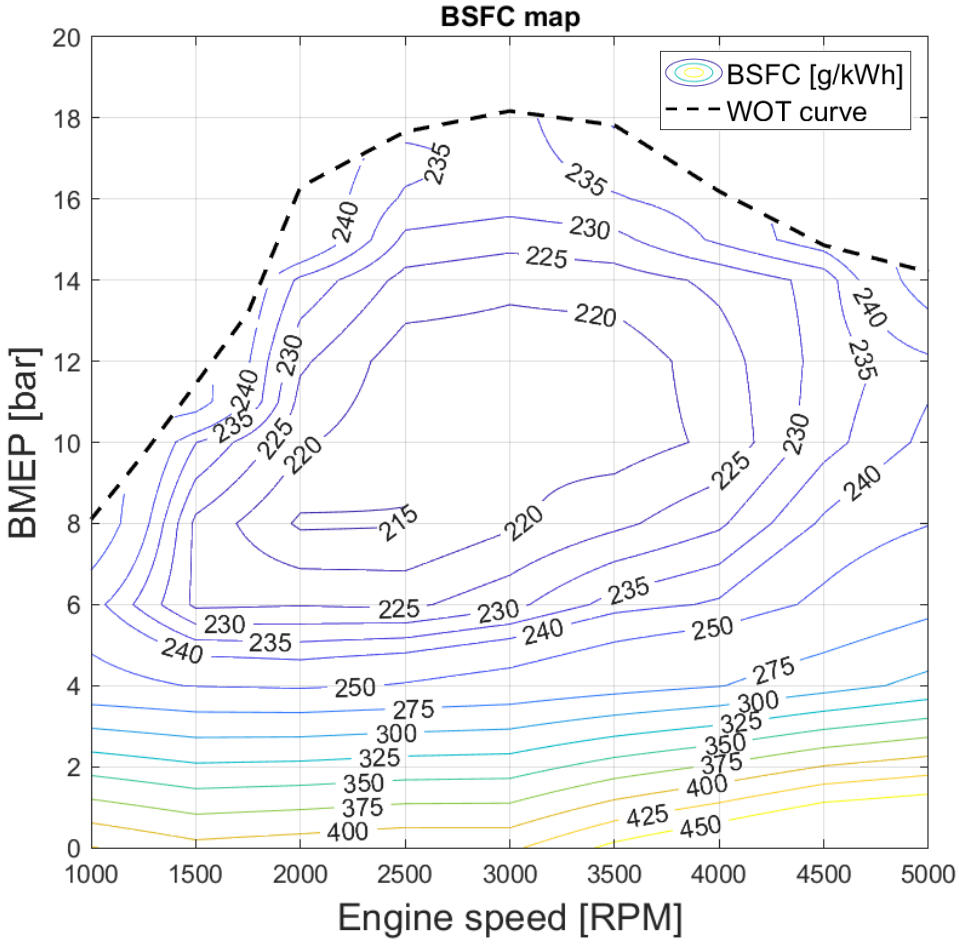

Figure 5 BSFC Map as Function of Engine Speed and BMEP

The illustrated experimental data served as basis for the analyses conducted during the thesis research work. Beside the engine combustion and performance investigation, the IFPEN data served for correlating the complete engine model, intended to represent a digital twin of the prototype physical engine, and for calibrating the predictive combustion model. On the other hand, the PoliTo experimental data were used for the numerical simulation of a real driving cycle, represented by the Worldwide Harmonized Light Vehicle Test Cycle (WLTC), and for optimizing the gearshift strategy.

2.3.2 Definition of the Experimental and Numerical Analyses

The experimental data acquired from both test facilities formed the foundation of our research. The analyses conducted in this thesis can be divided into two groups: experimental analyses and numerical simulations. The experimental analyses, starting from the test bench data, assess the influence of the several innovative implementations on engine functioning, emissions and fuel consumption to achieve the target peak indicated efficiency of 47%. The numerical simulations complement the study by providing reliable engine models that can be used to extend the experimental investigations.

The experimental analyses begin with a CPOA model based on IFPEN data, used to examine the combustion process parameters. This study characterizes the dual dilution approach by analysing efficiency and duration of the combustion as the air-fuel ratio and EGR rate vary. This experimental analysis concludes with an examination of performance indices, highlighting the impact of the technological solutions introduced in the PHOENICE project.

The second part of the experimental investigation consists of a 0D transient simulation based on the WLTC, referencing fuel consumption and engine-out emissions maps obtained from the PoliTo calibration tests. Specifically, three operating conditions are studied, respectively a stoichiometric mixture without EGR, a stoichiometric mixture with EGR, and a lean mixture with EGR. This simulation aims to determine the ideal fuel consumption and emissions that the prototype engine can achieve in a real driving scenario, to have a trustworthy term of comparison for the benchmark transient tests. The results of the 0D simulation are considered as ideal since the engine maps used in this study are based on the engine's steady-state calibration and do not account for the engine warm-up phase, which naturally impacts the real outcome.

The analysis of the engine behaviour under transient conditions is complemented by a study of the gearshift strategy. Since the shifting strategy significantly impacts fuel consumption and emissions, selecting an optimal strategy should lead to a reduction in both. Therefore, two possible optimizations of the baseline gearshift are examined, identifying the most frequently used operating region concerning BSFC and BSCO maps.

Regarding the numerical analyses, the primary objective is to develop a digital twin of the prototype engine, serving as a complementary tool for benchmark activities. Specifically, a reliable engine model enables to extend the evaluation of the potential

and impact of various features introduced in the PHOENICE project. The engine model is created using GT-Suite, with its correlation procedure based on experimental data provided by IFPEN.

A further step in the model development is the implementation of a predictive combustion model. The implemented model must account for the dual dilution approach, which is a fundamental aspect of the PHOENICE project. Therefore, the calibration procedure must ensure an accurate estimation of the factors influencing the flame propagation derived from the homogenous lean combustion coupled with the Swumble^{TM} charge motion.

The final analysis in this research focuses on evaluating the contributions of the various technological solutions introduced in the PHOENICE prototype engine to achieve the project targets. This analysis relies on examining the impact of the key features introduced in the prototype engine with respect to the peak indicated thermal efficiency target. To accomplish this task, the most important features are individually removed from the model, and the obtained results are analysed.

3. Experimental Data Analysis

3.1 Introduction

The scope of this chapter is to investigate the engine operating parameters to understand the real capabilities of the initial prototype. This analysis is conducted using experimental data acquired during the IFPEN test campaign for the steady-state calibration of the engine.

The starting point of this analysis is the pressure traces acquired during the research activity, from which the average pressure cycles were calculated. Using these traces in a GT-Suite Cylinder Pressure Analysis, the key indicators of the engine combustion process were identified to characterize the influence of the main features of the PHOENICE project, such as the Dual Dilution Combustion Approach and the aggressive Millerization.

The CPOA results were incorporated into the existing experimental data to enhance the understanding of the engine's behaviour due to the synergistic use of various technological solutions across different tested operating conditions.

As a final step, a study of the compressor map is conducted. This analysis aims to evaluate the efficiency of this component, which was built ad hoc for this application, under different working conditions. In particular, the goal of this study is to assess the possible limitations imposed by homogeneous lean burn operations on the functioning of the turbo group.

3.2 Methodology

To establish a well-structured and comprehensive study of the engine characteristics, the combustion process was analysed prior to the performance evaluation to ensure the completeness of the investigated parameters. This approach allowed for a clear distinction between the two procedures and methodologies used to obtain the desired results.

3.2.1 Combustion Process Analysis

The study of the combustion process is based on the IFPEN steady-state calibration acquired data. The calibration approach covered a large spectrum of possible engine functioning conditions, tested through sweeps of engine speed, load request and combinations of λ and EGR.

The combustion parameters are analysed through a Cylinder Pressure Analysis. CPOA is a simple tool implemented in GT-Suite that enables the calculation of the burn rate and mass fraction burned, along with other combustion parameters, based on measured pressure traces. This tool operates using a basic model of a single-cylinder engine, into which the average pressure cycle is fed. The main advantage of this approach lies in its simple modelling and fast computation. However, its primary drawback is the requirement for certain input parameters (e.g., residual fraction and cylinder trapping ratio), which can be difficult to estimate in many cases but are essential for obtaining accurate results.

Particularly, the data used for this model include:

- *Geometric Information*: bore, connecting rod length, compression ratio, exhaust and intake valve diameters.
- *Combustion Specifications*: spark advance, injected fuel mass, residual fraction, air volumetric efficiency, unburned fuel concentration, CO concentration.
- *Thermal Initial Conditions of the Combustion Chamber*: cylinder, piston, and head temperatures.

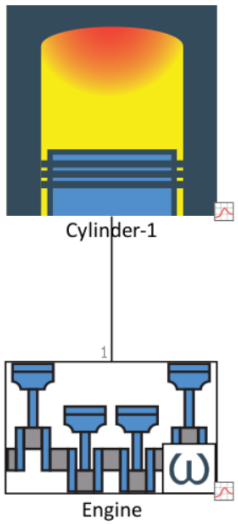

Figure 6 CPOA model

Since this simple model represents a closed-volume analysis, the initial conditions of ambient pressure and temperature must be imposed. Therefore, to account for boosting operations when necessary, the initial pressure and temperature are set to the intake plenum conditions.

As first instance, the Friction Mean Effective Pressure (FMEP) are simulated using the Chen-Flyn model. The coefficients used for the calculation of the frictions are referred to the baseline engine (GSE T4), therefore a certain level of inaccuracy is attended.

The last required experimental data are the pressure cycles. For each engine point, the average cycle of the four cylinders is inserted in the CPOA model. The cycles data were recorded at every tenth of crank angle degree, resulting in a total of 7200 points describing each pressure trace.

For this study, a separate CPOA model is built for each engine point. Every model incorporated the corresponding average pressure cycle and specific case setup, settled for the different combinations of air-fuel ratio and EGR rate tested at IFPEN.

Once the model is prepared, a fine-tuning of its parameters is required to ensure the accuracy of the results. The parameters that can be modified are essentially three: compression ratio, heat transfer multiplier and crank angle shift (or encoder error). Adjusting these parameters helps minimize the error between measured and simulated pressure cycles.

The Compression Ratio affects the maximum in-cylinder pressure reached during the cycle, as well as the slope of the compression line in the logp-logV chart.

The Heat Transfer Multiplier ensure the correct modelling of the heat transfer within the cylinder, primarily influencing the expansion line.

For these two specific parameters, the tuning was manually performed to achieve the best possible pressure cycle simulation. The final values of these parameters are reported in Table 7.

CPOA parameters	
Compression Ratio	13
Heat Transfer Multiplier	0,75

Table 7 Compression Ratio and Heat Transfer Multiplier values of the CPOA model

More challenging is instead the Encoder Error tuning. The encoder error represents the offset between the pressure sensor within the combustion chamber and the encoder that detects the crank angle at which a specific pressure value is associated.

Upon inspecting the pressure traces, it was found that the engine points with the lower load request (i.e. 1000 RPM x 2 bar BMEP, 1500 RPM x 2 bar BMEP, 1500 RPM x 5,5 bar BMEP and 2000 RPM x 5,5 bar BMEP) exhibited low encoder error computation. However, its value cannot be selected without further considerations. In fact, modifying the encoder error directly affects the simulation results. Specifically, an increase of the encoder error prevents consistency check failures across the different case, but it also reduces the calculated FMEP in the simulation. Thus, a trade-off must be found between these two conflicting effects.

To determine the optimal encoder error value, multiple trials were conducted, each with different encoder error adjustments. The corresponding FMEP values were recorded and compared to the reference values estimated using the Chen-Flyn friction model. The best correction of the encoder error was univocally determined as the one where the consistency check equals 1 (indicating a valid simulation) and the FMEP is as close as possible to the reference value. An example of this procedure, specifically for the 2600 RPM x 20 bar BMEP case, is presented in Table 8.

Encoder Error Analysis for 2600 RPM x 20 bar BMEP			
		λ = 1,00	***λ = 1,11***
Encoder Error = 0°	*Consistency check*	1,00	1,00
	Simulated FMEP [bar]	1,08	1,00
	Reference FMEP [bar]	1,22	1,19
Encoder Error = 0,5°	*Consistency check*	1,00	0,00
	Simulated FMEP [bar]	0,77	0,77
	Reference FMEP [bar]	1,22	1,19
Encoder Error = 1°	*Consistency check*	0,00	0,00
	Simulated FMEP [bar]	0,46	0,46
	Reference FMEP [bar]	1,22	1,19

Table 8 Example of Encoder Error Analysis Procedure

At the end of this brief analysis, the encoder error was set to 0,5 °CA for low BMEP engine points, whilst it was maintained at 0 °CA for all other cases.

Once the case setup is finalized and the tuning of the model parameters is accomplished, the combustion process analysis can proceed with the simulation of the different engine points.

3.2.2 Performance Analysis

The second part of the analysis consists of investigating the characteristics of the prototype engine. The behaviour of this particular engine is influenced by the various technological solutions implemented to achieve the project's targets. Therefore, this analysis aims to highlight the influence of such implementations on fuel consumption, emissions and brake thermal efficiency of the engine.

The data used in this study are still derived from the IFPEN steady-state calibration acquisition. In addition, the outputs of the combustion process analysis provide further insight into the engine understanding, offering information on burn durations (BD), mass fraction burnt (MFB), indicated mean effective pressure (IMEP), and pumping mean effective pressure (PMEP).

A simple MATLAB script is used for the analysis of the experimental data. The outputs of this script are various charts that primarily illustrate the influence of homogeneous lean combustion, combined with a high EGR rate, on the engine main performance indices.

3.3 Analysis Results

The results of the analysis of the experimental data are shown in this section. The aim is to examine the engine behaviour, emphasizing the influence of the dual dilution combustion approach and of the aggressive Millerization in achieving the project target of 47% peak indicated thermal efficiency.

Three different engine operating conditions representative of low, medium, and high load and speed are reported. Specifically, the three cases are:

- 1500 RPM x 5,5 bar BMEP
- 2200 RPM x 20 bar BMEP
- 3000 RPM x 7 bar BMEP.

The last case is of paramount importance, since the transition between naturally aspirated and boosted operation occurs precisely at a load of 7 bar of BMEP.

For each of the three select engine points, a brief illustration of pressure cycles, combustion events and main performance indices is provided to enhance the understanding of the prototype engine's operations.

3.3.1 Case 1: 1500 RPM x 5,5 bar BMEP

The analysis of this case is representative of the engine working conditions at low speed and low load. The engine is not in boosted operation and functions as naturally aspirated. As result, the effects of the aggressive Millerization is clearly visible, along with the contribution of the dual dilution combustion approach.

Figure 7 and Figure 8 display the pressure cycles in both in logp-logV and p-θ charts, as well as the Heat Release Rate as function of the crank angle, for λ equal to 1,00 and 1,11 respectively.

The impact of the Late Intake Valve Closure Miller Cycle is evident: as the piston moves towards the TDC, the intake valves remain open, causing part of the in-cylinder mass to be expelled. This results in a lower effective compression ratio compared to the geometrical one, thereby increasing the thermal efficiency of the cycle at the cost of reduced output work.

Furthermore, as the EGR rate increases from 0 to higher values, the engine's de-throttling effect becomes more pronounced. This occurs because a greater intake mass flow is induced, leading to a reduction in pumping work.

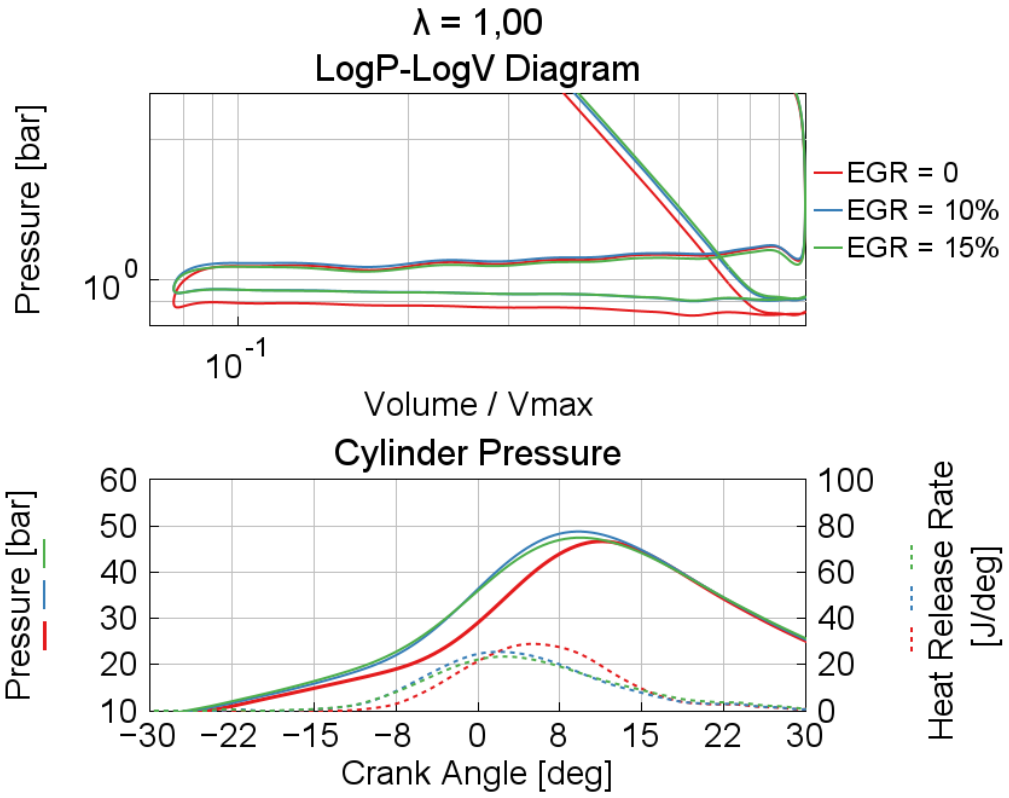

Figure 7 1500 RPM x 5,5 bar BMEP: Pressure Cycles and Heat Release Rate for λ = 1,00

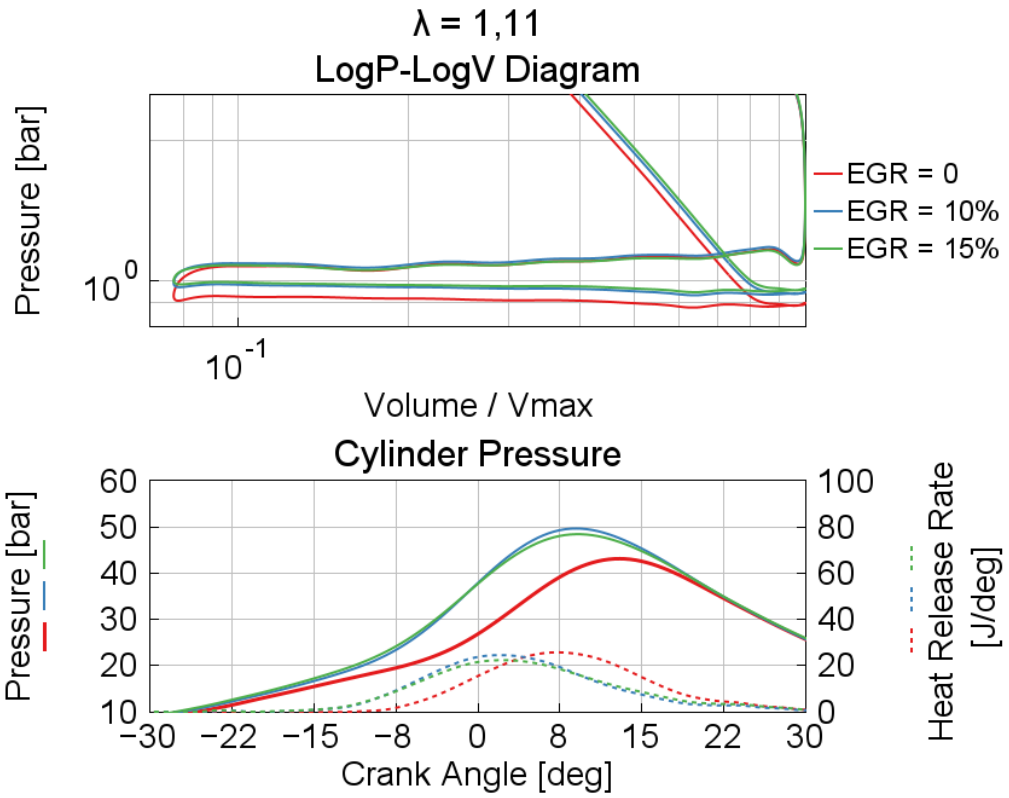

Figure 8 1500 RPM x 5,5 bar BMEP: Pressure Cycles and Heat Release Rate for λ = 1,11

For the same λ value, an increase in the EGR rate allows for a more advanced spark timing. This effect is due to the lower in-cylinder temperature, a consequence of EGR dilution, which also reduces in-cylinder pressure. As the mixture becomes more diluted, the Spark Advance can be advanced relative to the firing TDC to achieve a higher peak pressure during the combustion phase and extract more work during the expansion stroke. This effect is visible in Figure 9, where variations in **λ** and EGR rate are shown.

Furthermore, the enleanment of the mixture results in a slower combustion process. Since combustion begins with a lower-temperature mixture, the overall combustion duration increases. This effect is also evident in Figure 9, where the trends of different MFB values can be observed.

With a higher dilution of the mixture, the SA can be more advanced, causing the MFB50 to tend to move to lower values. However, a clear trend cannot be identified since this parameter is an outcome of the combustion phasing. It can also be noted that the MFB90 moves to higher values as the air-fuel ratio or EGR increases, which is a result of the slower combustion process.

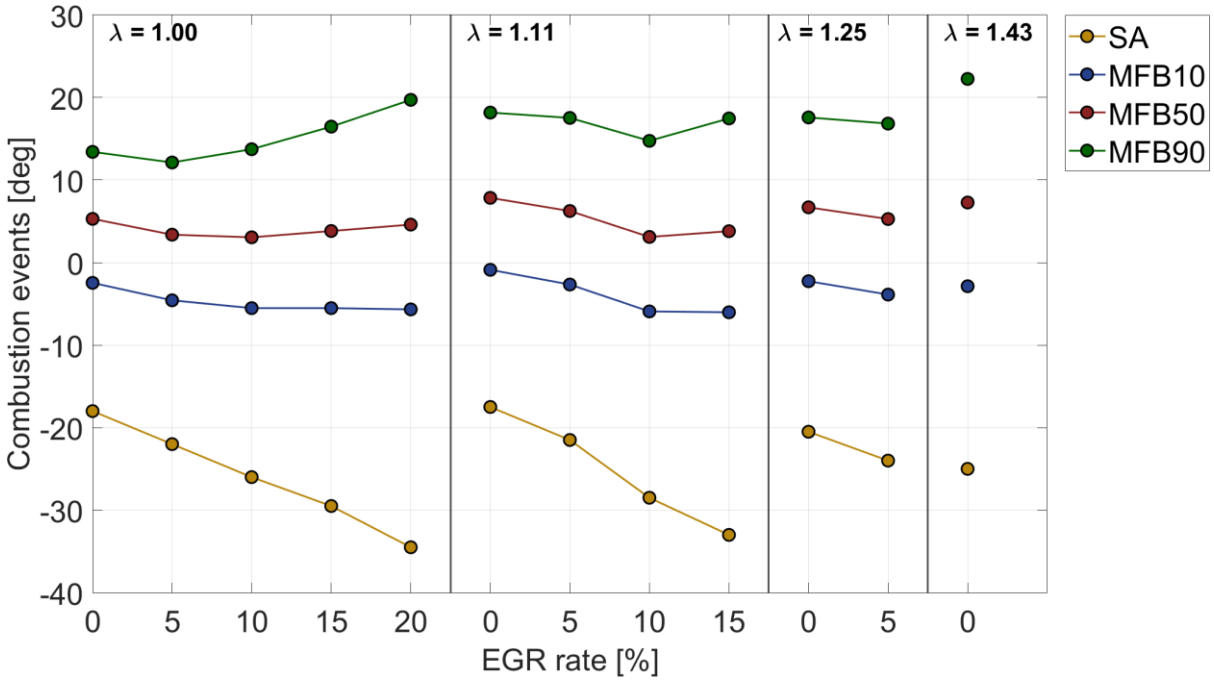

Figure 9 1500 RPM x 5,5 bar BMEP: Combustion Events

When the EGR rate increases or a larger λ is used, the Coefficient of Variation of the Indicated Mean Effective Pressure (CoV_{IMEP}) tends to increase. This parameter

is of paramount importance as it describes the cyclic variation of the IMEP and is related to vehicle drivability. The CoV_{IMEP} must be limited to 3–4% to prevent fluctuations in engine power that could be perceived by the driver.

Figure 10 shows the trend of the CoV_{IMEP}. Notably, as the EGR rate increases for the same λ, the CoV_{IMEP} tends to rise, limiting the possible EGR rates. Additionally, the CoV_{IMEP} imposes a restriction on the maximum λ that can be achieved. At λ = 1.43, the 3% CoV_{IMEP} threshold is already exceeded, even in the absence of EGR.

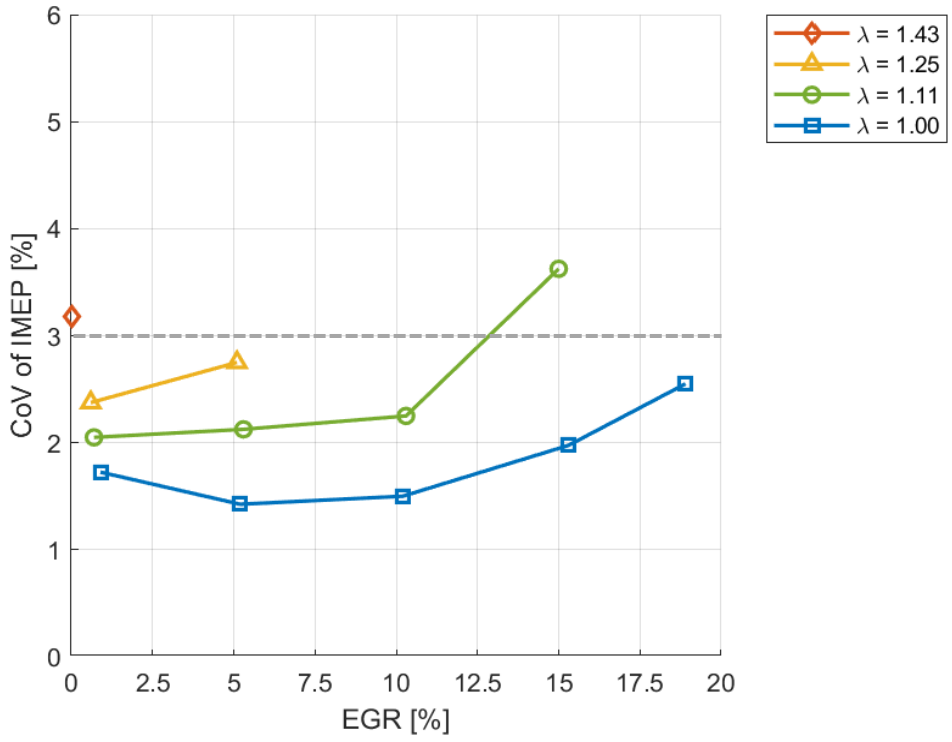

Figure 10 1500 RPM x 5,5 bar BMEP: CoV of IMEP

With an increase in the EGR rate or λ, the pumping work tends to decrease. This reduction is a result of engine de-throttling: as the intake flow increases, the throttle valve opens wider, reducing pressure drops in the intake manifold.

As a result of the reduction in pumping work due to engine de-throttling and the lower heat losses caused by the dilution effect, both Brake Thermal Efficiency and Gross Indicated Efficiency increase with a higher EGR rate or a larger air-fuel ratio. This trend is shown in Figure 12 and Figure 13.

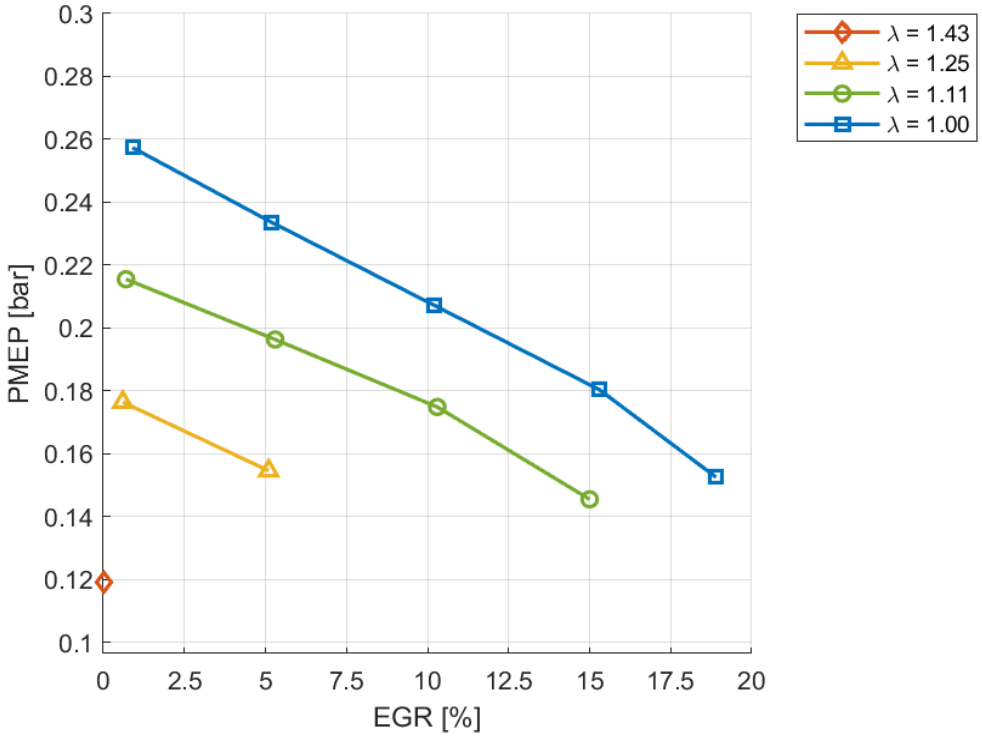

Figure 11 1500 RPM x 5,5 bar BMEP: Pupming Mean Effective Pressure

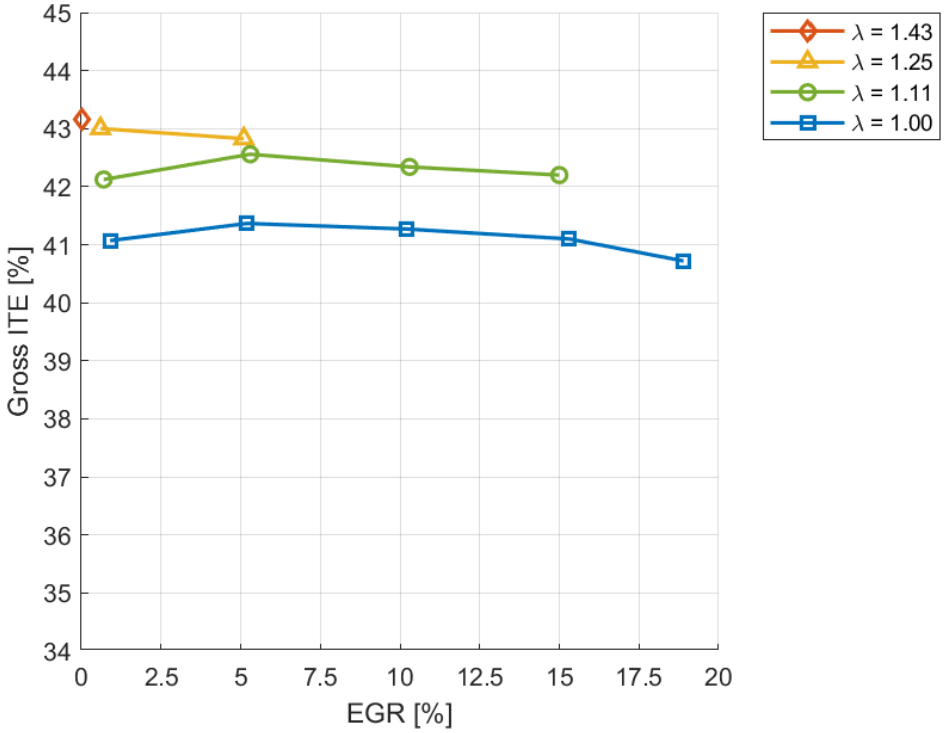

Figure 12 1500 RPM x 5,5 bar BMEP: Gross Indicated Thermal Efficiency

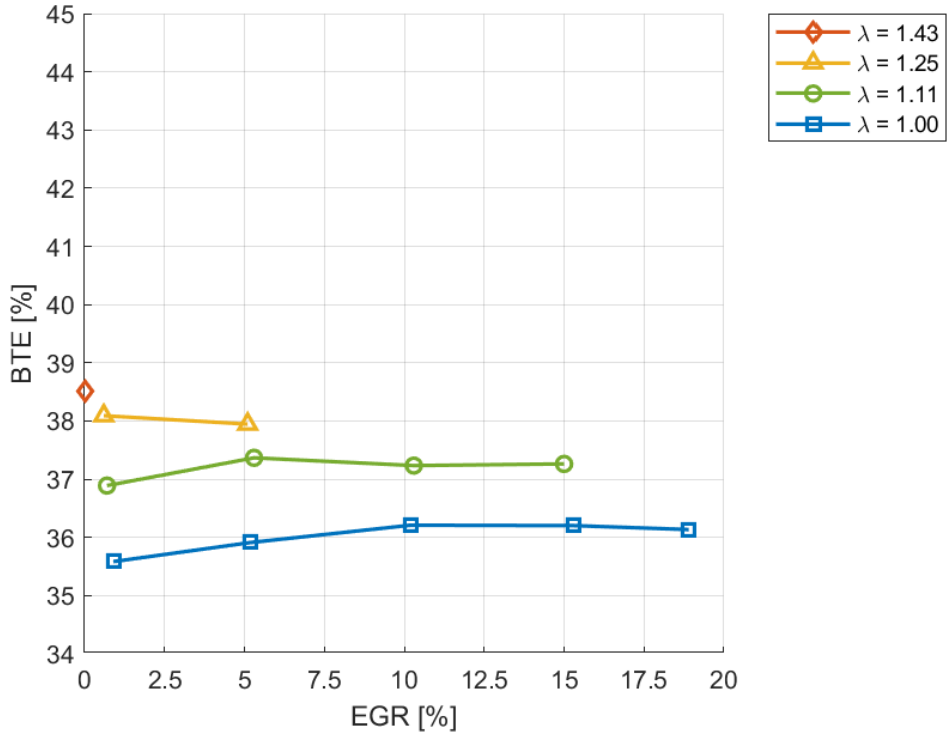

Figure 13 1500 RPM x 5,5 bar BMEP: Brake Thermal Efficiency

Regarding engine-out emissions, our focus is on HC, CO, and NOx, as they are the primary pollutants in automotive engines.

Thanks to higher O_2 concentrations and lower in-cylinder temperatures, using a leaner mixture or a higher EGR rate results in lower engine-out CO emissions. Moreover, the dissociation phenomenon is less likely to occur due to the lower combustion chamber temperature.

The primary effect of the temperature decrease resulting from mixture dilution is the reduction of engine-out NOx emissions. For example, as shown in Figure 15, an approximate 80% reduction can be observed at $\lambda = 1{,}00$ when increasing the EGR rate from 0% to 19%. However, a leaner mixture requires a dedicated NOx after-treatment system, which in our case consists of an SCR combined with an ASC.

It is also important to note that mixture enleanment does not necessarily result in lower NOx emissions. In fact, at $\lambda = 1{,}11$ and $1{,}25$, NOx emissions are higher than in the case of $\lambda = 1{,}00$. For these specific cases, the increased oxygen content due to mixture dilution has a greater impact than the reduction in in-cylinder temperature.

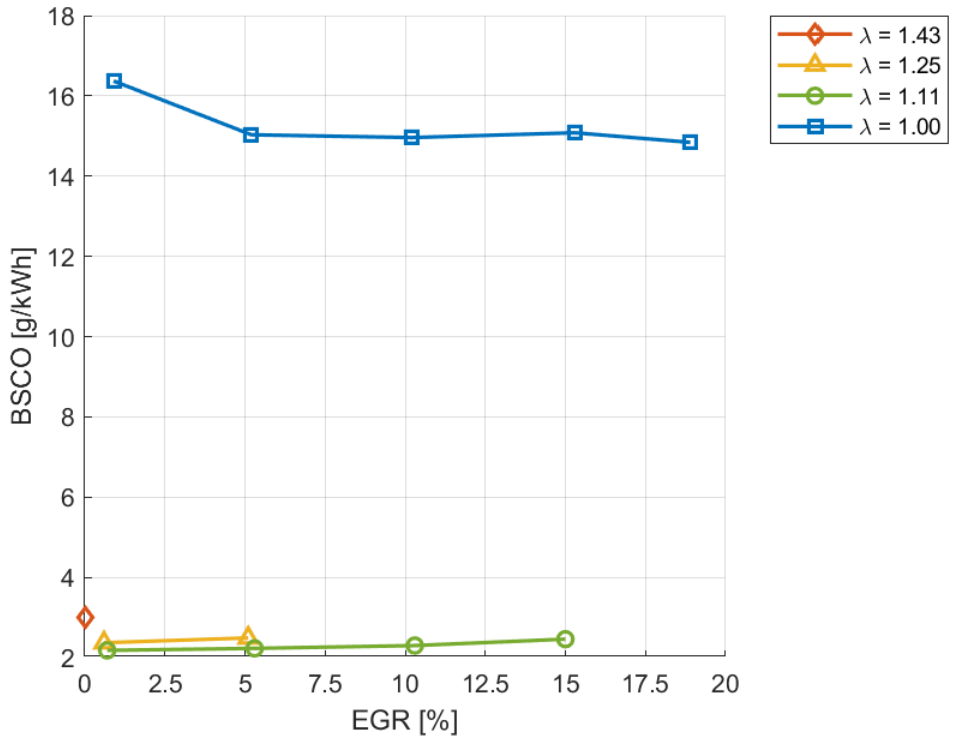

Figure 14 1500 RPM x 5,5 bar BMEP: Engine-out Brake Specific CO

On the other hand, a more diluted mixture can create an environment inside the cylinder that is more prone to HC formation mechanisms, such as flame quenching due to lower in-cylinder temperatures. As the air-fuel ratio or EGR rate increases, HC emissions at the engine exhaust also rise. However, this variation is limited, with a maximum increase of approximately 1,5 g/kWh in the case of $\lambda = 1{,}00$, as shown in Figure 16.

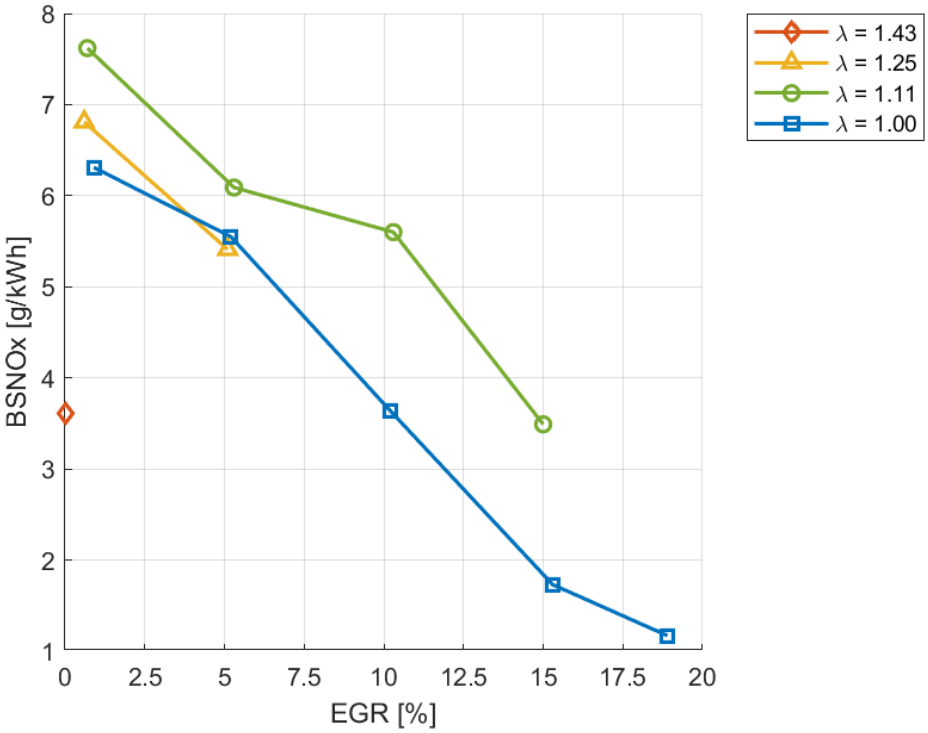

Figure 15 1500 RPM x 5,5 bar BMEP: Engine-out Brake Specific NOx

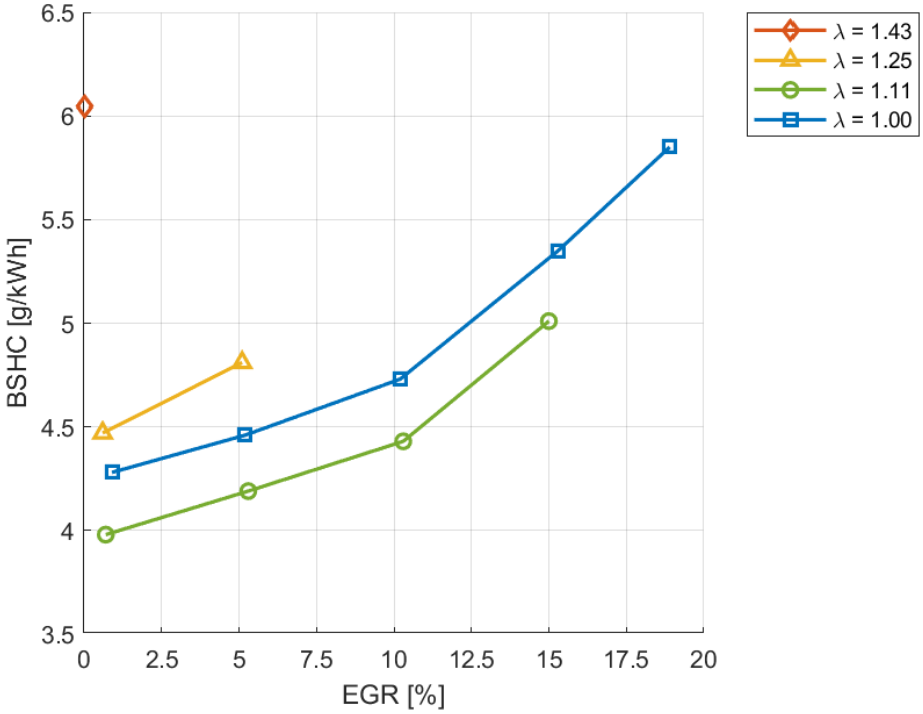

Figure 16 1500 RPM x 5,5 bar BMEP: Engine-out Brake Specific HC

3.3.2 Case 2: 2200 RPM x 20 bar BMEP

When moving to a case with higher speed and load, spark advance must be further retarded to prevent excessive in-cylinder pressure and ensure proper knock suppression. However, increasing the EGR rate allows for a greater advance of the SA while maintaining effective knock suppression. This is because the peak pressure inside the cylinder is lower due to the dilution effect.

This trend is evident in Figure 17, where it is notable that as the EGR rate increases, the peak pressure of the cycle rises and occurs at a lower crank angle.

From the Logp-LogV diagram, it can be observed that increasing the EGR rate leads to an increase in pumping work. This is due to the larger amount of air that must be drawn into the cylinder. However, since the engine speed is higher, the intake process has less time to complete, potentially leading to a reduction in volumetric efficiency.

At the same time, to achieve the correct level of boosting, as the intake mass flow increases, the VNT rack must close further, causing the boost pressure to rise and stabilizing the intake pressure at a higher level. Notably, in the case with EGR = 0, the lower backpressure results in negative pumping work (work done by the fluid). In contrast, with EGR = 15%, the higher backpressure causes the pumping work to become positive (work done on the fluid).

As previously discussed, with increased mixture dilution, the spark advance can be further advanced without negatively affecting knock suppression. However, as the mixture becomes more diluted, the burn duration increases due to the slower combustion process.

This trend is illustrated in Figure 18 in terms of the mass fraction burned. It is particularly noticeable that as the EGR rate increases or λ becomes larger, the MFB90 extends significantly. Meanwhile, the MFB50 is adjusted to achieve optimal combustion phasing.

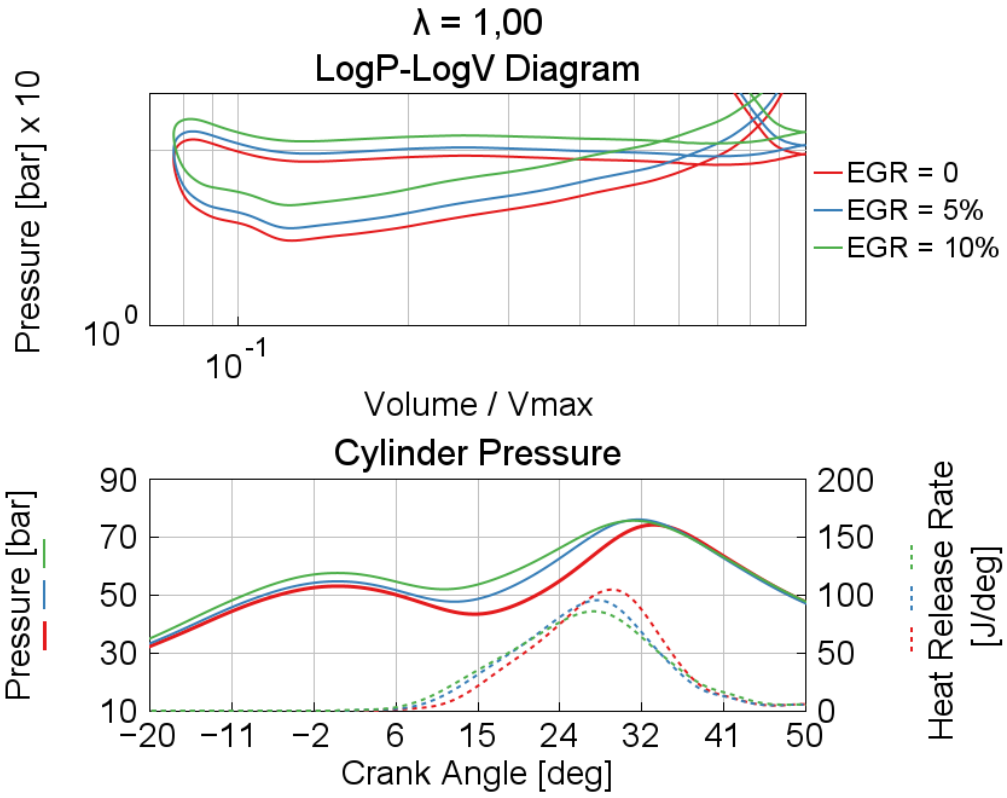

Figure 17 2200 RPM x 20 bar BMEP: Pressure cycles and Heat Release Rate for λ = 1

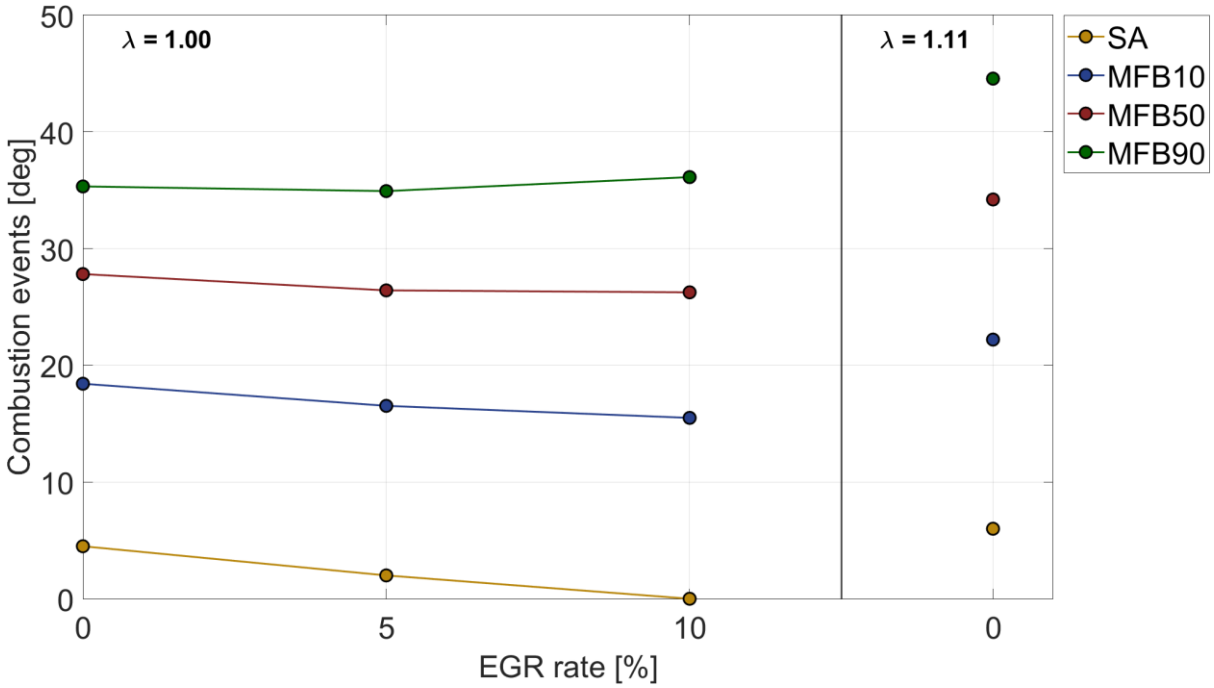

Figure 18 2200 RPM x 20 bar BMEP: Combustion Events

Regarding CoV_{IMEP}, similar considerations can be made as in the previous case. An increase in the EGR rate leads to greater variability in IMEP, which affects vehicle drivability.

For example, as shown in, when $\lambda = 1{,}00$, the EGR rate must be limited to 10% to stay within the upper threshold of 3%. However, in the case of $\lambda = 1{,}11$, this threshold is already exceeded even without the presence of EGR.

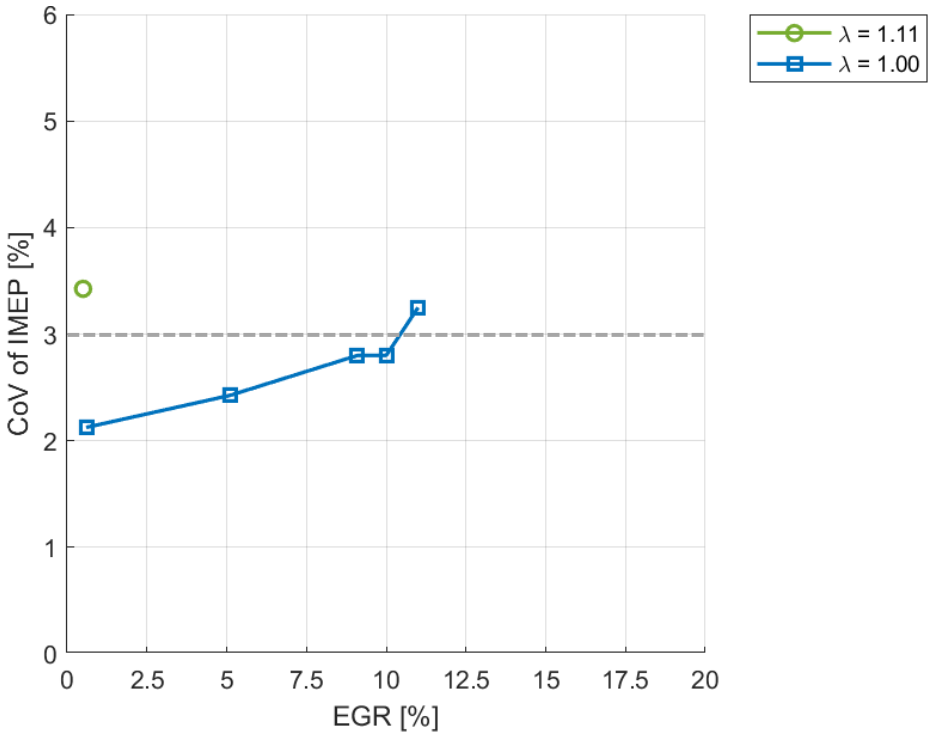

Figure 19 2200 RPM x 20 bar BMEP: CoV of IMEP

At higher speeds, the engine requires more air and fuel to maintain stable combustion. Due to the increased amount of inducted air, losses in the intake system also rise. Additionally, a reduction in volumetric efficiency may occur due to insufficient time for the intake process to complete.

These effects, combined with higher backpressure under high-speed and high-load operating conditions, result in increased pumping losses. Figure 20 further illustrates that as the EGR rate increases, pumping work also rises due to the greater intake flow (air plus EGR).

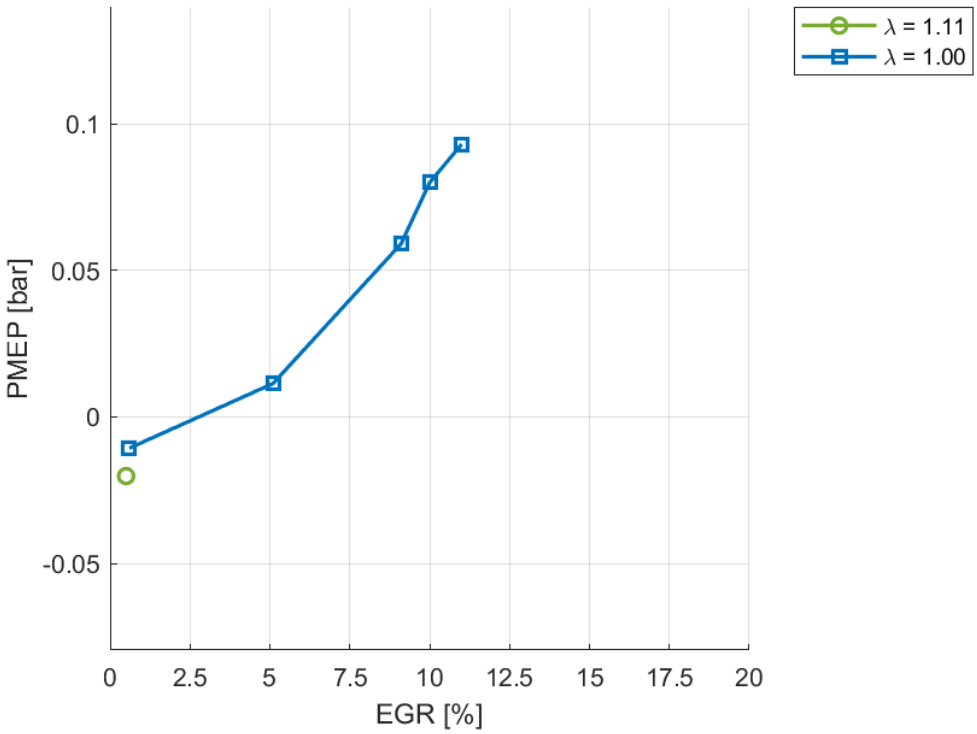

Figure 20 2200 RPM x 20 bar BMEP: Pumping Mean Effective Pressure

Whether using a leaner mixture or a higher EGR fraction, the combustion process tends to become more efficient. This is because the moderate increase in pumping work has a smaller impact compared to the significant improvement in fuel conversion efficiency. As a result, both Gross Indicated Thermal Efficiency (Gross ITE) and Brake Thermal Efficiency (BTE) increase as function of the EGR rate.

The final consideration for this engine operating point concerns engine-out emissions, with a specific focus on key pollutants such as CO, NOx, and HC.

Regarding engine-out CO emissions, Figure 23 shows that a more diluted mixture leads to a reduction in CO levels, as the increased availability of O_2 in the combustion chamber enhances oxidation.

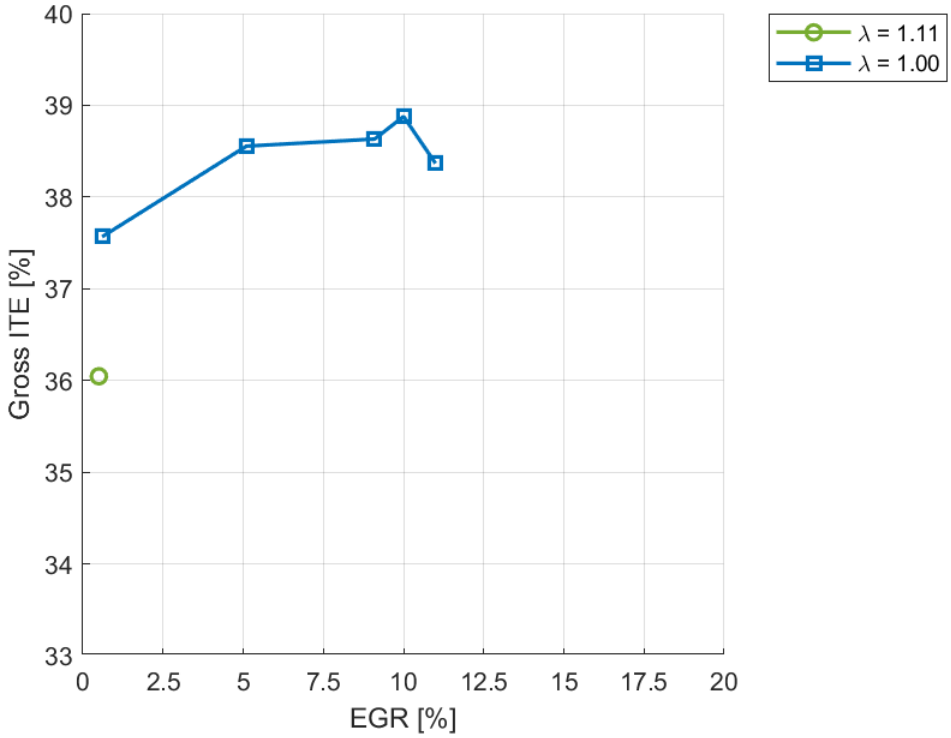

Figure 21 2200 RPM x 20 bar BMEP: Gross Indicated Thermal Efficiency

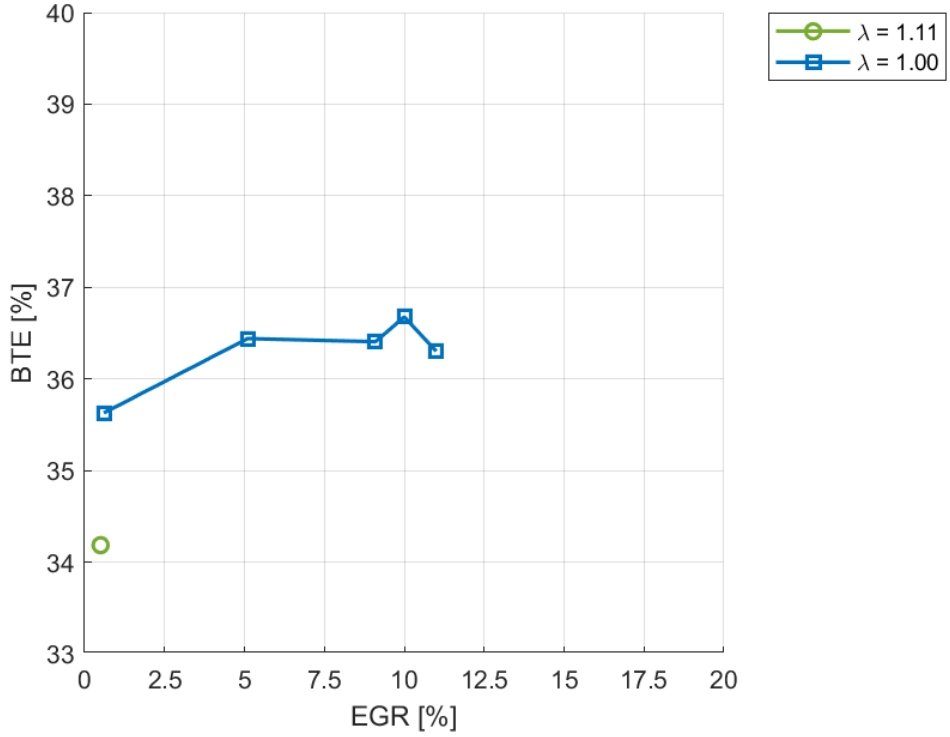

Figure 22 2200 RPM x 20 bar BMEP: Brake Thermal Efficiency

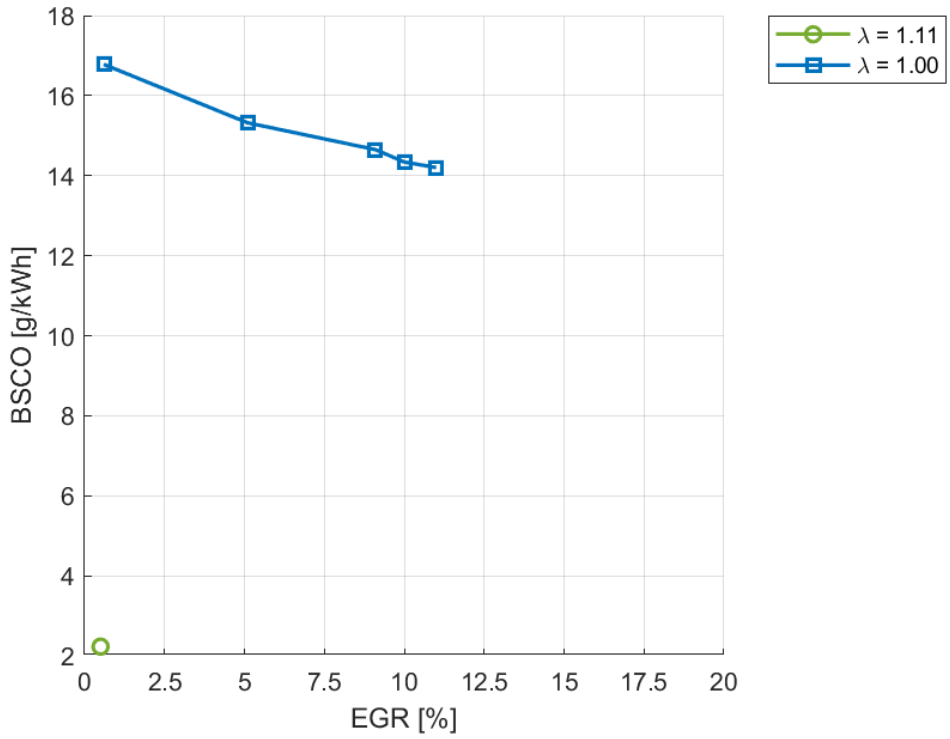

Figure 23 2200 RPM x 20 bar BMEP: Engine-out Brake Specific CO

About engine-out NOx emissions, it is clear that increasing the EGR rate leads to a reduction in these species due to the dilution effect. Specifically, for $\lambda = 1{,}00$, an increase in the EGR rate from 0% to 11% results in a reduction of NOx emissions by approximately 67%, as shown in Figure 24.

Finally, due to the more diluted mixture composition, HCs are more likely to be present in the engine-out emissions, as their formation mechanisms, such as flame quenching at the cylinder wall, are more likely to occur. However, as with the previous case, this increase in HC emissions is quite limited. As shown in Figure 25, increasing the EGR rate from 0% to 11% leads to an increase in brake-specific engine-out HC emissions by about 0,5 g/kWh.

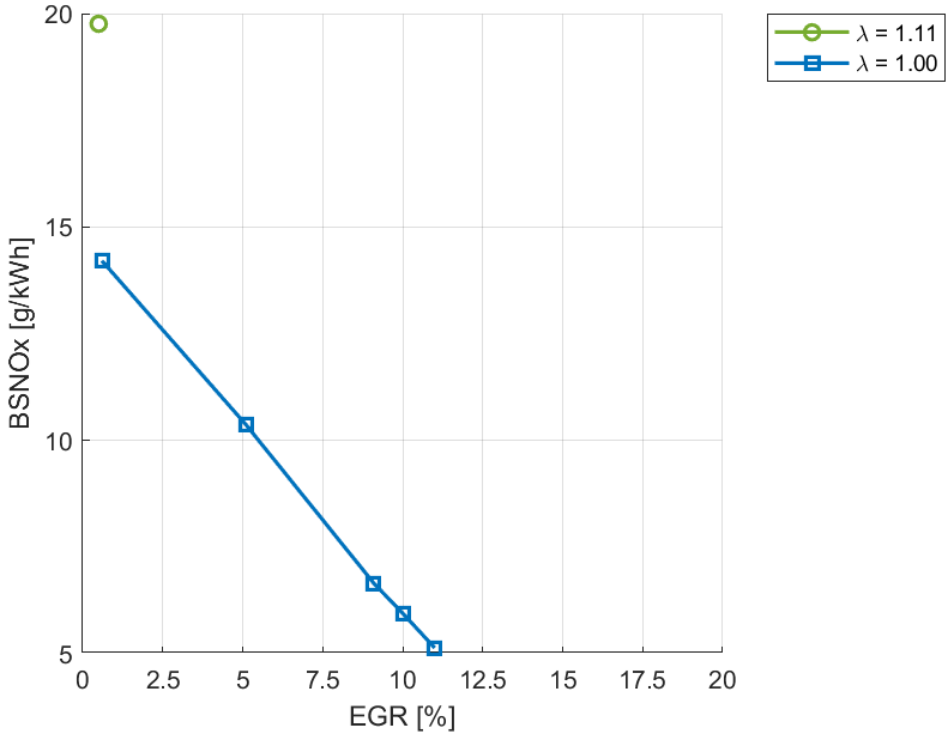

Figure 24 2200 RPM x 20 bar BMEP: Engine-out Brake Specific NOx

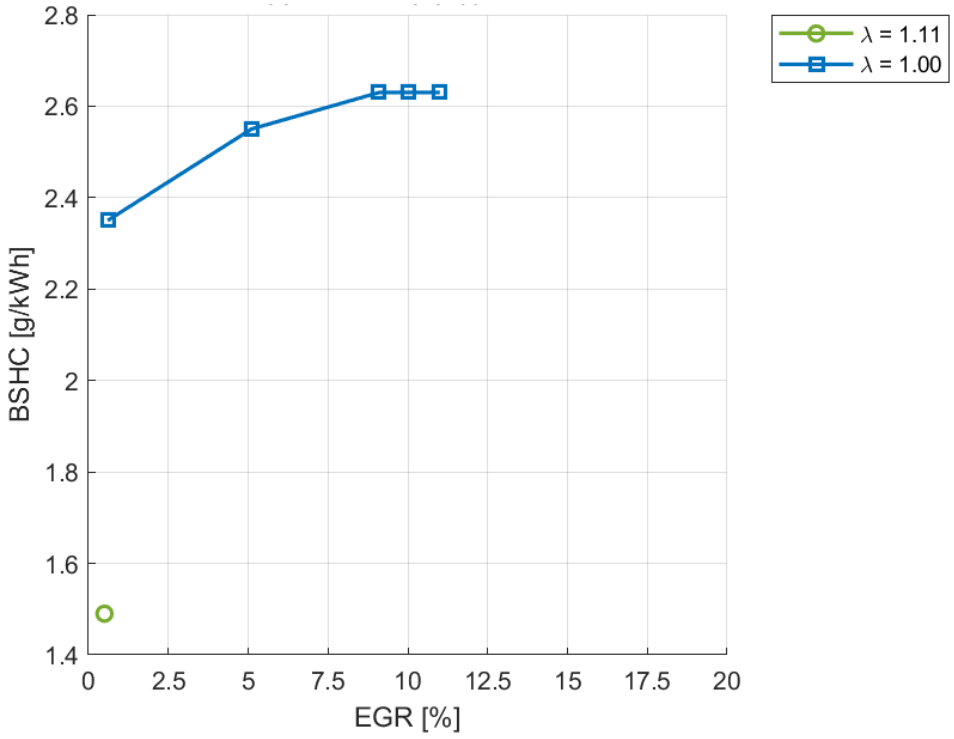

Figure 25 2200 RPM x 20 bar BMEP: Engine-out Brake Specific HC

3.3.3 Case 3: 3000 RPM x 7 bar BMEP

This engine point represents the most tested conditions at IFP, in terms of EGR rate and air-fuel ratio. Moreover, it is of significant importance, as the transition between naturally aspirated and boosted operation occurs precisely at 7 bar BMEP.

The dilution of the mixture allows for the advancement of the spark advance (SA), enabling higher pressure inside the cylinder and, therefore, a larger amount of work to be collected by the piston during the expansion stroke. This results in a higher peak pressure, occurring at a lower crank angle, as shown in Figure 26, Figure 27 and Figure 28.

Considering the Logp-LogV diagram, it can be noted that the case with $\lambda = 1{,}00$ behaves like a naturally aspirated engine point: as the EGR rate increases, the pumping area reduces, and the PMEP tends to decrease, as shown in Figure 25.

A similar behaviour is observed for the case with $\lambda = 1{,}11$, but with higher backpressure due to the increased mass flow. This effect becomes more pronounced as the EGR rate increases.

Moving to the case of $\lambda = 1{,}25$, it is clear that an increase in the EGR rate facilitates the transition from aspirated to boosted operating conditions. To accommodate a larger intake mass flow rate, the VNT rack must close to increase the boost level, raising the intake pressure above atmospheric levels. This effect is clearly visible in the Logp-LogV chart of Figure 28 for the case with an EGR rate of 15%.

Furthermore, by comparing the cases with EGR rates of 0% and 15%, it is noticeable that, for the first case, the backpressure is lower compared to the second case, due to the lower amount of entrained mass.

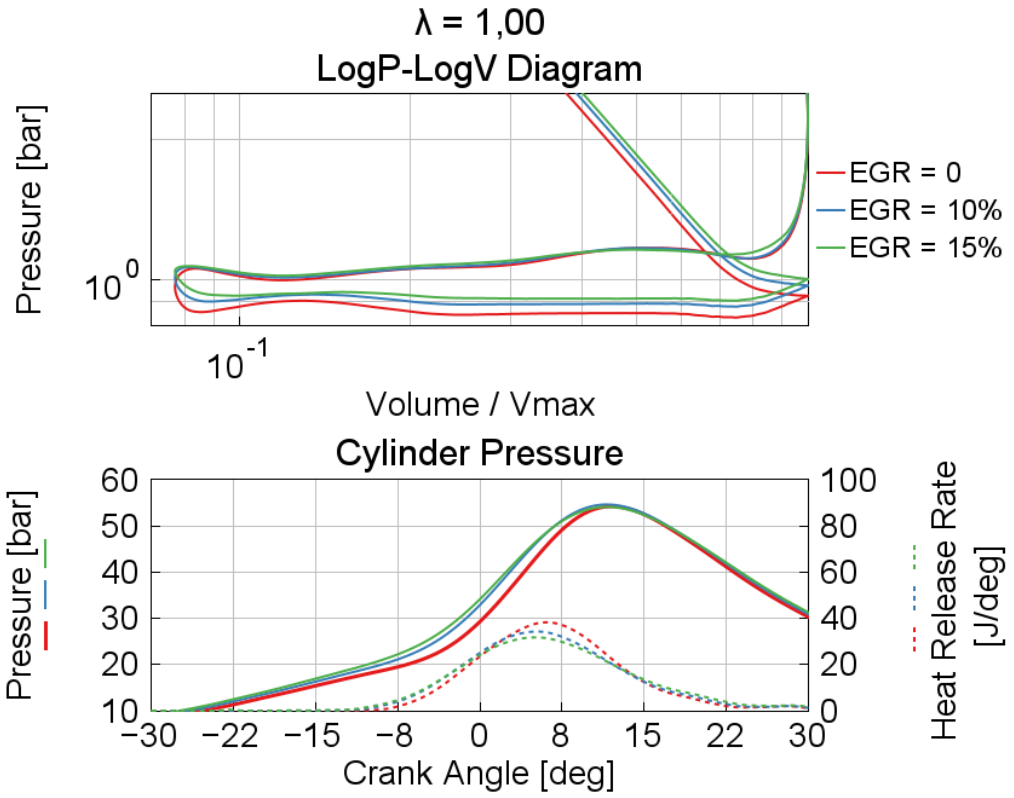

Figure 26 3000 RPM x 7 bar BMEP: Pressure Cycles and Heat Release Rate for λ = 1,00

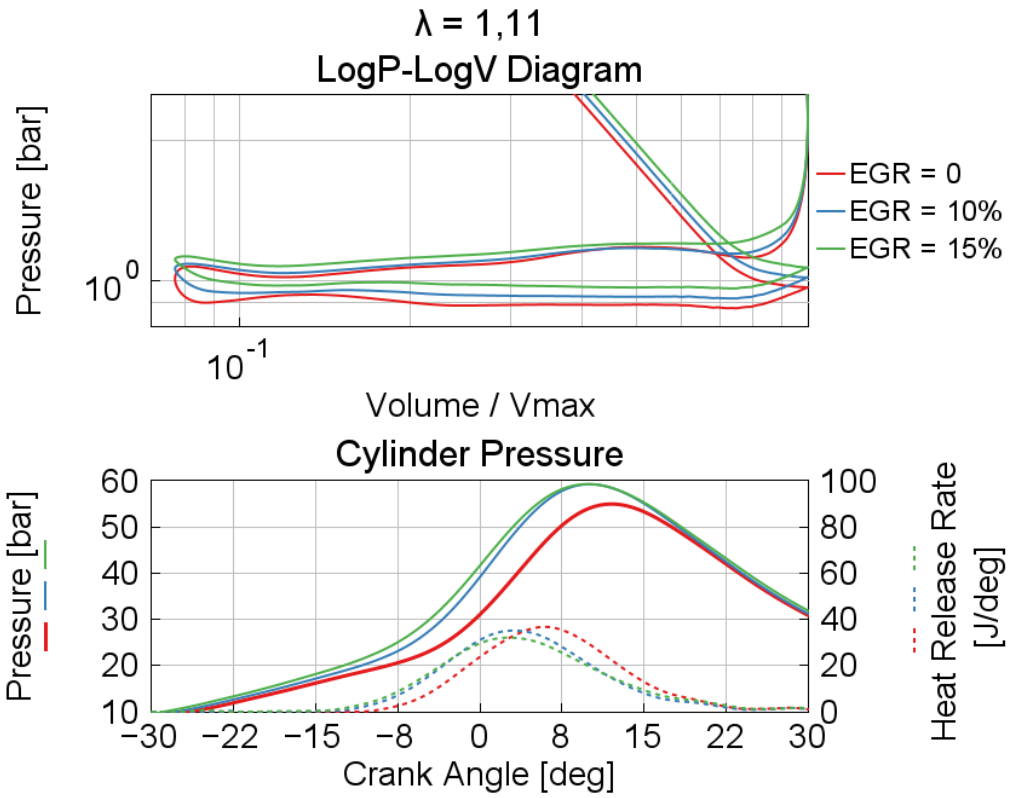

Figure 27 3000 RPM x 7 bar BMEP: Pressure Cycles and Heat Release Rate for λ = 1,11

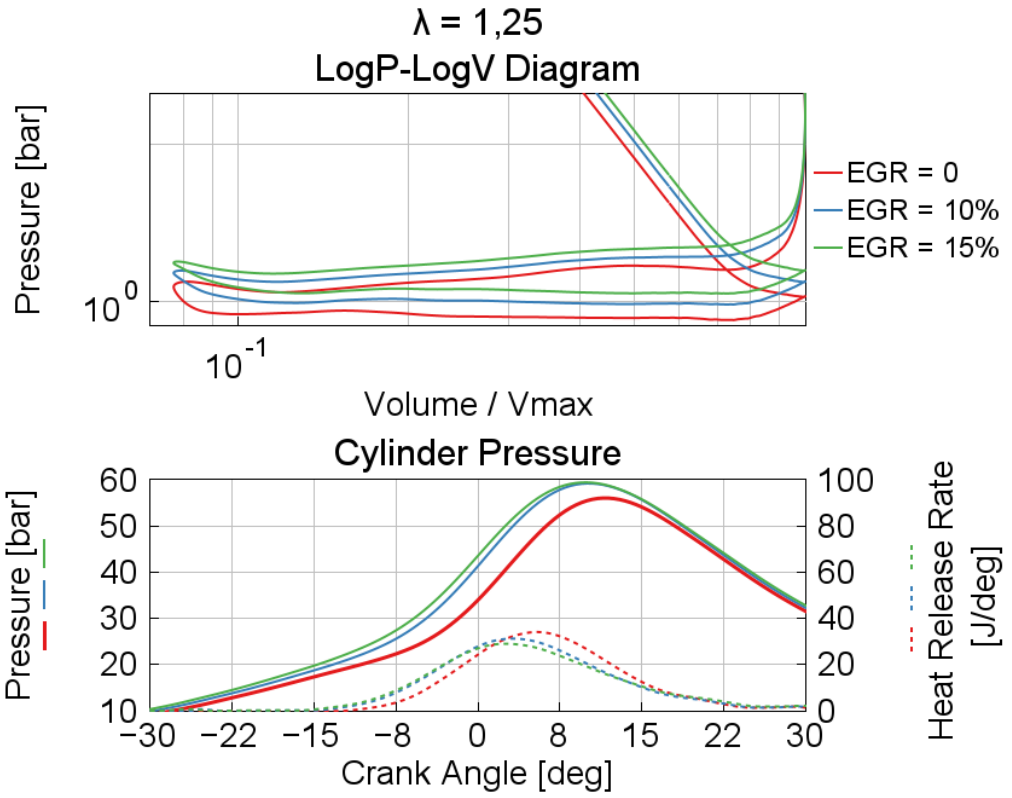

Figure 28 3000 RPM x 7 bar BMEP: Pressure Cycles and Heat Release Rate for λ = 1,25

Besides ensuring the advance of the SA, the second effect of the dilution is the increase in burn duration, which results from a slower combustion process due to lower temperatures inside the combustion chamber. Once again, this trend is visible in terms of MFB, as shown in Figure 29.

For this engine point, it is noticeable from Figure 30 that the 3% CoV_{IMEP} threshold is exceeded only in the case of $\lambda = 1{,}11$ and an EGR rate of 20%. This limits the maximum EGR that can be used. Moreover, a clear trend emerges, with CoV_{IMEP} increasing as the air-fuel ratio and EGR rate increase, due to a depletion of the combustion process.

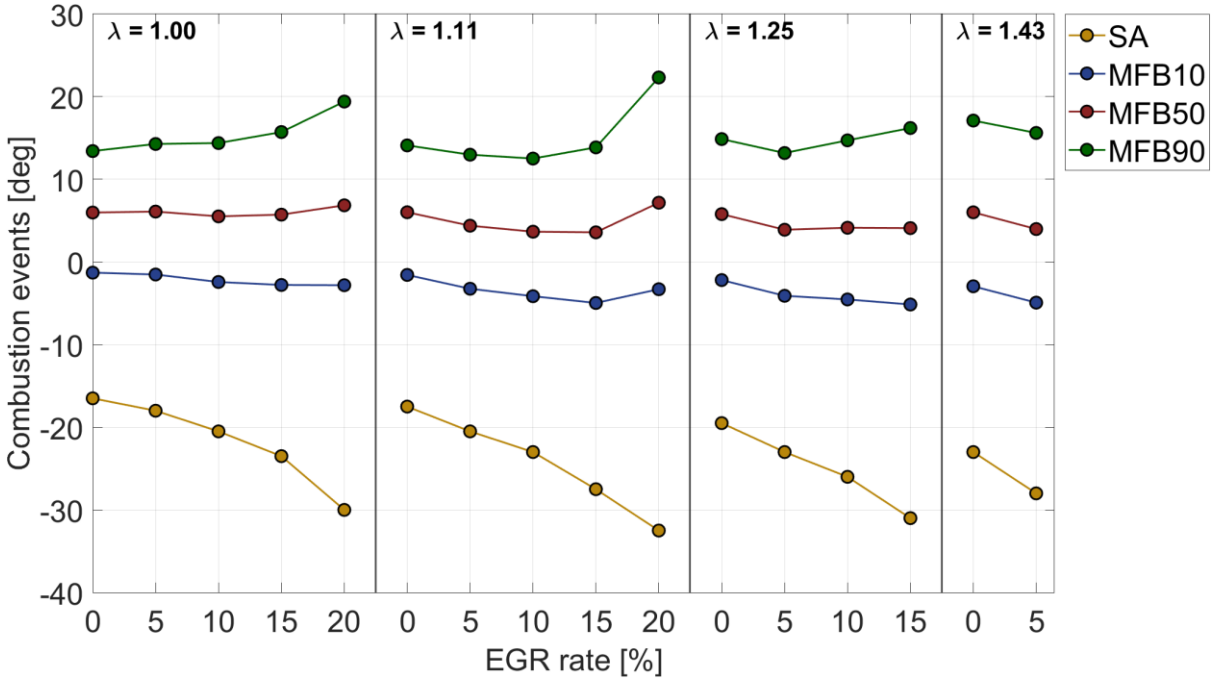

Figure 29 3000 RPM x 7 bar BMEP: Combustion Events

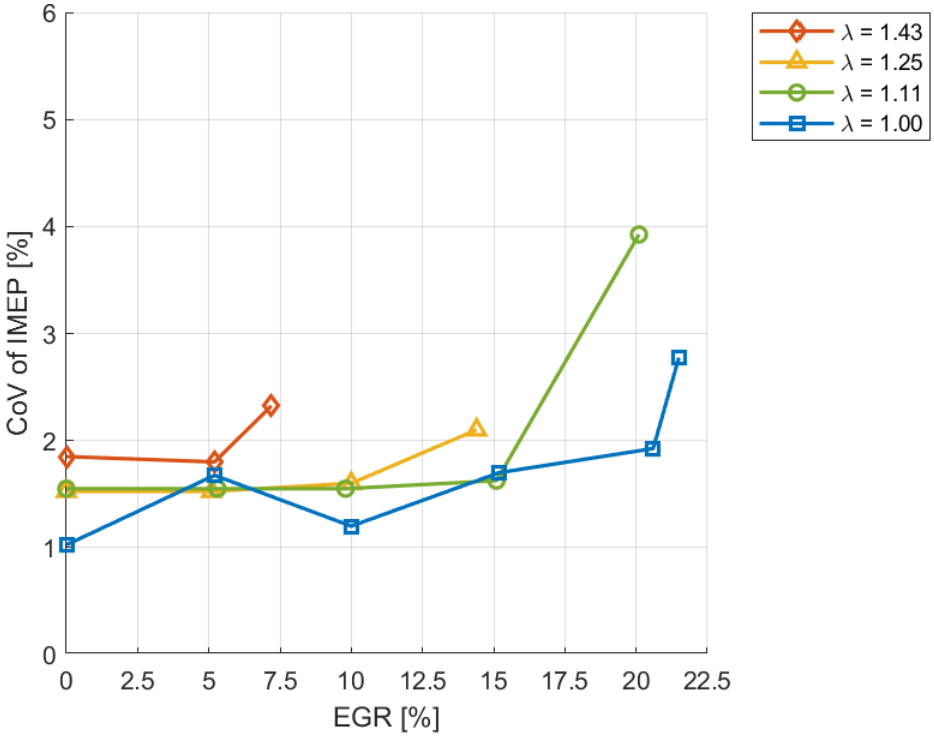

Figure 30 3000 RPM x 7 bar BMEP: CoV of IMEP

Considering the pumping work, it is evident from Figure 31 that PMEP decreases as the EGR rate increases, as the engine becomes more de-throttled with a larger intake mass flow.

For the case of $\lambda = 1{,}25$, it can be observed that the transition from aspirated to boosted operating conditions is starting to occur. This is evident as no clear reduction in PMEP is visible, and, as seen in the Logp-LogV chart, the intake pressure tends to be higher than atmospheric pressure.

In the case of $\lambda = 1{,}43$, the trend is reversed compared to the other cases. This can be explained by the fact that the throttle valve is already fully open to allow such a large amount of air. As a result, a certain level of boost is required. The VNT rack begins to close, the boost pressure rises, and the correct amount of inducted mass is ensured. However, the pumping work increases to accomplish the gas exchange process.

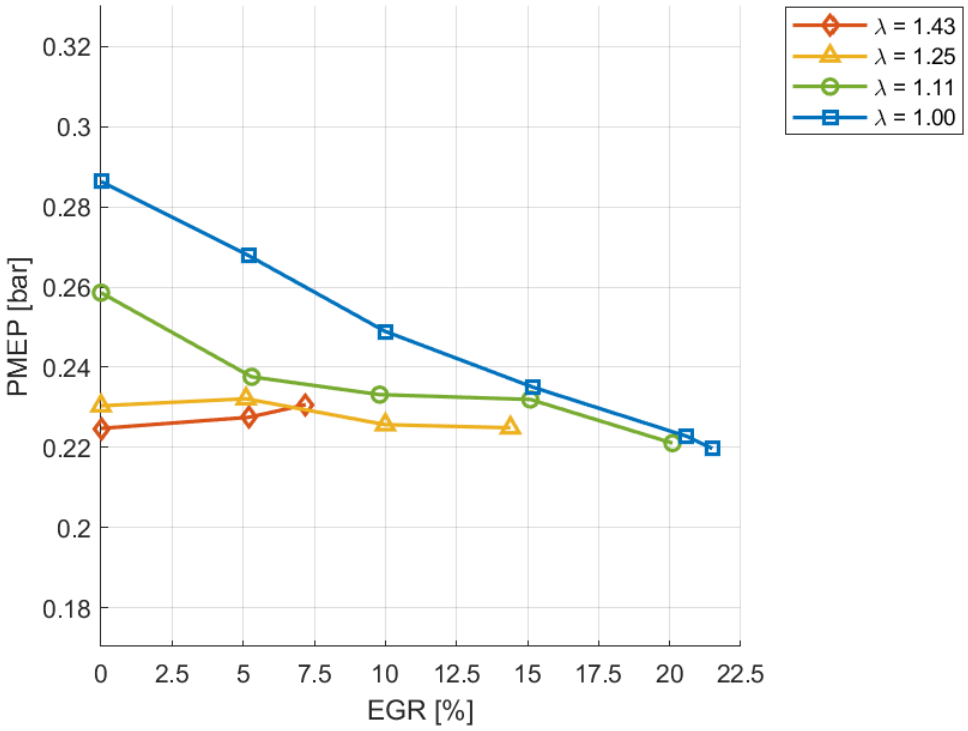

Figure 31 3000 RPM x 7 bar BMEP: Pumping Mean Effective Pressure

Once again, it is evident that as the EGR rate increases or the mixture becomes leaner, the engine's fuel conversion efficiency improves, both in terms of Gross ITE and BTE.

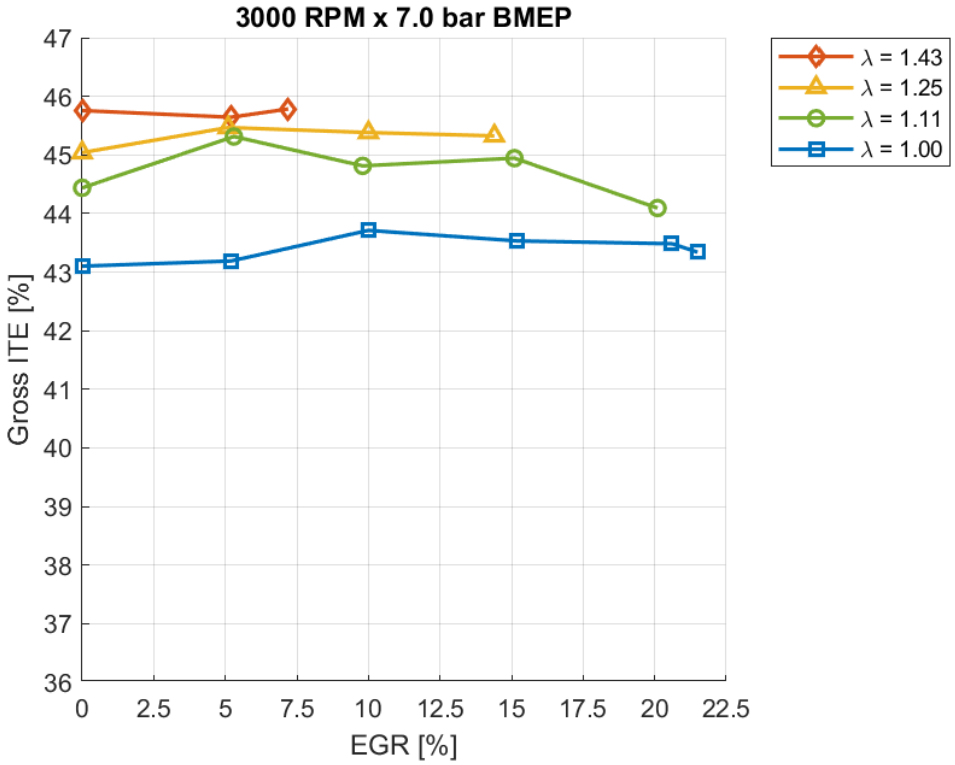

Figure 32 3000 RPM x 7 bar BMEP: Gross Indicated Thermal Efficiency

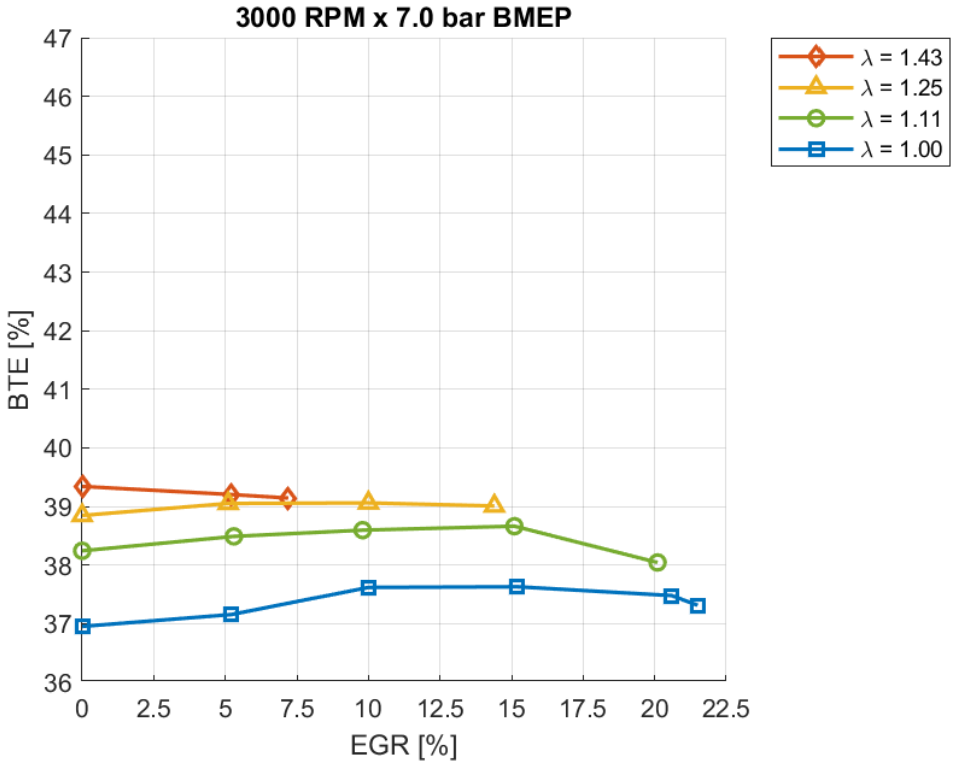

Figure 33 3000 RPM x 7 bar BMEP: Brake Thermal Efficiency

The final step in the analysis of this engine point is a brief discussion of the engine-out emissions.

Regarding CO emissions, as the mixture becomes more diluted, CO emissions tend to decrease because more oxygen is available in the combustion chamber, making oxidation occur more easily.

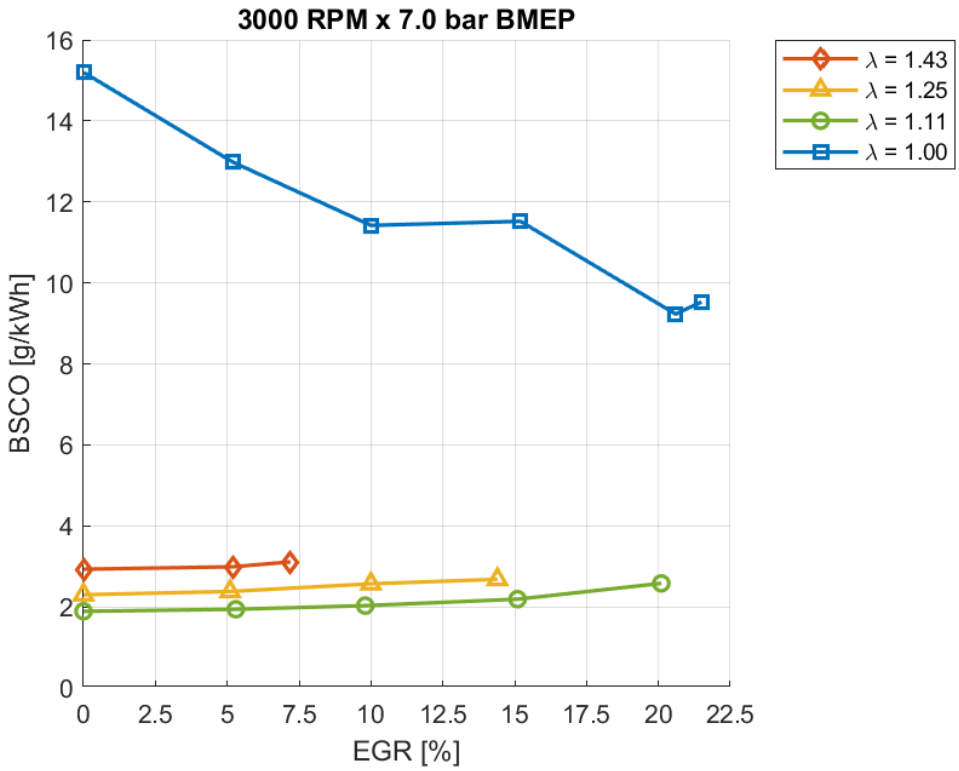

Figure 34 3000 RPM x 7 bar BMEP: Engine-out Brake Specific CO

Increasing either the air-fuel ratio or the EGR rate leads to a reduction in NOx emissions. This effect is due to the lower temperatures reached inside the combustion chamber, which results in a reduced NOx formation mechanism.

During combustion, due to the higher extent of mixture dilution, the temperature reached is lower, and phenomena such as flame quenching are more likely to occur. As a result, HC formation increases, leading to a rise in engine-out brake-specific HC emissions as the EGR or air-fuel ratio increases.

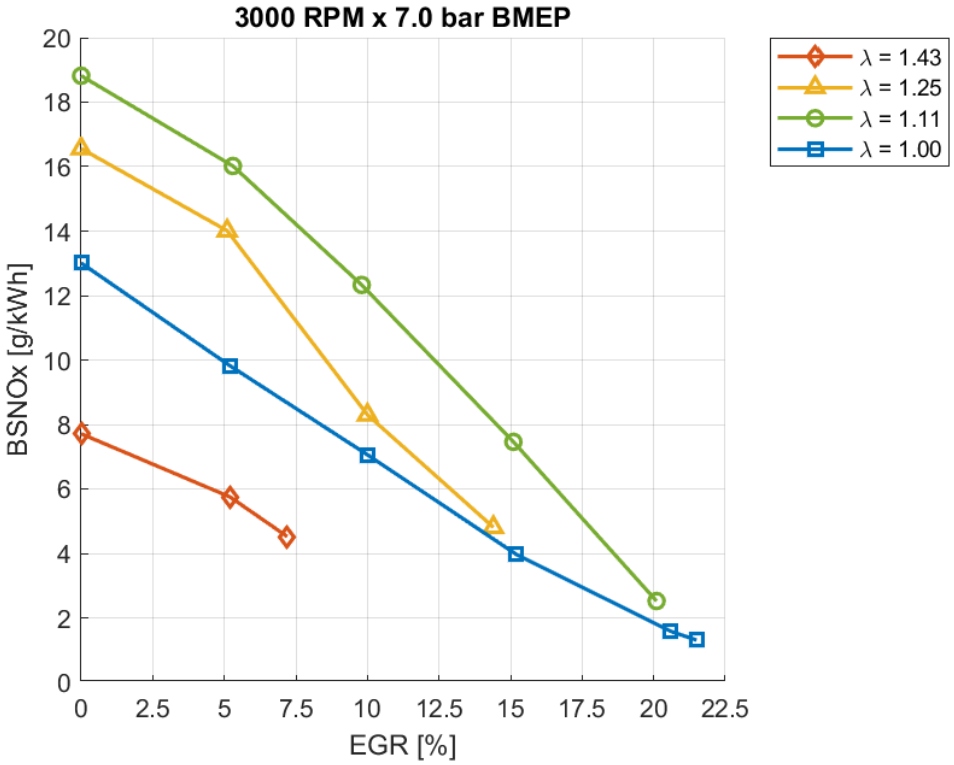

Figure 35 3000 RPM x 7 bar BMEP: Engine-out Brake Specific NOx

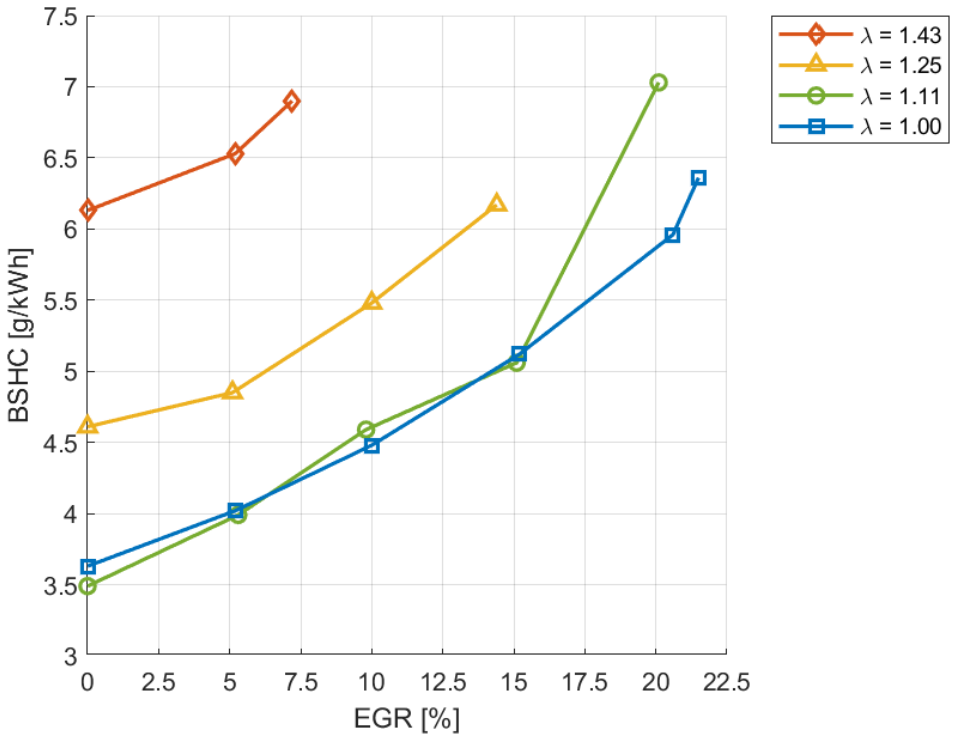

Figure 36 3000 RPM x 7 bar BMEP: Engine-out Brake Specific HC

3.4 Compressor Map Analysis

In this paragraph, a brief analysis of the compressor map is conducted, highlighting the most commonly adopted working conditions and the limits imposed by the use of a lean mixture.

It must be reminded that the compressor used in this application is specifically designed for the PHOENICE project. It offers a higher pressure ratio capability, though at the cost of a reduced mass flow capacity compared to the baseline engine's wastegate turbocharger. These features enable an expansion of the high-efficiency area, improving the behaviour of this component for most of the boosting operating conditions.

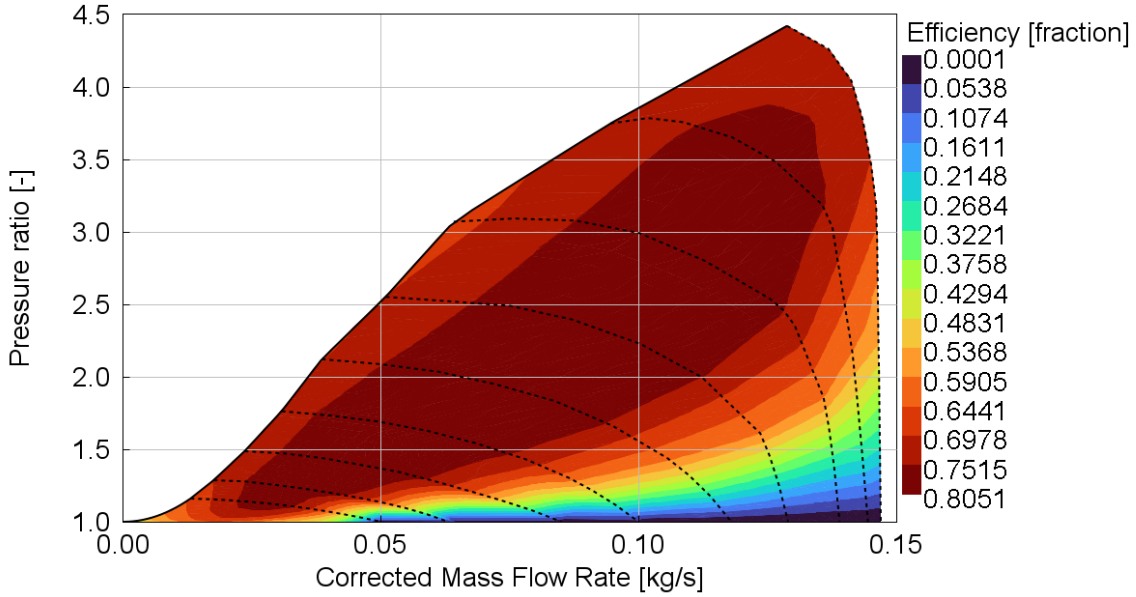

Figure 37 Efficiency Contour Map of the compressor

First, a comparison is made between engine points at the same speed but different load requests (e.g., 2600 RPM × 15 bar BMEP and 2600 RPM × 20 bar BMEP). It is clear that, in the case of a BMEP of 20 bar, a larger amount of air is required for proper combustion. Therefore, to accommodate a larger intake mass flow (air plus EGR), the boost pressure must increase. As a result, the operating points shift to higher corrected mass flow rates, moving into a higher efficiency region. Thanks to the improved efficiency of the custom-built compressor, this component operates much more efficiently as the load increases, as shown in Figure 38 and Figure 39.

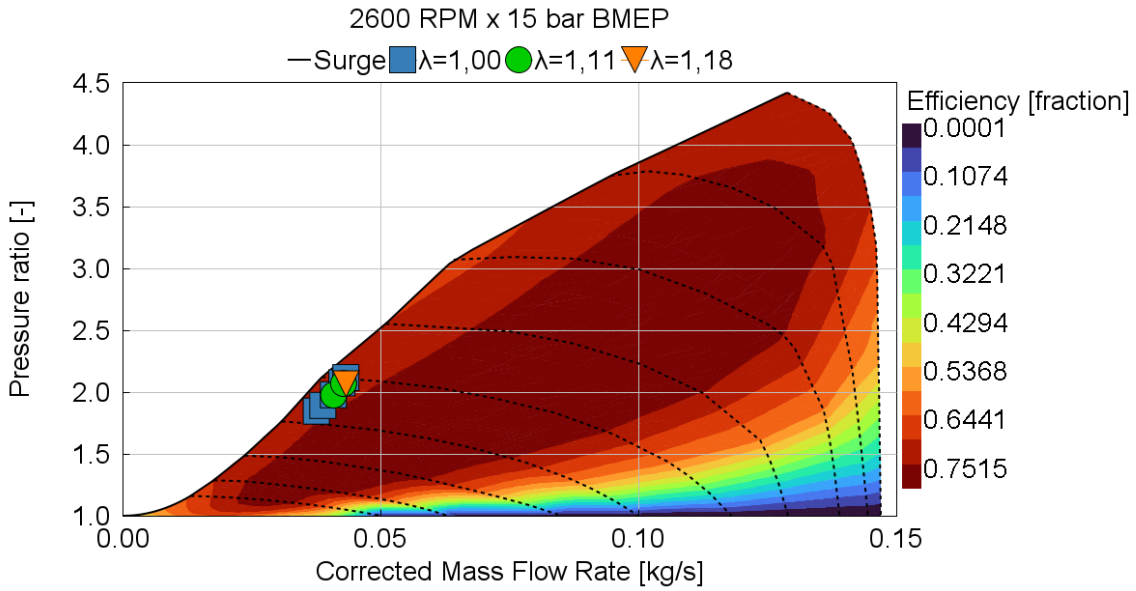

Figure 38 Compressor Analysis: 2600 RPM x 15 bar BMEP Working Conditions

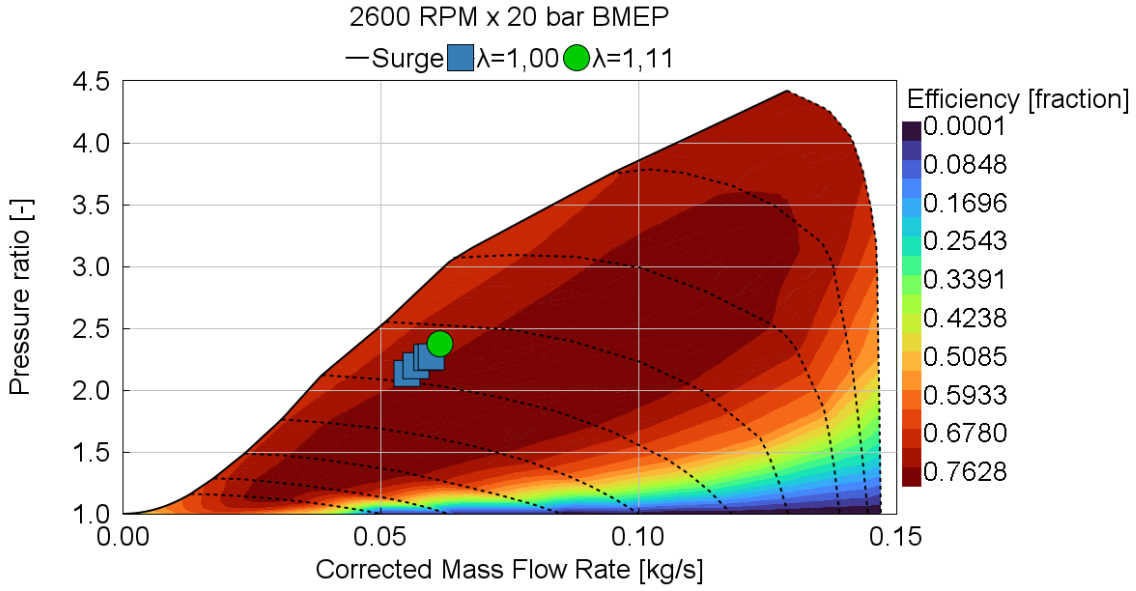

Figure 39 Compressor Analysis: 2600 RPM x 20 bar BMEP Working Conditions

Considering two engine operating conditions at the same speed but different BMEP, specifically referring to the cases 2600 RPM × 20 bar BMEP shown in Figure 39 and the working point 2200 RPM × 20 bar BMEP shown in Figure 40, it is clear that moving to a higher speed results in a more efficient working condition for the compressor. To maintain stable combustion at higher speeds, more air is required, shifting the points on the compressor map to larger corrected mass flow rates while maintaining a similar pressure ratio. Furthermore, by increasing the EGR, the

compressor speed must increase to ensure the correct boost level, which is necessary to entrain the requested amount of EGR and air into the intake.

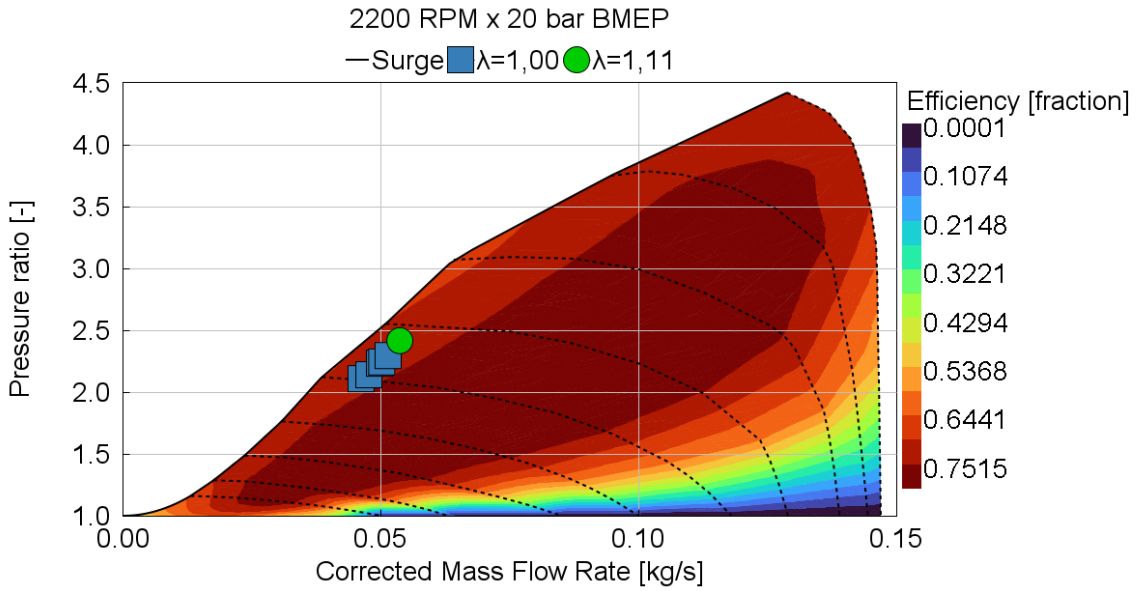

Figure 40 Compressor Analysis: 2200 RPM x 20 bar BMEP Working Conditions

The last consideration regards the limits imposed by the use of a lean mixture. This effect is evident for the engine points where the required boost level is in the medium-low range. For example, considering two engine points at medium boost levels - 1500 RPM × 11.5 bar BMEP and 2000 RPM × 13.5 bar BMEP, shown in Figure 41 and Figure 42, respectively - it can be concluded that the leaner or more diluted the mixture, the closer the working points are to the surge limit on the compressor map. Therefore, the maximum possible mixture enleanment must be limited to avoid compressor instability. In fact, for the mentioned engine points, the maximum value of the air-fuel ratio used during the steady-state calibration tests at IFPEN was restricted to 1,11.

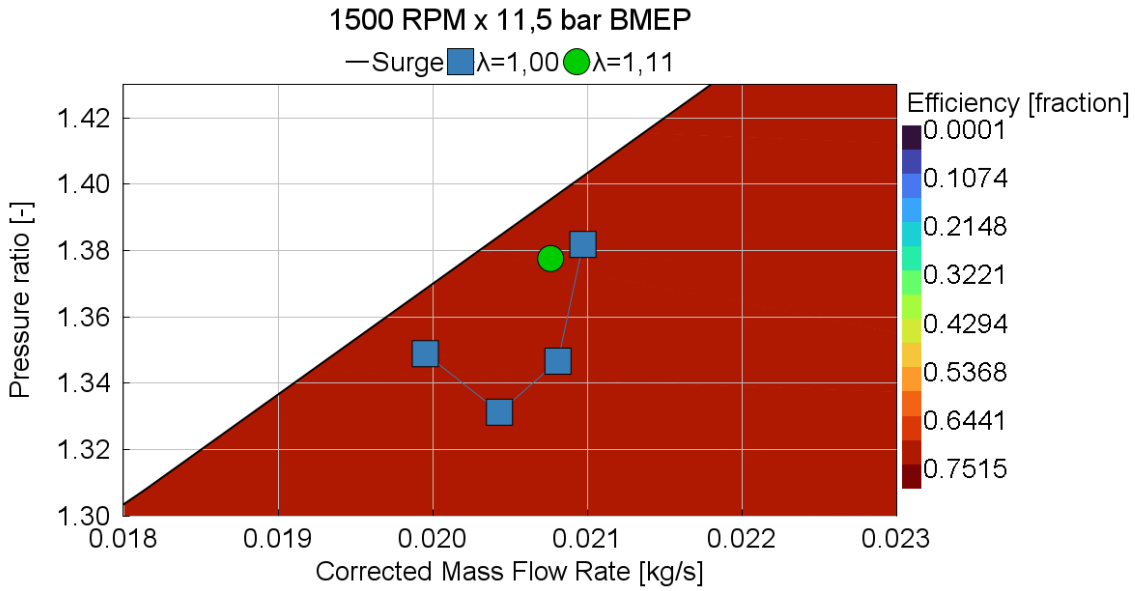

Figure 41 Compressor Analysis: 1500 RPM x 11,5 bar BMEP Working Conditions

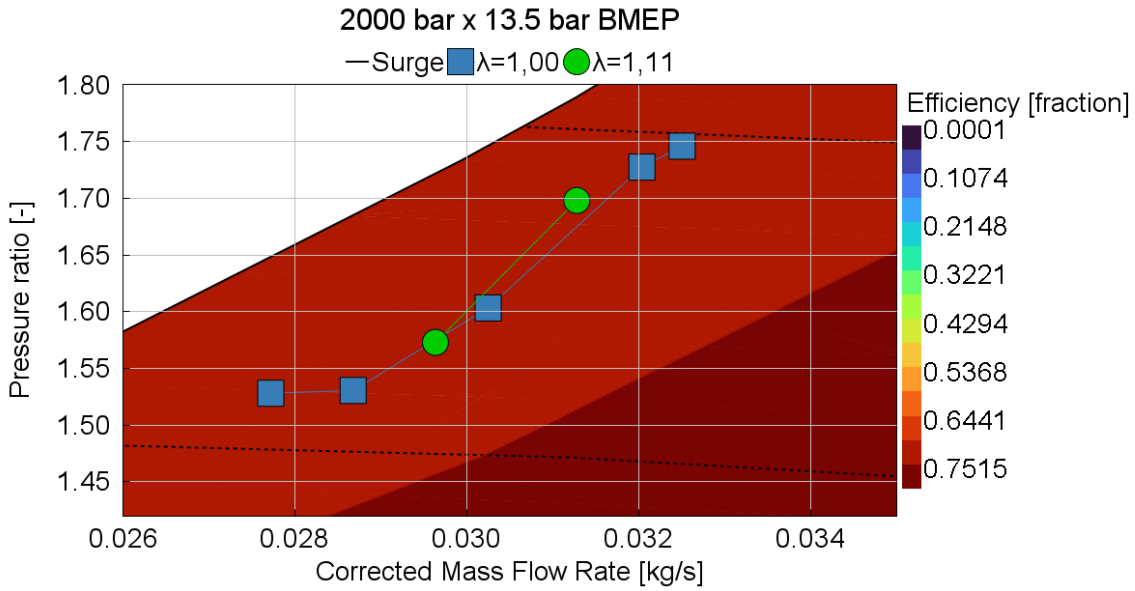

Figure 42 Compressor Analysis: 2200 RPM x 13,5 bar BMEP Working Conditions

3.5 Conclusions

In this chapter, the analyses conducted on the combustion process and performance indices were presented.

Starting from the available data, the procedures for studying the combustion process and performance indices were briefly described.

To present the obtained results, three different engine points (1500 RPM $\times$ 5.5 bar BMEP, 2200 RPM $\times$ 20 bar BMEP, and 3000 RPM $\times$ 7 bar BMEP) were considered. All these points were thoroughly examined in terms of pressure cycles, combustion events, thermal efficiencies, and engine-out emissions, pointing out the outstanding results of emission reduction and increment of the engine thermal efficiency.

Finally, a brief discussion on the compressor was included, focusing on how efficiently this component operates and the limits imposed by the use of a lean combustion mixture.

These analyses served as the starting point for this thesis, providing the necessary understanding of the engine behaviour under different speeds and load conditions, and laying the foundation for the subsequent research activities.

4. Transient Analysis

4.1 Introduction

The aim of this chapter is to analyse engine consumption and emissions over a real driving cycle, represented by a Worldwide Harmonized Light Vehicles Test Cycle (WLTC) trace.

The starting point of this analysis is the engine fuel consumption and CO, NOx, and HC emissions maps, obtained at PoliTo during steady-state calibration. These maps are implemented to provide the interpolation basis for the different quantities over the driving cycle.

The study is based on a 0D kinematic approach and is repeated for different combinations of mixture composition and EGR rate. As a first attempt, the initial standard vehicle gear-shifting strategy is used.

It is important to emphasize that, due to the methodology used in this analysis, it represents only the ideal fuel consumption and emissions that the engine could achieve over a real driving cycle. Since the steady-state calibration maps of the engine are used, the warm-up phase of the engine is not taken into account. It follows naturally that this phase has a significant impact on engine consumption and emissions. Therefore, the results of this transient analysis are used solely for comparison and reference against real test outcomes.

The second part of this chapter focuses on analyzing the gear-shifting strategy, which is a key aspect of the PHOENICE project due to its impact on vehicle emissions and fuel consumption.

The PHOENICE project prototype features a six-speed automatic transmission gearbox, which, along with the engine, is mounted in the conventional front transverse powertrain position.

After the initial study using the baseline vehicle gearshift, an optimization of this strategy is proposed. Two possible solutions are presented: the first is an optimization developed at FEV, while the second is an attempt at optimization carried out at the Polytechnic of Turin. The common goal of both optimizations is to improve the baseline gearshift strategy, particularly by reducing fuel

consumption and carbon monoxide emissions. Therefore, for each analysed strategy, a comparison with the baseline gearshift is provided to assess progress toward the study's main objective.

4.2 Methodology

Even though the procedures for the transient simulations and the optimization study are similar, in order to maintain better clarity, the methodology is described as split into two parts, representing the two conducted analyses, respectively.

4.2.1 Transient Simulation

The simulation is based on WLTC traces for Class 3 vehicles, which describe vehicle speed, engine speed, and engine torque throughout the cycle. These traces have a sampling time of 0,1 seconds, covering the standard 1800 second duration of the WLTC, resulting in a total of 18000 data points representing the cycle.

WLTC Specification	
Duration [s]	1800
Stop Duration [s]	235
Cover Distance [m]	23266
Average Speed [km/h]	46,5

Table 9 WLTC Specification

The WLTC traces used in this simulation are shown in Figure 43. In particular, when analysing the vehicle speed trace, the four segments of the cycle can be identified:

- Low-speed segment: 0 to 600 seconds
- Medium-speed segment: 600 to 1,000 seconds
- High-speed segment: 1,000 to 1,450 seconds
- Extra-high-speed segment: 1,450 to 1,800 seconds.

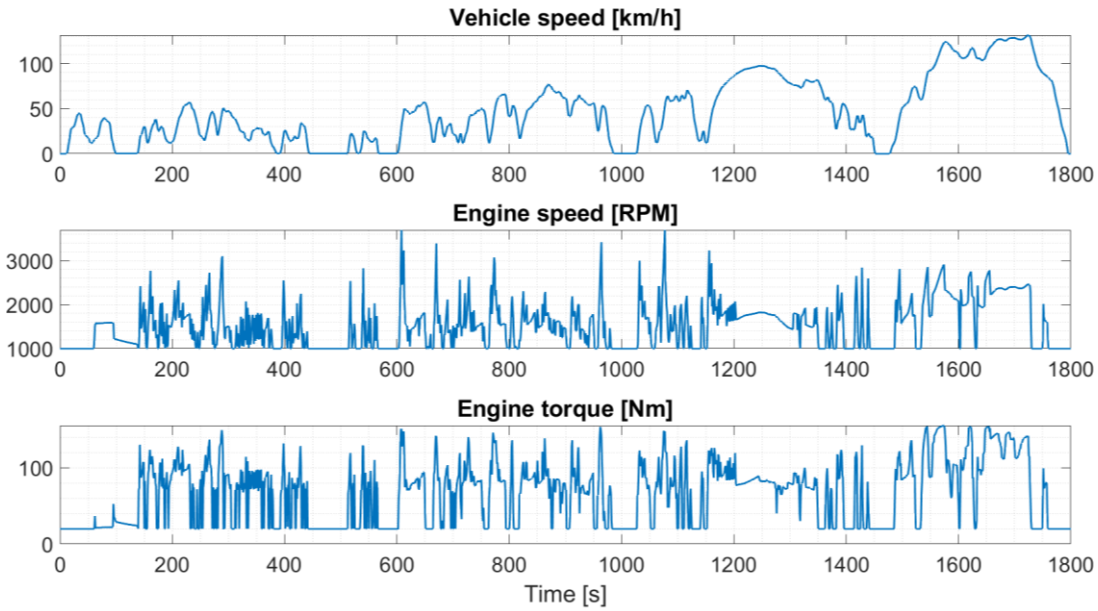

Figure 43 WLTC Traces for Vehicle Speed, Engine Speed and Engine Torque

The second key element required for the transient analysis are the engine maps for fuel consumption and emissions.

During the PoliTo steady-state test campaign, fuel consumption and engine-out emissions maps were acquired. These maps were obtained for various engine operating points, defined by different combinations of engine speed and load request. For each engine point, data acquisition was repeated under different mixture compositions and EGR rates.

Specifically for the transient simulation, fuel consumption and emissions over the WLTC are evaluated under three different operating conditions:

- Stoichiometric mixture without EGR
- Stoichiometric mixture with EGR
- Lean mixture with EGR.

The data acquired from the test bench expressly include brake specific fuel consumption (BSFC), brake specific engine-out CO emissions (BSCO), brake specific engine-out NOx emissions (BSNOx), and brake specific engine-out HC emissions (BSHC), all as functions of engine speed and BMEP.

Since the engine maps were obtained from stationary test acquisitions, the spectrum of speeds and loads must be extended to cover the possible requests of the WLTC simulation. To achieve this, for each tested BMEP, a trendline for fuel consumption

and engine-out emissions is identified as a function of speed. This approach makes it possible to determine values for BSFC, BSHC, BSCO, and BSNOx across a broader range of feasible engine speeds. Therefore, this method allows for the expansion of the cluster containing the engine map information, enabling more accurate interpolation for the different quantities.

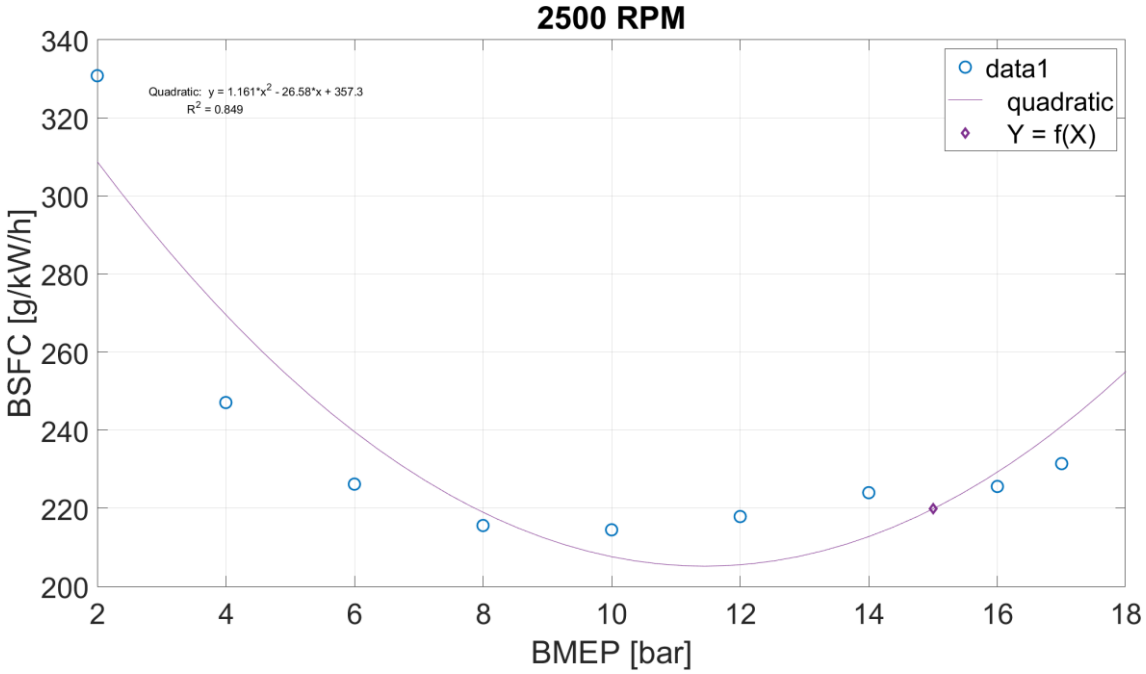

Figure 44 Example of the Trendline Identification for the BSFC at 2500 RPM

However, the simulations carried out, especially in the case of low engine speed and low engine load, may suffer from computational errors. This outcome can be attributed to a potentially weak trendline prediction used to extend the steady-state maps obtained from the PoliTo test bench, but in many cases it is difficult to estimate a better trendline than the one used. Additionally, the absence of the warm-up phase, which is not considered in engine maps coming from the steady-state calibration, reduces the simulation's prediction accuracy. Therefore, the simulations are intended only as an ideal representation of a real driving cycle and are used solely for comparing the data obtained from real tests.

The final element required for the driving cycle simulation was the gearshift strategy. As a first attempt, the baseline gear shifting of the initial standard vehicle is used.

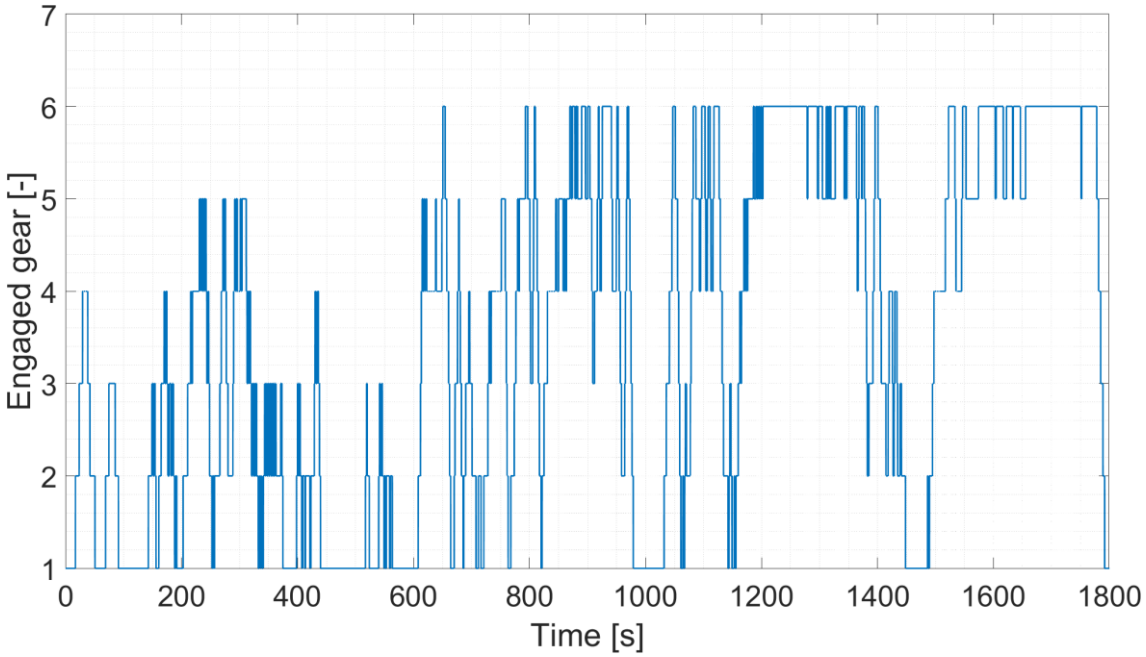

Figure 45 Baseline Gearshift Strategy

All the described data are implemented in an interpolation algorithm used to calculate the consumption and emissions over the WLTC. It is produced as a simple MATLAB script that, starting from the engine maps and the WLTC traces, calculates the instantaneous and cumulative values of fuel consumption and engine-out CO, NOx, and HC emissions.

4.2.2 Optimization Analysis

Regarding the analysis of the gearshift optimization, two additional traces are needed.

The first trace is provided by the FEV gearshift strategy, which is an optimization of the baseline strategy obtained through an internal-use algorithm and is reported in Figure 46.

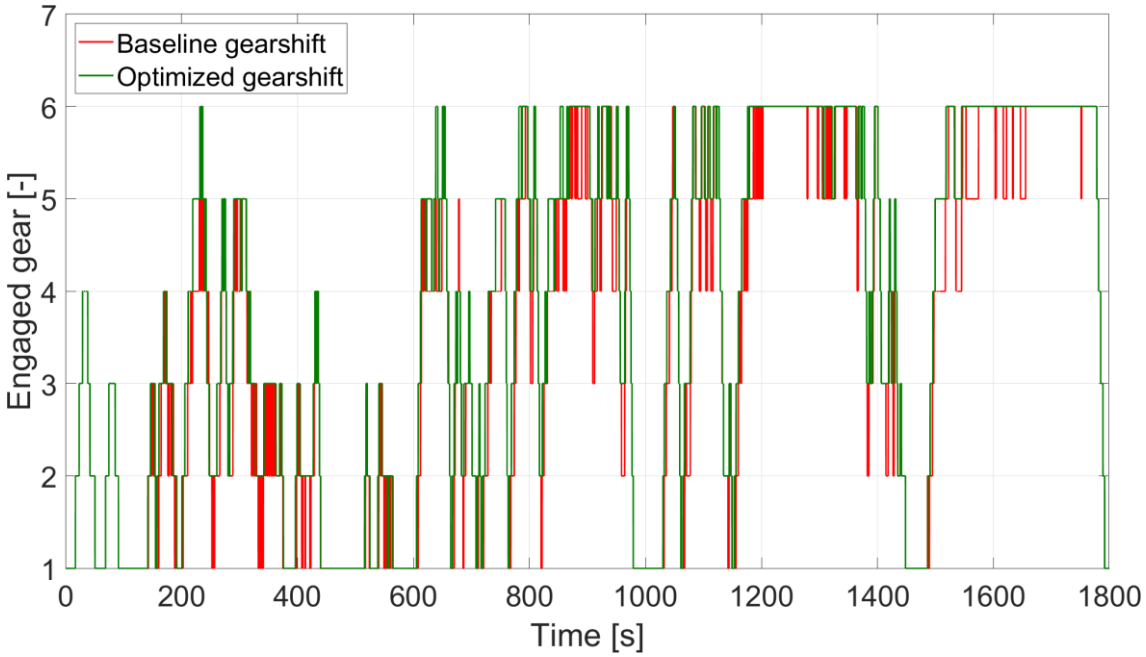

Figure 46 Baseline Gearshift Strategy and FEV Optimized Strategy

It can be noted that the FEV strategy attempts to avoid extended use of low gears and to maintain the highest gear when the vehicle is moving at high speed. These two precautions are certainly reducing the engine's fuel consumption, which is the primary result requested from the gearshift optimization.

The FEV shared trace is simply implemented in MATLAB and, through a simple interpolation algorithm, enables the estimation of fuel consumption and pollutant emissions over the WLTC.

To better analyse the outcome of the simulation, the time distribution of the studied gearshift strategy is examined. This procedure allows estimation of how much time the strategy spends in specific engine operating conditions, defined as interplay of engine speed and requested load. The time distribution is analysed with respect to the BSFC map, as well as the BSCO map, to evaluate the consumption and emissions of the strategy.

After analysing the FEV gearshift, a second possible optimization is explored. This optimization results from a simple rule-based algorithm developed at PoliTo and based on a kinematic approach. For each point in the WLTC trace, the fuel consumption corresponding to the six available gears is evaluated. Then, the algorithm selects the gear that meets the engine speed and load requirements while ensuring the lowest consumption.

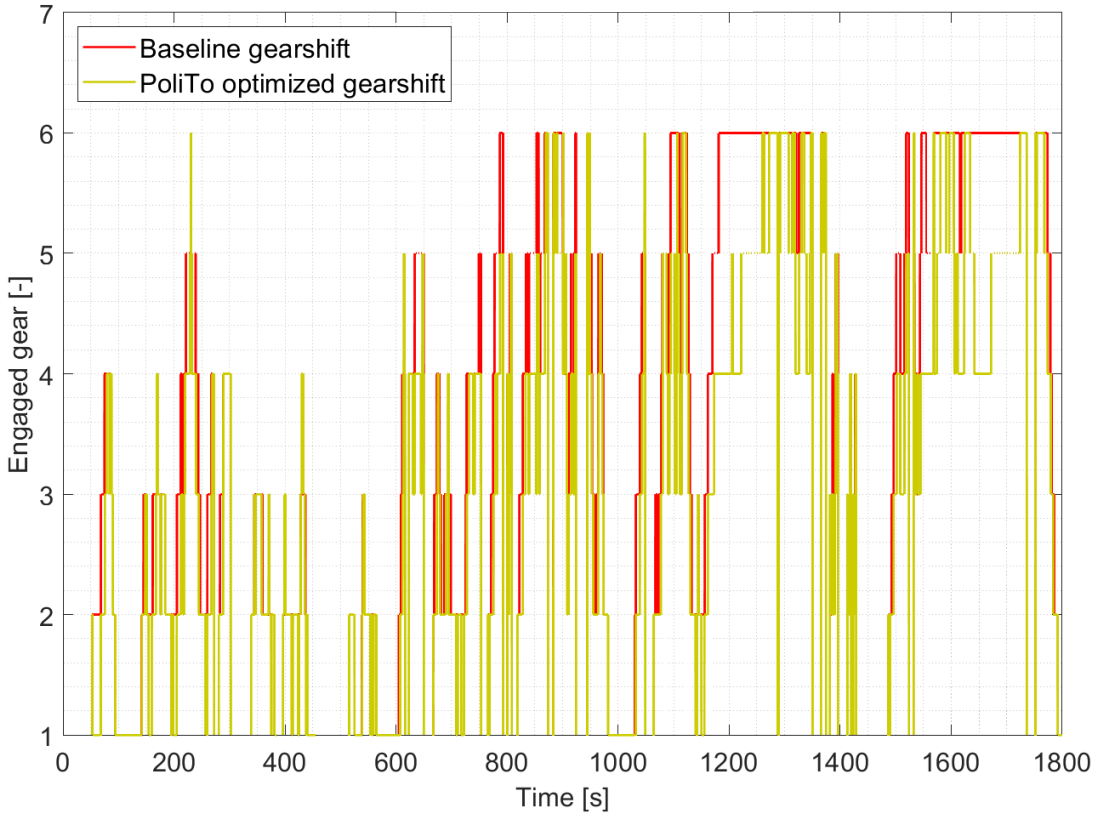

Figure 47 Baseline Gearshift Strategy and PoliTo Optimized Strategy

Finally, the gearshift strategy trace is implemented in the MATLAB interpolation algorithm to obtain the simulation outcomes, including both cumulative and instantaneous values, as well as the time distribution over the BSFC map.

It must be underlined that the optimization analysis is conducted only for the case of engine functioning with a λ equal to 1,43 in presence of EGR, as this is the core of the PHOENICE project, representing the maximum enleanment reached during the steady-state calibration at both IFPEN and PoliTo.

4.3 Transient Simulation Results

In this section, a brief discussion of the 0D simulation results is presented.

As previously mentioned, the simulation over the WLTC is performed for three different mixture compositions:

- $\lambda = 1$ without EGR
- $\lambda = 1$ with EGR
- $\lambda > 1$ with EGR.

The objective of this study is to highlight the impact of EGR induced dilution and mixture enleanment on fuel consumption and engine-out emissions.

4.3.1 Fuel Consumption

The first considerations concern fuel consumption, as reported in Figure 48 and Figure 49, which show the instantaneous and cumulative fuel consumption over the WLTC, respectively.

Regarding instantaneous fuel consumption, it can be observed that the lowest fuel economy corresponds to the case with $\lambda = 1{,}00$ without EGR.

However, at certain points, the highest fuel consumption occurs in the case of a stoichiometric mixture with EGR. These peaks in consumption correspond to rapid increases in load demand. This can be explained by the need to supply a greater intake mass flow rate (air plus EGR) to meet the high load request, which requires a certain level of boost. Consequently, the pressure before the turbine (p3) must increase, leading to a reduction in the engine's volumetric efficiency. Excessive backpressure under high operating conditions negatively impacts engine performance, affecting the intake phase and resulting in a fuel consumption penalty.

For the remainder of the simulation, the expected trend is observed: fuel consumption decreases as λ and the EGR rate increase. This is consistent with the well-known principle that a leaner mixture improves engine fuel conversion efficiency, while the presence of EGR helps reduce heat transfer losses.

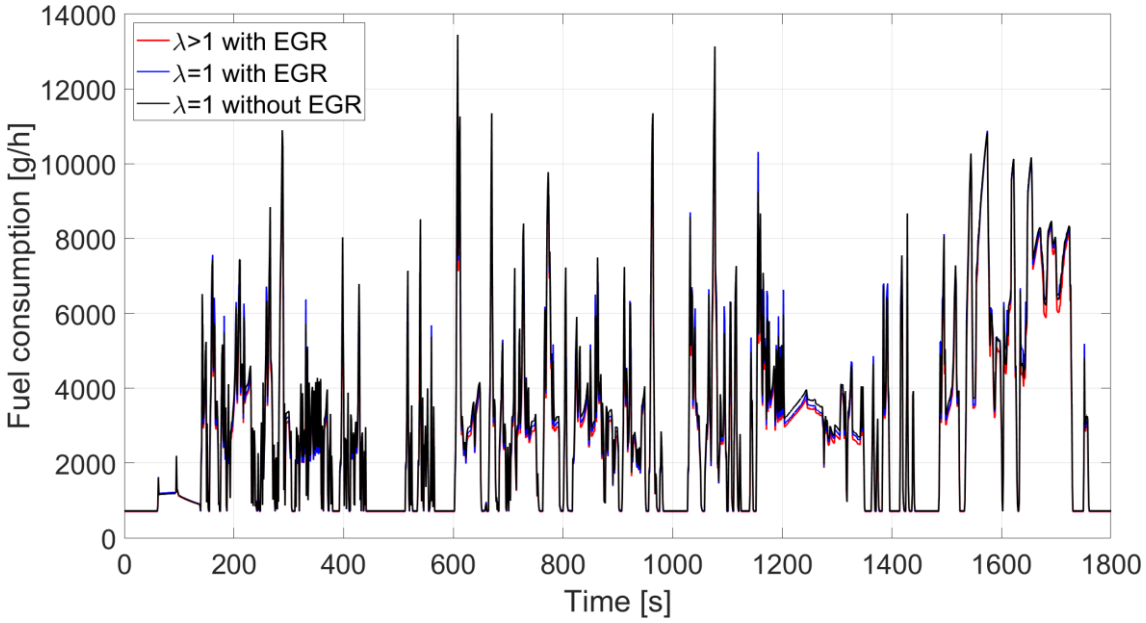

Figure 48 Instantaneous Fuel Consumption over the WLTC

Nevertheless, despite some contradictory effects at certain cycle points where rapid transient conditions occur, the overall impact of a leaner mixture combined with EGR usage is a reduction in engine fuel consumption. Specifically, transitioning from $\lambda = 1$ without EGR to $\lambda > 1$ with EGR results in an approximate 5% fuel savings.

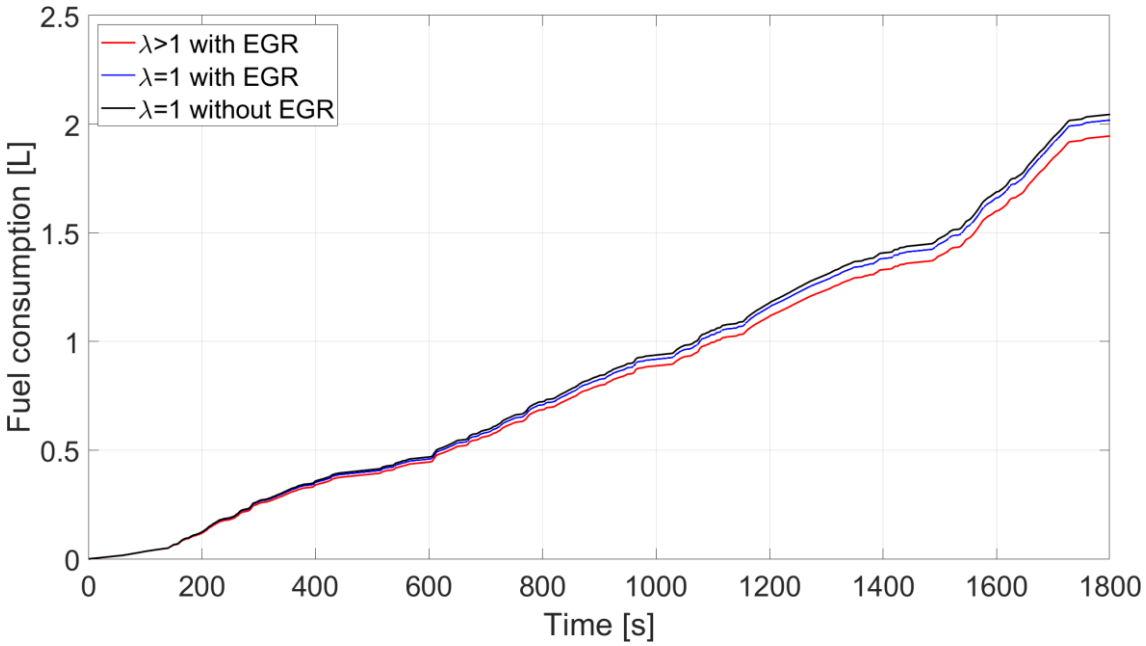

Figure 49 Cumulative Fuel Consumption over the WLTC

4.3.2 Engine-out Emissions

Regarding CO emissions, Figure 50 clearly shows that the introduction of EGR leads to lower engine-out CO emissions. Additionally, a leaner mixture further enhances this effect.

This can be explained by the fact that a more diluted mixture results in a lower in-cylinder temperature, which counteracts the CO_2 dissociation phenomenon - the primary mechanism for CO formation. Furthermore, in a lean mixture with EGR, a higher oxygen concentration is present during combustion, facilitating the oxidation of a greater amount of CO.

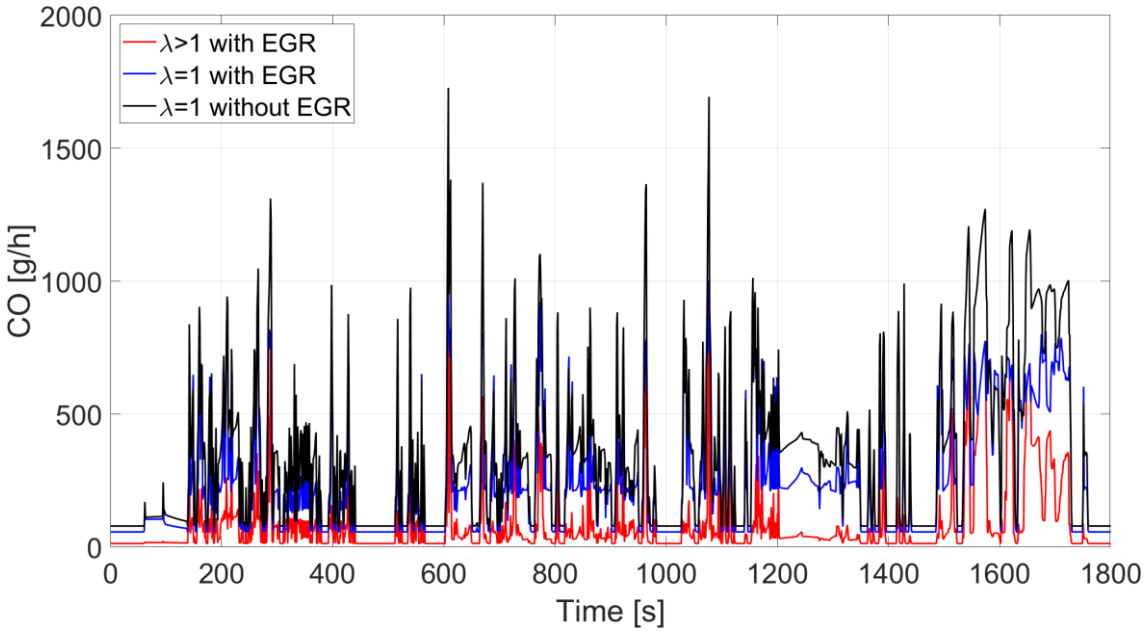

Figure 50 Instantaneous CO Emissions over the WLTC

The plot of engine-out cumulative CO emissions, shown in Figure 51, clearly demonstrates that the combination of a leaner mixture and the use of EGR leads to a massive reduction in CO emissions.

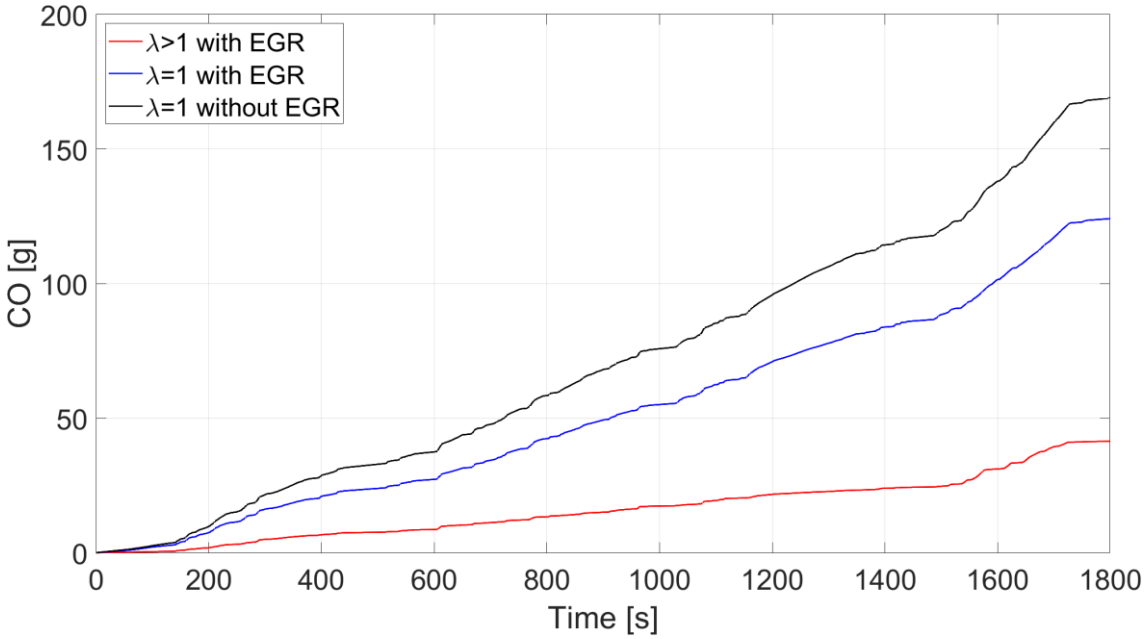

Figure 51 Cumulative CO Emissions over the WLTC

However, it should be noted that the simulation for the case of $\lambda > 1$ with EGR may be affected by computational errors, potentially leading to an underestimation of the cumulative CO emissions. As discussed in the previous section, this outcome may be attributed to the limitations of the trendline prediction, particularly at low engine speeds and low BMEP conditions.

Regarding HC emissions, it must be considered that this species is extremely sensitive to engine operating conditions and mixture composition. Due to lower in-cylinder temperatures, mechanisms such as flame quenching are more likely to occur with a diluted mixture, increasing the engine-out HC emissions. This effect is shown for the instantaneous HC emissions in Figure 52, where an increase in emissions is visible for mixtures containing a certain amount of EGR or those under lean conditions, compared to the stoichiometric mixture without EGR.

The greatest extent of HC production occurs with the stoichiometric mixture with EGR during fast-transient load requests, in accordance with the instantaneous fuel consumption trend. When a certain level of boost is required to entrain a higher intake flow rate, backpressure must increase, volumetric efficiency decreases, and, for the same amount of injected fuel, combustion tends to be less efficient, resulting in an increased concentration of HC in the exhaust.

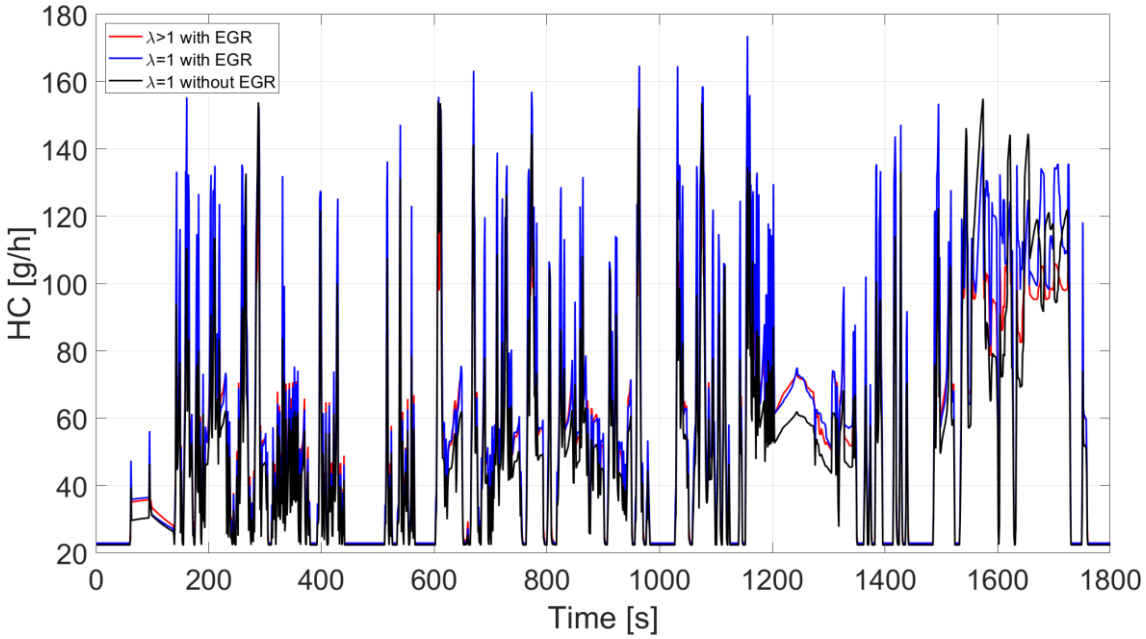

Figure 52 Instantaneous HC Emissions over the WLTC

In Figure 53, the trends of the cumulative emissions are shown, and it is evident how the grams of engine-out HC increase with the rise in λ and EGR. However, the increase in HC content is quite restrained, amounting to about 4 g when transitioning from a stoichiometric mixture without EGR to the same mixture composition but with EGR.

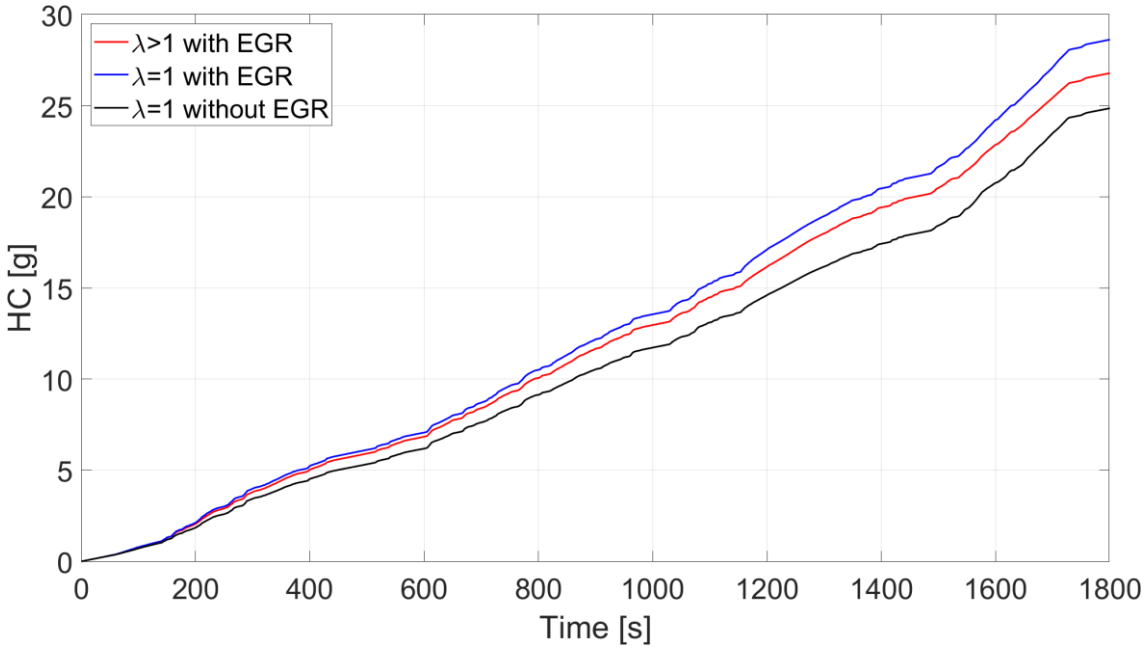

Figure 53 Cumulative HC Emissions over the WLTC

The NOx formation mechanism is based on three key factors: high temperatures, oxygen availability, and time for the reactions to occur. The implementation of EGR helps reduce the in-cylinder peak temperature, consequently lowering NOx formation. Therefore, as depicted in Figure 54, the engine operating conditions that use EGR show lower engine-out NOx emissions over the WLTC.

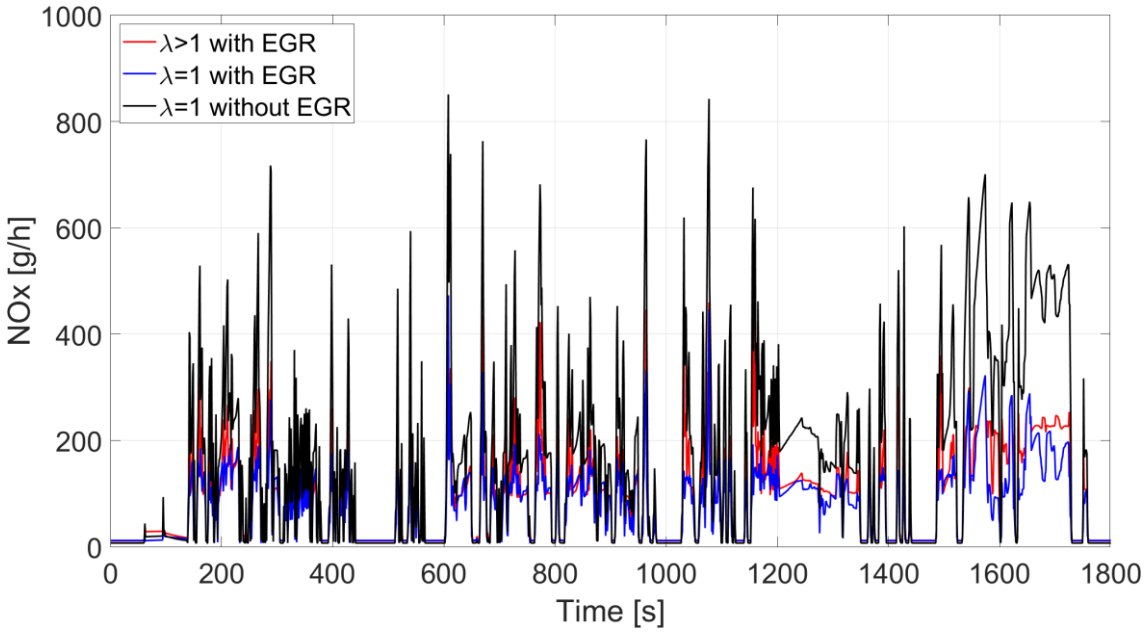

Figure 54 Instantaneous NOx Emissions over the WLTC

The same conclusion can be drawn from Figure 55, which shows the cumulative engine-out NOx emissions. By employing EGR with a stoichiometric mixture, the NOx emissions are reduced by about 53% compared to the case where EGR is not used.

The higher content of nitrogen oxides observed in the simulation with lean mixture operating conditions, compared to the case with λ equal to 1 with EGR, can be justified by the fact that a lean mixture contains a larger amount of O_2 and allows for more advanced spark advance (SA) without compromising knock suppression and combustion stability. Therefore, as the SA is advanced further, due to the higher pressure reached inside the combustion chamber, more work can be extracted from the engine, which is beneficial during high load requests over the driving cycle. However, at the same time, the temperature also increases, and this, combined with the higher oxygen content from the lean mixture, creates a more favourable environment for the NOx formation mechanism.

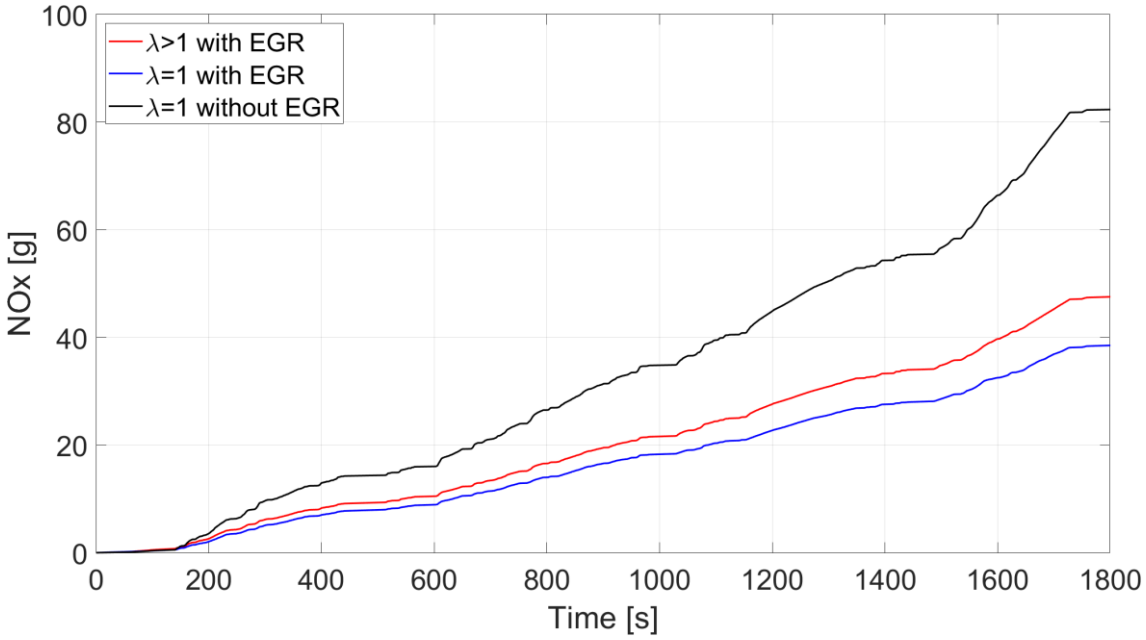

Figure 55 Cumulative NOx Emissions over the WLTC

4.4 Gearshift Optimization Results

The results of the gearshift strategy optimization are presented here. The results are analysed using a time distribution chart, which shows how much time the gearshift strategy spends at specific combinations of engine speed and load. The time distribution is represented as a bubble chart: the larger the bubble, the more time the engine spends in that specific operating condition, thereby impacting consumption and emissions.

The first analysed strategy is the baseline gearshift, reported in Figure 56. The baseline strategy covers a well-distributed portion of the BSFC map but never enters in the minimum fuel consumption region. This is the main reason for researching an optimization strategy.

The aim of the optimization procedure is to reduce not only fuel consumption but also CO emissions, without affecting the energy split between the electric and mechanical energy provided by the electric machine and the ICE, respectively.

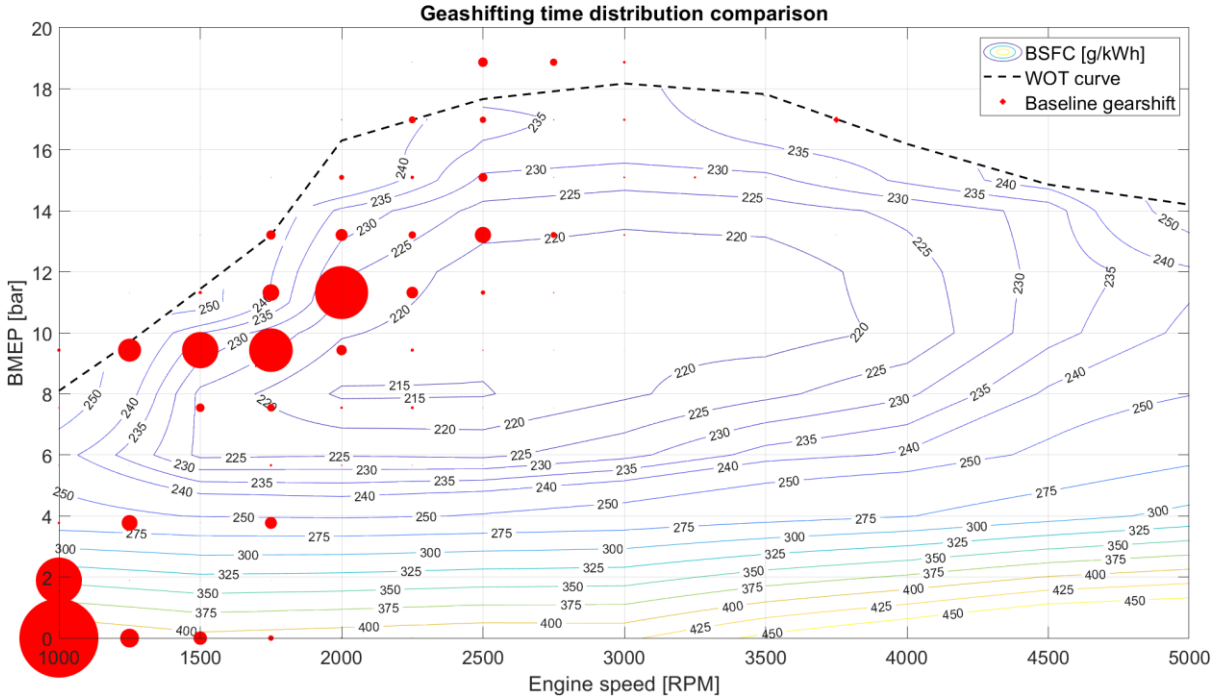

Figure 56 Baseline Gearshift Time Distribution

The algorithm used by FEV to find an optimized gearshift strategy fulfills the fuel consumption reduction requirement. In fact, it is evident that the FEV optimized strategy operates on a more concentrated portion of the BSFC map for most of the WLTC cycle. However, this strategy never reaches the minimum BSFC region.

A comparison between the baseline and FEV strategies is summarized in Figure 58. The FEV optimized strategy results in a reduction of the mechanical requested energy by about 10%, but this decrease does not correspond to a proportional reduction in fuel consumption, which only decreases by about 5%.

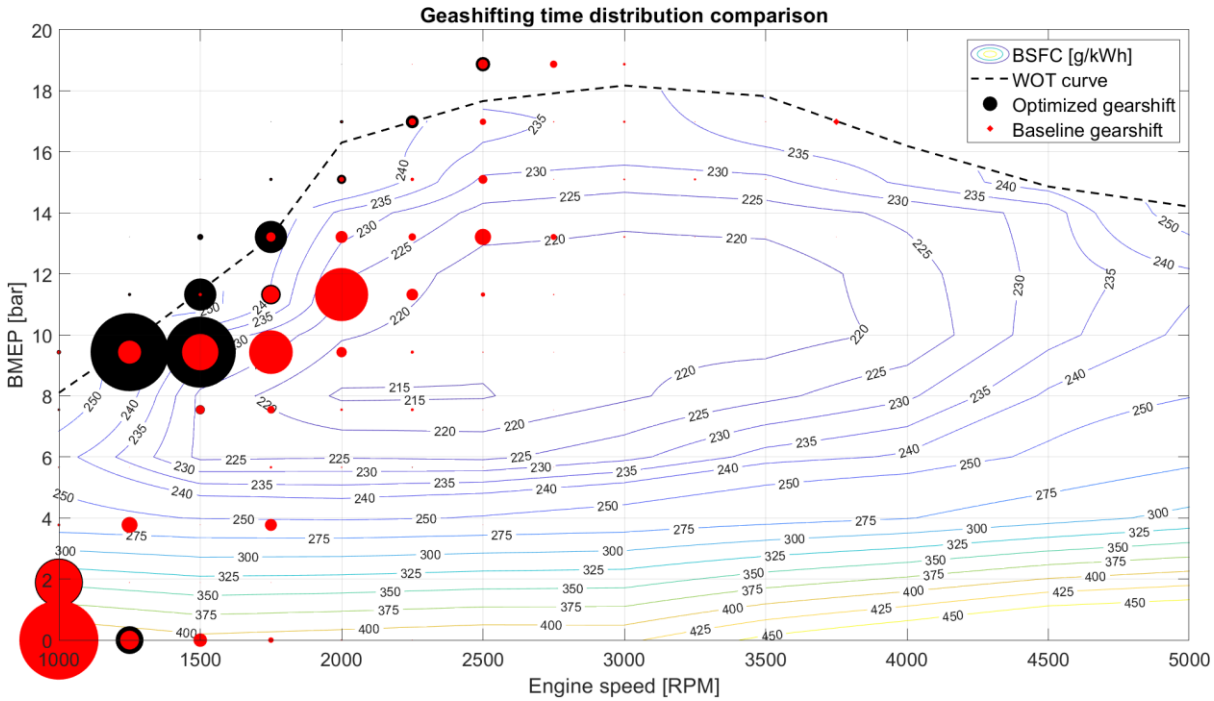

Figure 57 FEV Optimized Gearshift and Baseline Gearshift Time Distributions

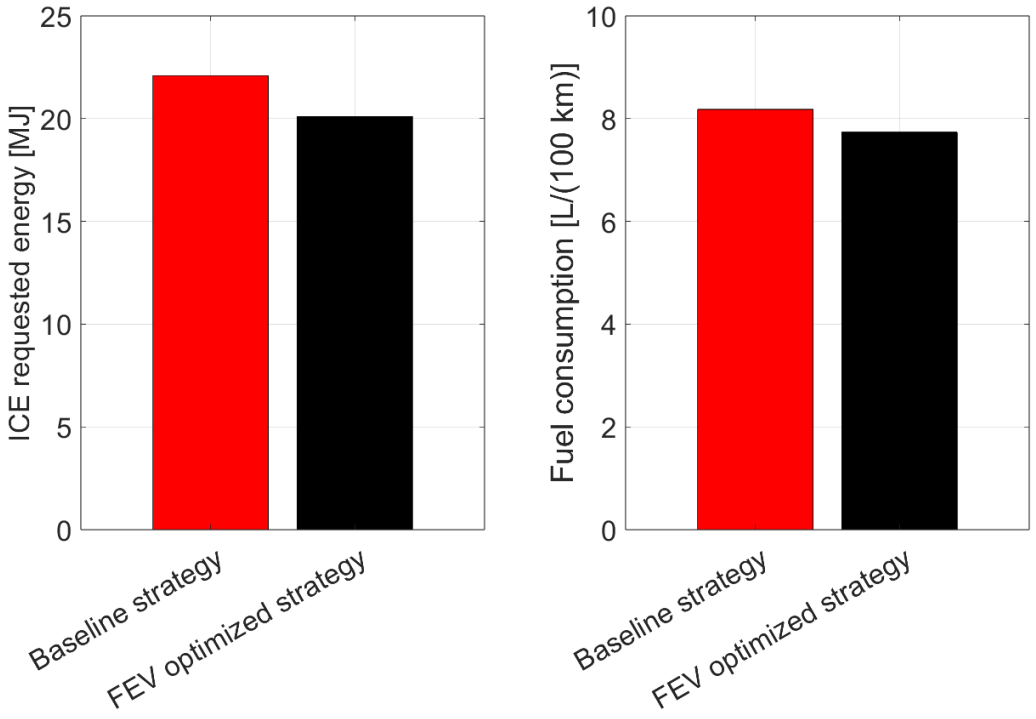

Figure 58 Mechanical Energy and Fuel Consumption Comparison for FEV and Baseline Strategies

Considering the engine-out emissions, CO increases by 10% when transitioning from the baseline strategy to the optimized one. However, as fuel conversion efficiency improves, HC and NOx tend to decrease with the implementation of the FEV optimized strategy.

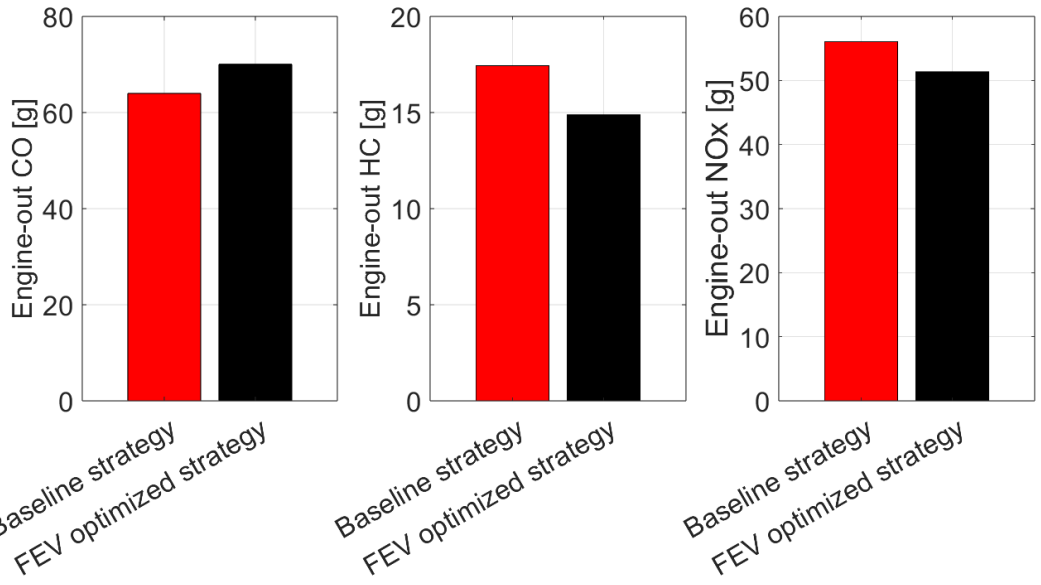

Figure 59 Engine-out Emissions Comparison for FEV and Baseline Strategies

From these results, it is clear that the two main objectives of the optimization procedure have not been completely achieved. Therefore, a new optimization strategy is implemented. The PoliTo optimization offers a gearshift strategy based on a simple rule-based algorithm that does not change the baseline energy demand, leaving the energy split between the ICE and the electric machine unaltered.

Figure 60 shows a comparison among the three analysed gearshift strategies. The PoliTo optimization covers a much wider area of the BSFC map compared to the previous strategies and never exceeds the full load curve. Moreover, this strategy spends most of the time in the minimum BSFC region, resulting in a significant improvement in fuel consumption.

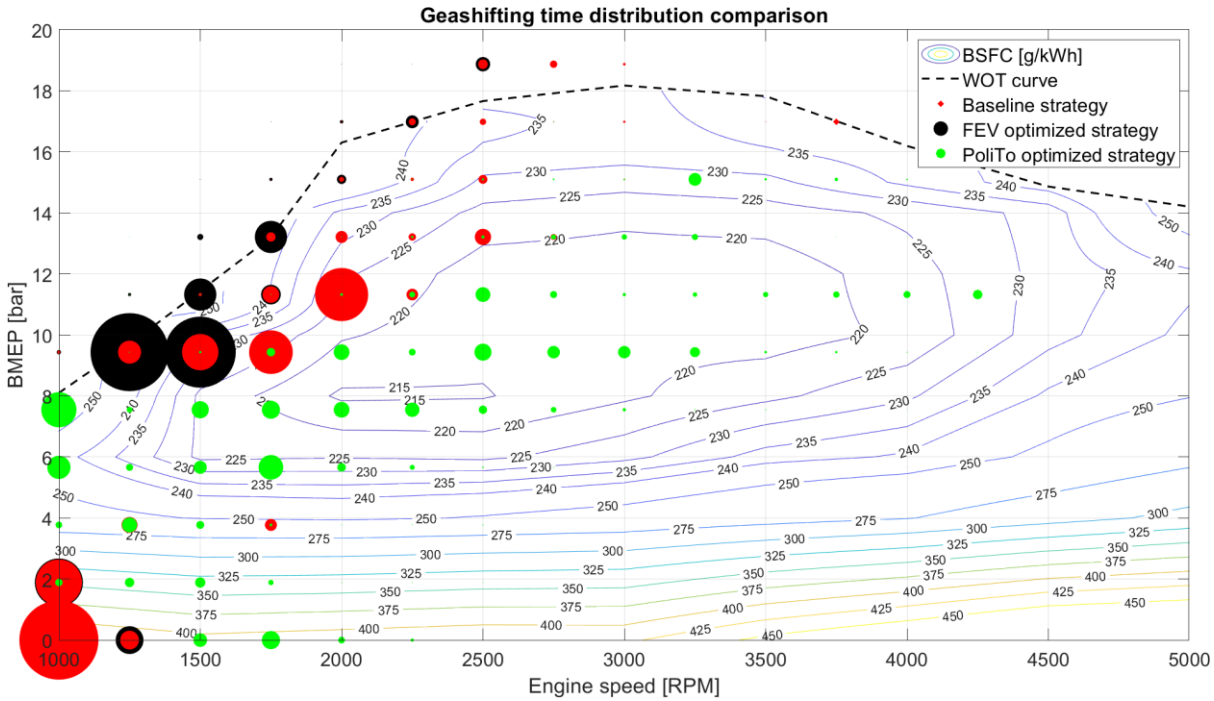

Figure 60 Baseline, FEV and PoliTo Gearshift Strategies Time Distributions

The PoliTo optimized strategy also leads to a decrement in fuel consumption of about 6,5%. For this strategy, this outcome gains more importance as the ICE requested energy is the same of the baseline strategy.

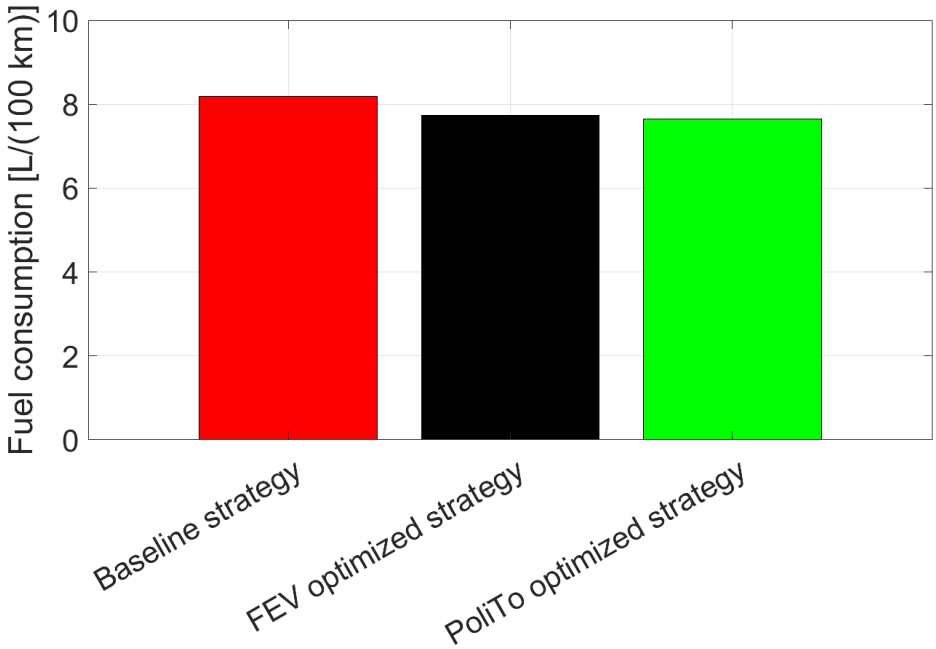

Figure 61 Fuel Consumption Comparison for Baseline, FEV and PoliTo strategies

Regarding the engine-out emissions, the adoption of the PoliTo strategy leads to a reduction of CO by about 47% compared to the baseline strategy. Therefore, the main objectives of the optimization procedure are fully achieved.

There is an increase in engine-out HC for the PoliTo strategy, but the increment is around 5 g compared to the baseline strategy over the entire WLTC.

Engine-out NOx remains at the same level as the FEV optimized strategy, indicating a decrease of about 8% compared to the baseline gearshift.

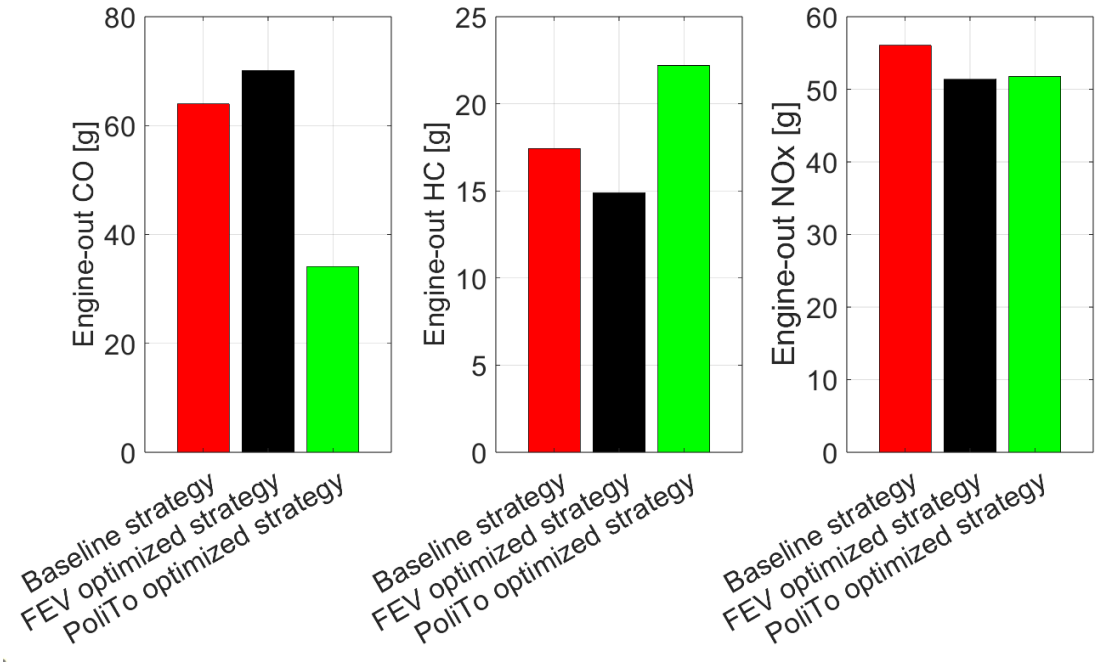

Figure 62 Engine-out Emissions Comparison for Baseline, FEV and PoliTo Strategies

4.5 Conclusions

In this chapter, the real driving cycle simulation of the PHOENICE prototype engine was presented. The first step involved collecting the necessary data, which consisted of engine steady-state maps for fuel consumption, CO, HC, and NOx emissions obtained from the PoliTo tests. These maps were then extended using a trendline prediction tool to cover a broader range of load and speed conditions, more closely matching the WLTC requirements.

The core of this chapter was the discussion of the simulation results - both instantaneous and cumulative - which served as a basis for comparison with the driving cycle test cell outcome. The simulation was carried out in MATLAB using a simple interpolation script that produced the results discussed, representing the ideal fuel consumption and emissions that the engine could achieve over the WLTC.

The second part of this research activity aimed to optimize the gearshift strategy to reduce engine fuel consumption and emissions. In particular, two optimizations of the baseline strategy were studied: the first was provided by FEV, and the second was a rule-based optimization algorithm developed at PoliTo. The best results were obtained from the PoliTo gearshift strategy, which met the targets without altering the vehicle's mechanical and electrical power split.

5. Engine Digital Twin Development

5.1 Introduction

The primary objective of this chapter is to illustrate the steps involved in developing a digital twin of the PHOENICE prototype engine. The digital twin is represented by a model of the engine that was built and calibrated in GT-Suite. Its primary purpose is to support the steady-state calibration of the high-efficiency spark-ignition ICE at the Polytechnic of Turin.

Therefore, the correlation procedure for the engine model is of paramount importance in developing a reliable simulation platform that fully exploits the various features introduced in the PHOENICE project. This correlation is performed using the experimental data acquired by IFPEN during the first engine steady-state calibration.

A further step in developing the engine digital twin is the introduction of a predictive combustion model, which enables the prediction of the in-cylinder burn rate, emissions, and knocking occurrence. This approach to combustion clearly explores the prototype engine's features without the limitations of an imposed combustion process, thereby extending the scope of the analysis.

The optimal combustion parameters of the predictive model are obtained as results of an optimization process that relies on calibration and validation based on a simple turbulence model.

5.2 Methodology

The development of the engine digital twin can be divided into two procedures, each with its specific methodology: the correlation of the complete engine model and the implementation of the predictive combustion model.

However, both procedures are fundamentally based on the experimental data acquired at the IFPEN benchmark during the steady-state calibration of the

prototype engine, represented by the eleven engine operating points and combinations of air-fuel ratio and EGR rate.

5.2.1 Model Correlation

The model built in GT-Suite for the simulations is shown in Figure 63. It clearly illustrates how all the engine components are modeled as different subassemblies, connected together to form the complete engine. The core of the model is the Cylinders subassembly, which contains the cylinders along with the exhaust and intake valves. It is important to underline that the valve lift within the model is managed through a specific subassembly, which starting from the imposed electrical valve lift opening (IVO) and closure (IVC), interpolates the correct IVO and IVC for the considered operating engine point. The intake line is divided into two sections: the low-pressure line and the high-pressure line, with the latter serving as the output of the compressor. The exhaust line includes the entire system as installed at the PoliTo facility. To complete the model, the integrated exhaust manifold, EGR loop, and turbocharger are incorporated.

The ECU is represented within the model by the Utility subassembly, which contains various controllers. In particular, these include:

- A throttle valve controller, provided by a GT built-in controller, which regulates the throttle valve opening to maintain the correct intake line pressure (p2) during naturally aspirated operations.
- A turbo controller, implemented as a PID controller. This controller adjusts the VNT rack to maintain the correct boost pressure when required, considering constraints such as compressor surge, maximum turbocharger speed, and turbine inlet pressure and temperature.
- A knock controller, represented by a PI controller, which detects and suppresses knock onset by analysing the average burn duration (0-50) and the average in-cylinder maximum pressure.
- An EGR controller, implemented as a GT built-in model-based controller, whose purpose is to regulate the EGR valve to ensure the correct amount of EGR is admitted into the loop.

The choice between throttle and turbo actuation is managed by an Event Manager. This block determines the optimal actuation strategy based on logical criteria to achieve the correct intake plenum pressure (p5).

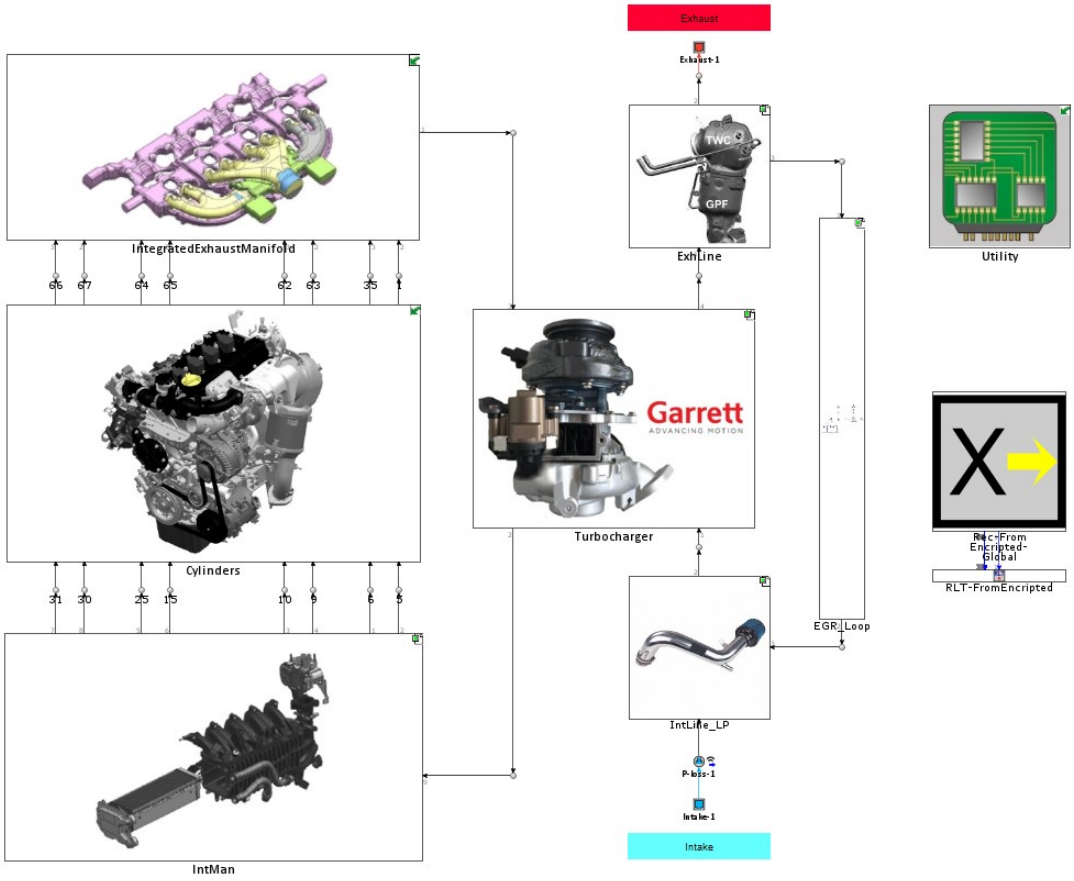

Figure 63 Complete Engine Model

Sensors are placed along the different lines to monitor engine conditions, specifically measuring pressures, temperatures, and mass flow rates in the various subassemblies.

During the correlation procedure, some adjustments to the complete engine model are necessary to achieve simulation results that satisfactorily match the experimental data.

In the cylinder subassembly, the discharge coefficients of the intake valves are adjusted, as they influence boost pressure. To achieve the correct boost level, these coefficients are reduced to 80% of their original values. On the exhaust side, the valve cam timing angle is changed from 0 to 5 °CA to properly phase the lift array within the cycle and more accurately simulate the exhaust phase.

To better characterize the intake line, an orifice is inserted before the throttle valve, and its discharge coefficients are appropriately tuned. This improves the pressure drops within the intake line. Additionally, the duct geometries are corrected by extrapolating appropriate values from the intake line CAD model.

A similar procedure is applied to the exhaust line. In particular, the discharge coefficients of the orifice upstream of the EHC are tuned to better simulate the backpressure at the turbine outlet (p4).

The turbo group maps are enhanced by using heat-corrected extrapolated maps provided by FEV. This approach results in a more accurately defined turbocharger, and its simulation more closely aligns with real outcome.

For the correlation procedure, the event manager is configured to control the air mass flow rate, ensuring that this parameter exactly matches the experimental data. Additionally, the model burn rate is set according to the CPOA analysis, and the injected mass of fuel is imposed to comply with the experimental test cell data.

To ensure accurate simulation results, an iterative process between the engine and CPOA models must be carried out. The complete model outputs residual fraction, as well as liner, head, and piston temperatures, which are extrapolated and used as boundary conditions in the CPOA. A new closed volume simulation is then performed, during which the compression ratio and heat transfer multiplier are adjusted to best match the measured and simulated cycles. These updated values, along with the revised burn rate, are reinserted into the complete model, and the iterative process continues until the simulation outcomes converge.

To assess the effectiveness of the correlation procedure, several key parameters are continuously monitored. Particular emphasis is placed on the air mass flow rate, EGR rate, maximum combustion pressure and its corresponding crank angle, as well as data related to the turbo group. Additionally, pressure and temperature values before and after the throttle valve are closely observed.

5.2.2 Predictive Combustion Model Implementation

The first step in integrating the predictive combustion into the complete model is the study of the turbulence generated by the innovative Swumble™ in-cylinder motion, whose scope is to enhance the mixture motion within the cylinder while mitigating the negative effects on turbulence associated with the dual dilution approach.

The turbulence model is examined through a Three Pressure Analysis (TPA) model in GT-Suite. For this analysis, estimating the residual fraction and trapping ratio is not required; however, three measured pressures – intake, cylinder and exhaust - are necessary. As a result, the accuracy of this simulation is improved compared to

a CPOA model, though the main drawback is the additional experimental data required for the simulation. The model is shown in Figure 64.

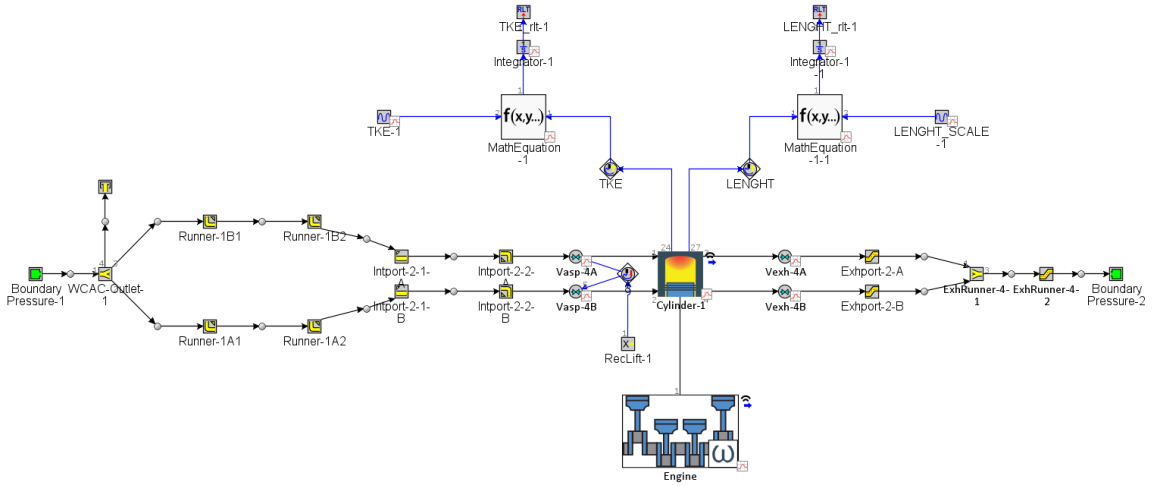

Figure 64 TPA Model

The TPA model is used to calculate Turbulent Kinetic Energy (TKE), turbulent length scale and mean flow strength, key parameters that define the turbulence characteristics of the PHOENICE prototype engine.

The reference experimental data of the turbulence model are obtained from a cold-flow 3D CFD simulation, which originates from the Swumble™ initial research activity. This simulation was used to investigate the flame propagation for Early and Late Intake Valve Closure Miller strategies and was conducted for specific engine operating conditions (2000 RPM, no fuel injection, no combustion).

Once the turbulence parameters of the engine are identified, the implementation of the predictive combustion model proceeds with its calibration and validation.

The predictive combustion model relies on the accurately estimating laminar and turbulent flame speeds. Therefore, an in-depth analysis of the parameters influencing these two speeds is essential to ensure precise simulation results.

The turbulent flame speed must correctly describe the transition between laminar and turbulent region. Its formulation is presented in (1)

$$S_T = C_s u' \left(1 - \frac{1}{1 + \frac{C_k {R_f}^2}{{L_t}^2}} \right) \quad (1)$$

where C_s is the turbulent flame multiplier, u' is the turbulent intensity, C_k the flame kernel growth multiplier, R_f the flame radius and L_t the turbulent length scale.

Instead, the laminar flame speed (S_L) limits the gas entrainment, and it is function of the dilution coming from residuals and enleanment. In particular, the dilution effect is considered as described in (2)

$$f(dilution) = 1 - 0{,}75 * DEM\ (1 - (1 - 0{,}75 * DEM * Dilution)^7) \quad (2)$$

in which DEM represents the Dilution Effect Multiplier and Dilution is the residuals mass fraction in the unburned zone.

The burn rate is influenced by both velocities and is proportional to the amount of unburned mixture behind the flame front, divided by a time constant τ, calculated as in (3)

$$\tau = \frac{\lambda}{S_L} \quad (3)$$

where λ is the Taylor length scale.

The burn rate, laminar flame speed, and turbulent flame speed are functions of some parameters that requires tuning, specifically:

- Flame Kernel Growth Multiplier
- Turbulent Flame Speed Multiplier
- Taylor Length Scale Multiplier
- Dilution Effect Multiplier.

The calibration process for predictive combustion focuses on optimizing these multipliers to ensure accurate simulation results. The optimization of these parameters is conducted using the GT-Suite built-in optimizer. The engine model

used in the optimization process is a CPOA model, where the combustion object is configured as the predictive combustion model, with imposed spark timing serving as the boundary condition. In particular, the objective function is designed to minimize the burn rate RMS error and the algorithm used is a genetic algorithm that runs for 40 generations, testing a total of 401 designs.

The engine operating points for the calibration procedure are selected to cover a wide variety of speed and load combinations within the IFPEN tested operating conditions. For each engine point, three different combinations of EGR rate and air-fuel ratio are considered, resulting in a calibration procedure based on 33% of the total IFPEN tested data. This selection of calibration points allows for a thorough evaluation of the influence of the dual dilution combustion approach, aggressive Millerization, and Swumble™ in-cylinder motion on the combustion process of the prototype PHOENICE engine.

The calibration optimization process is divided into two phases. First, the four multipliers are optimized using sweep cases, resulting in four parameters that are consistent across all calibration points. The second step consists of a separate optimization run for the DEM, with the other three parameters fixed at the values obtained in the first step, allowing for a different DEM to be obtained for each calibration condition. This approach was adopted because the various implementations of the PHOENICE project significantly influence the in-cylinder residual fraction, which in turn affects the DEM. Therefore, by running a second independent optimization, we ensure that the DEM is properly tuned as a function of the residuals for all optimization cases, improving the objective function definition.

Passing to the validation of the predictive combustion model, it is necessary to find a mathematical function that estimates the DEM for the test points not included in the calibration procedure. Using MATLAB's curve fitting tool, a 3D interpolating surface is identified to establish a reliable model for accurately calculating the DEM. This surface is obtained as a function of the residual fraction, air-fuel ratio, and DEM of the calibration points, as shown in Figure 65.

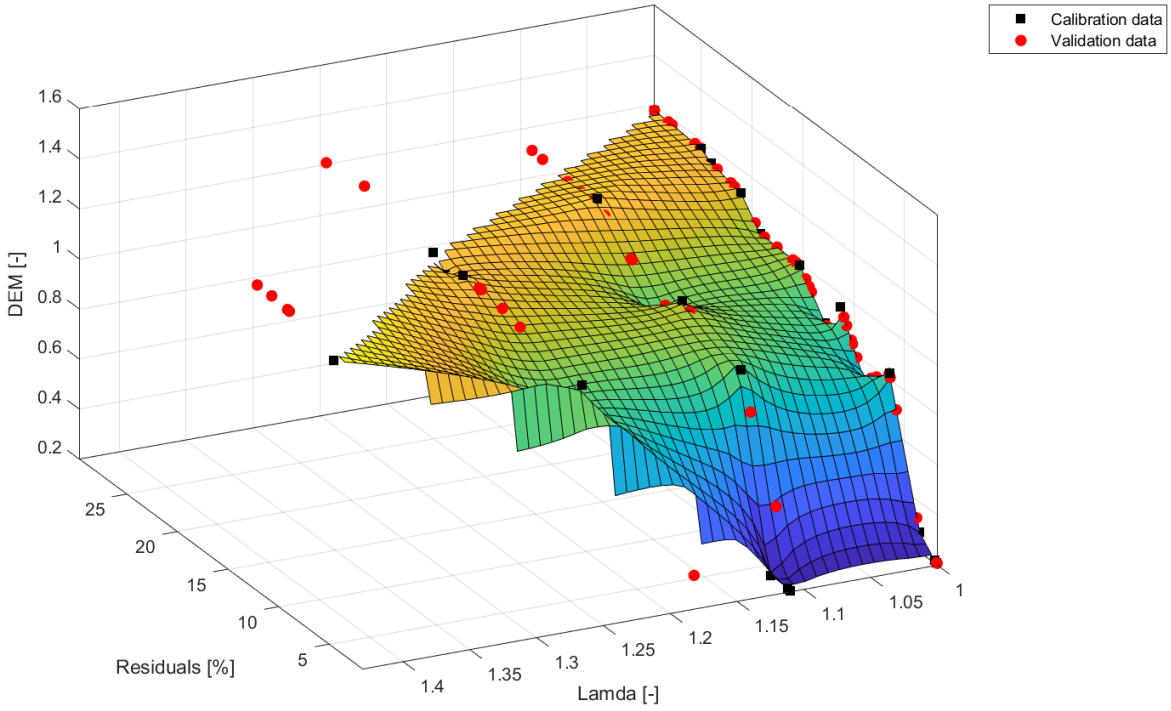

Figure 65 DEM Fitting Surface

Based on the interpolating surface, the DEM for the remaining IFPEN-tested operating conditions is predicted, allowing validation to proceed with the simulation of the entire test data set using the predictive combustion model. In this case, the validation is conducted using the complete engine model, which incorporates the same predictive combustion model used during the CPOA calibration procedure.

5.3 Digital Twin Development Results

In this paragraph, the results of the model development are presented. First, an overview of the correlation plots for the different monitored quantities is provided for the final version of the model. Then, some pressure cycles are reported to assess the quality of the correlation procedure. Finally, the results of the predictive combustion model are shown.

5.3.1 Correlation Plots

Correlation plots are an important tool for evaluating the accuracy of the procedure. They illustrate the relationship between two variables, which, in our

case, are represented by the experimental and simulated quantities. Specifically, the key parameters monitored in the model are:

- Air Mass Flow Rate
- EGR Rate
- Maximum in-cylinder pressure during the cycle and its corresponding crank angle
- Pressure and Temperature at the Compressor Outlet
- Pressure and Temperature at the Intake Plenum
- Pressures and Temperatures at the Turbine Inlet and Outlet
- Turbocharger Speed.

It is important to note that the model correlation is performed using an imposed burn rate from the CPOA model. Moreover, the controllers are set to target the intake air mass flow rate. To ensure reliable simulations, the Friction Mean Effective Pressure (FMEP) and the injected fuel mass are set based on experimental data.

Regarding the Air Mass Flow Rate, it is visible in Figure 66 that the controller completely fulfils the implemented target. In fact, all the correlation points lie on the reference line.

About the volumetric efficiency of the engine, Figure 67 depicts optimal correlation results for most points. However, the volumetric efficiency is underestimated at low engine loads, while the opposite trend is observed at high loads. This effect results from an imprecise estimation of the pressure inside the intake plenum (p5).

The complete model accurately simulates the EGR rate, as shown in Figure 68. A few points fall outside the $\pm 5\%$ error tolerance relative to the reference. Nonetheless, the reliable performance of the EGR controller is confirmed. To improve controller stability and prevent misleading oscillations, engine points with an EGR rate below 5% - indicative of internal EGR due to the gas exchange process - are assigned an EGR value of 0.

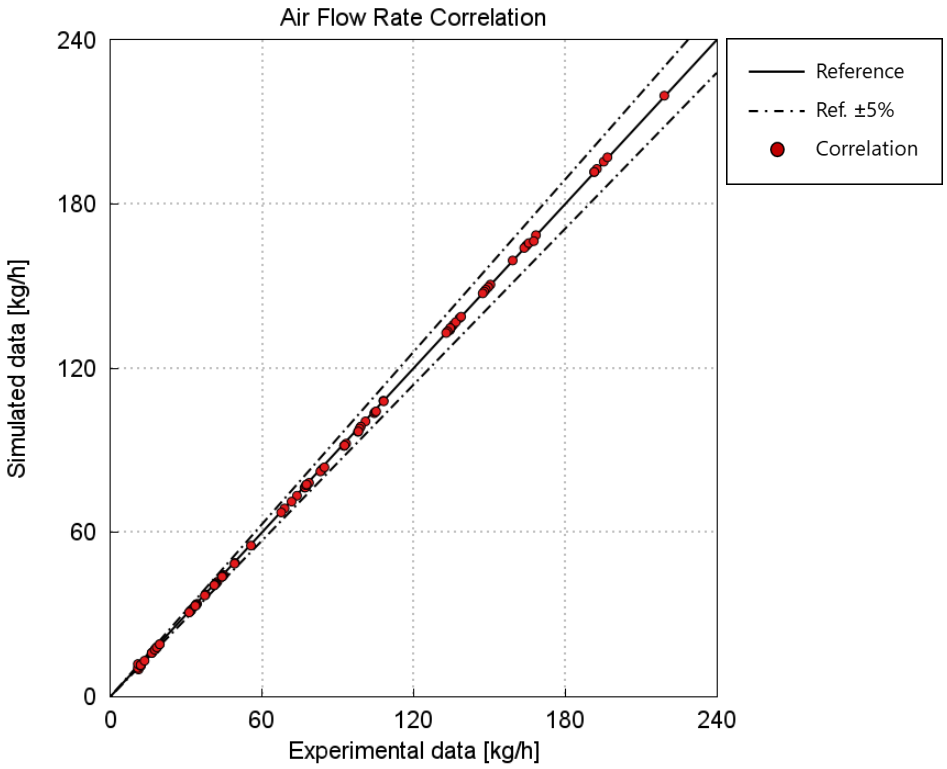

Figure 66 Air Flow Rate Correlation

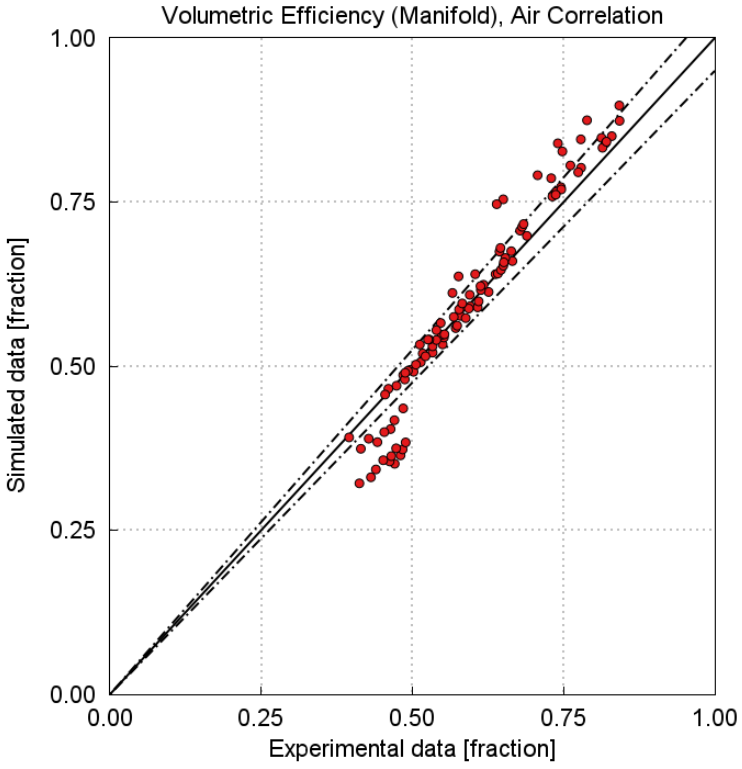

Figure 67 Volumetric Efficiency Correlation

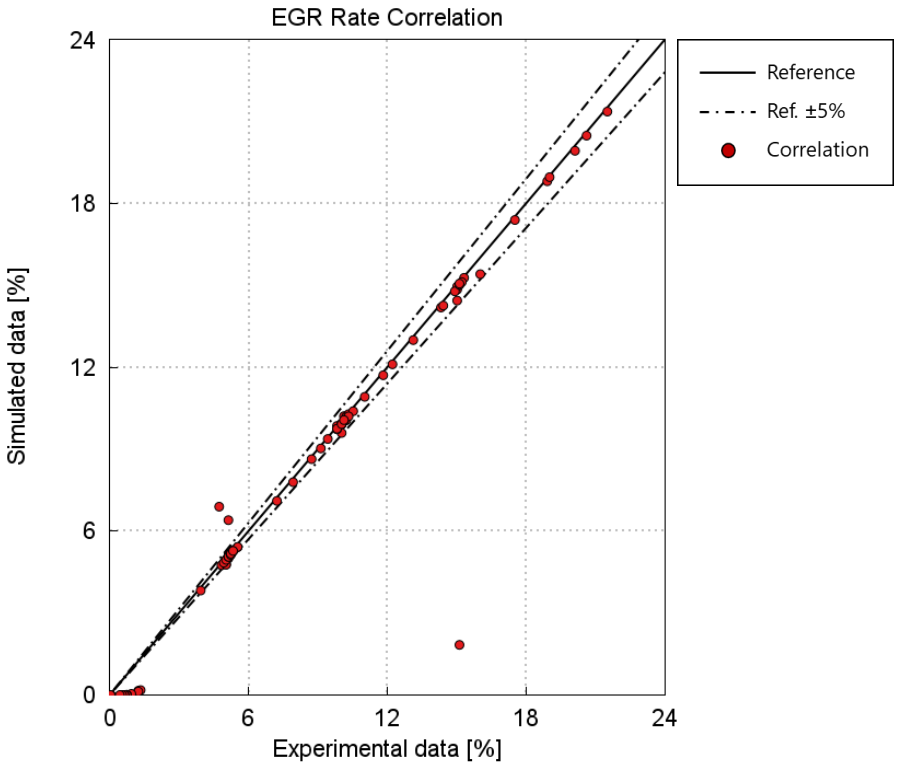

Figure 68 EGR Rate Correlation

To inspect the combustion outcome, the in-cylinder maximum pressure within the cycle and the corresponding crank angle are considered, since the burn rate is imposed from the CPOA.

Figure 69 shows the correlation of the cycle maximum pressure. In most cases, the values fall within the accepted error boundaries. A slight overestimation is observed for low-speed, low-load engine points, primarily due to the air mass flow rate trend.

The angle at which the maximum pressure occurs is satisfactorily correlated for all the tested cases, as illustrated in Figure 70.

To analyse the correctness of the turbocharger behaviour simulated by the complete model, various parameters were monitored.

The pressure and temperature at the outlet of the compressor are shown in Figure 71 and Figure 72, respectively. Regarding p2, an optimal trend can be observed. In particular, for low-load engine points, this pressure is regulated by the throttle controller, while when boost is required, p2 matches p5. In both cases, the event manager ensures the correct pressure is maintained.

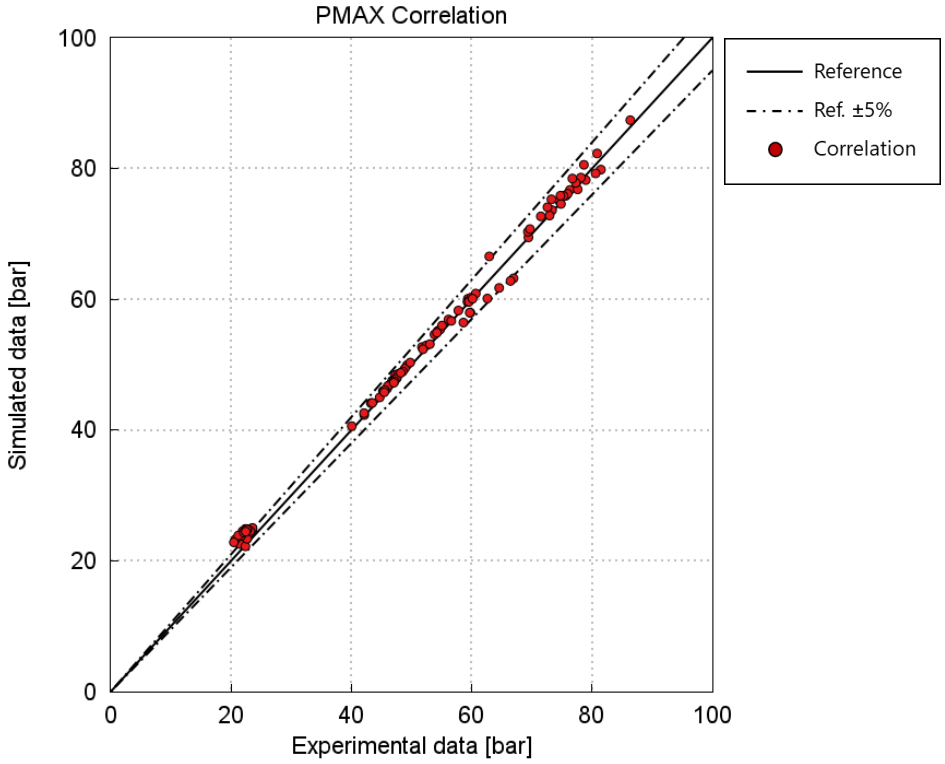

Figure 69 In-cylinder Maximum Pressure

As for T2, there is an underestimation of the temperature for most engine points. This discrepancy may be due to differences in the measurement points between the experimental acquisitions and the simulation monitoring.

Considering the boost pressure (p5), Figure 73 shows that most simulated engine points remain within the acceptable error range of ±5% relative to the reference values. However, a certain level of overestimation is present for low-speed and low-load engine points.

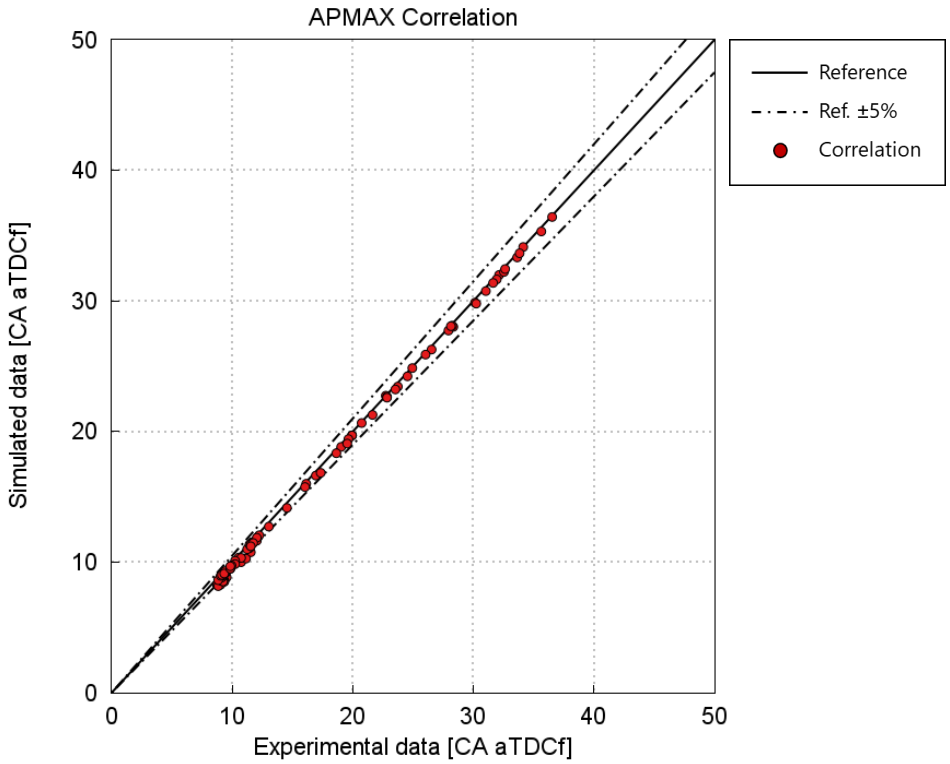

Figure 70 Crank Angle of the Maximum Pressure

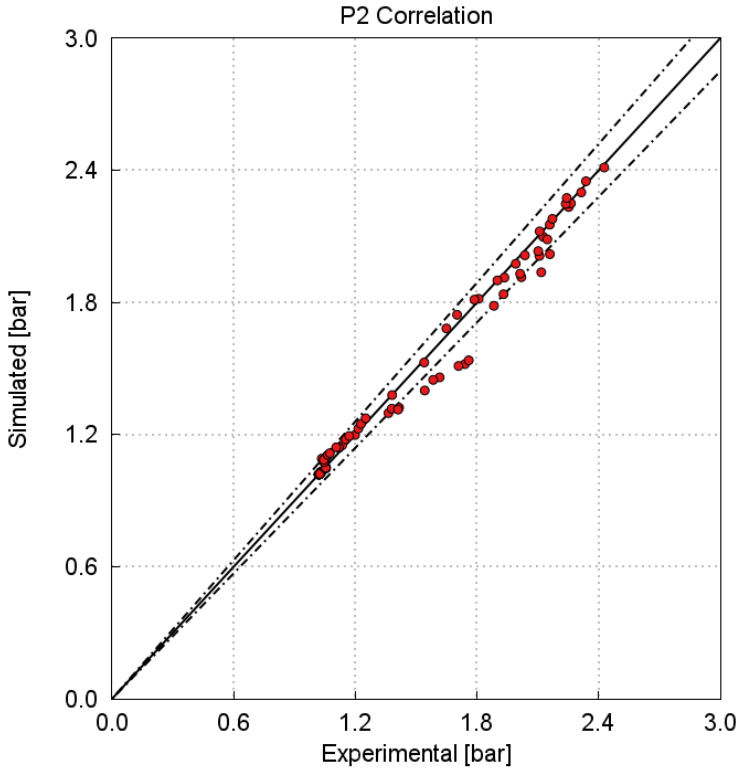

Figure 71 Compressor Outlet Pressure Correlation

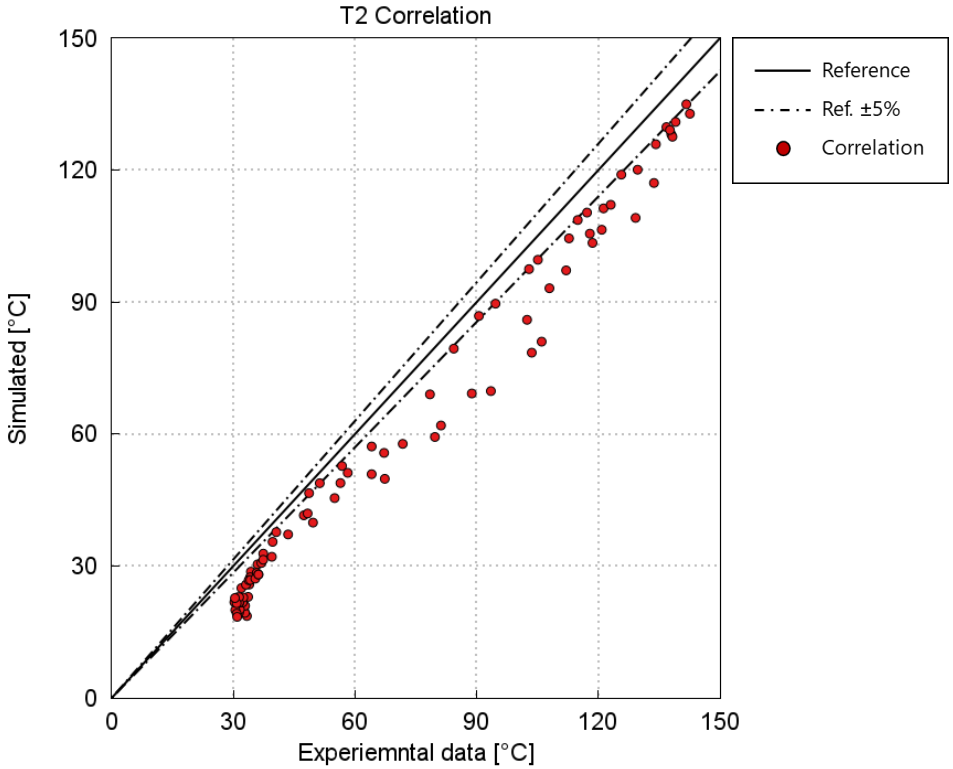

Figure 72 Compressor Outlet Temperature Correlation

Regarding the temperature inside the intake plenum (T5), a satisfactory level of correlation is achieved, indicating that the controller of the turbocharger is functioning properly.

On the turbine side, Figure 75 clearly shows an underestimation of the inlet pressure, particularly for medium-to-high engine speeds and loads. This results in an increased pumping work in the simulated engine model compared to the experimental outcome. A possible cause of this underestimation could be the discharge coefficients of the exhaust valves, which are imposed in the model, though no information is provided about their experimental measurement region. Another plausible cause may be the flow splits in the pipes of the integrated exhaust manifold, as accurately replicating the real geometry in the complete model was challenging.

Similar conclusions can be drawn when considering the temperature at the turbine inlet (T3), shown in Figure 76, for which the model simulation introduces a clear overestimation.

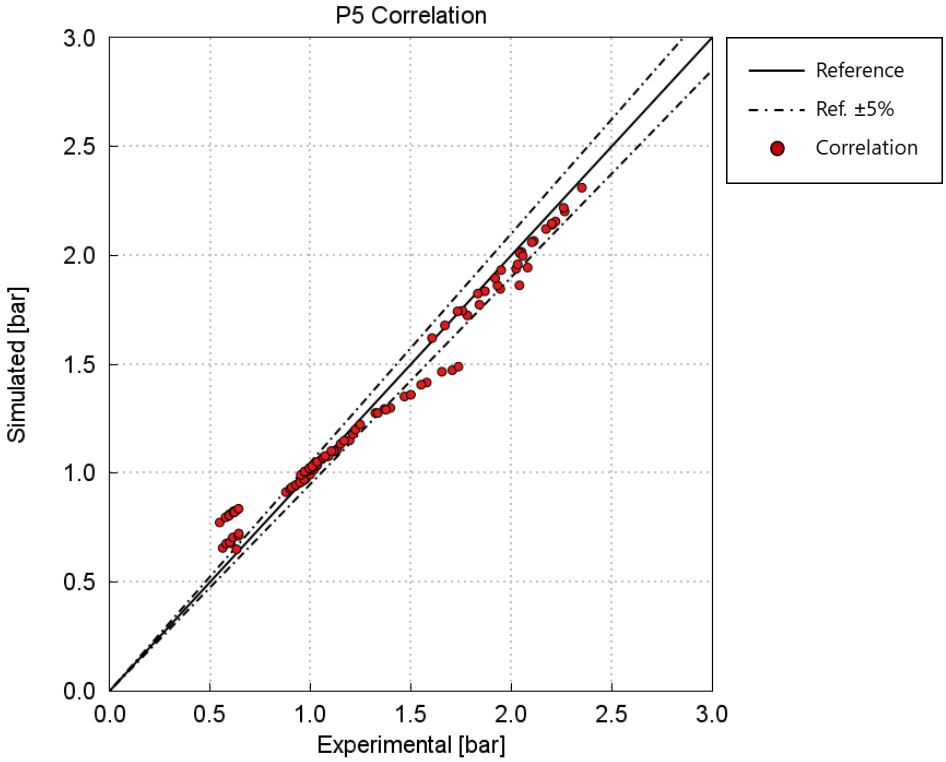

Figure 73 Intake Plenum Pressure Correlation

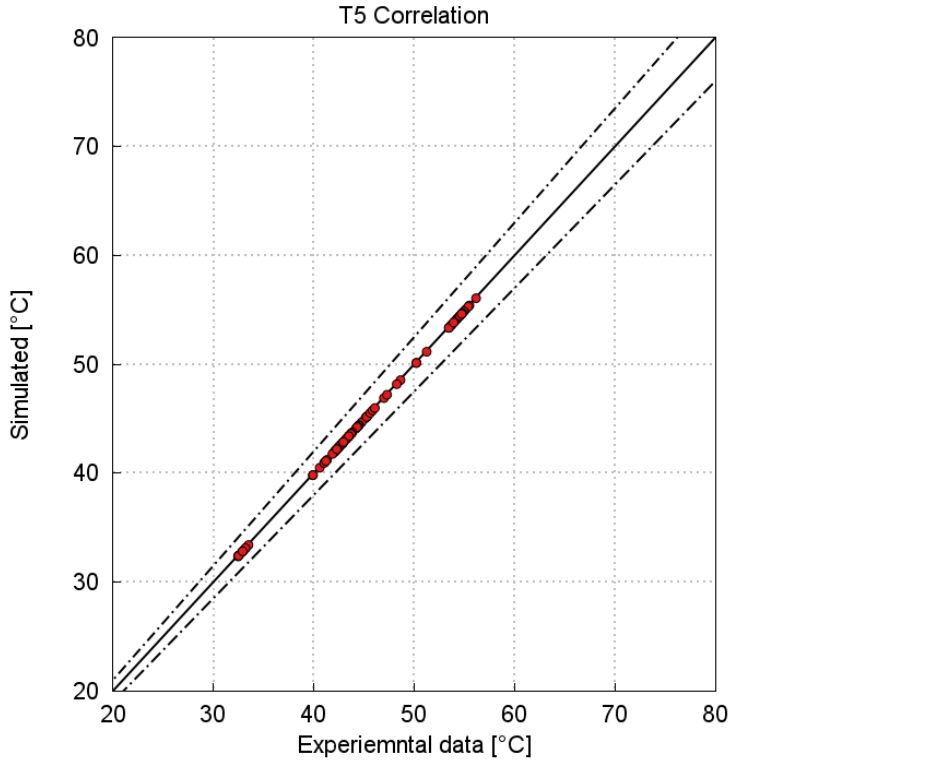

Figure 74 Intake Plenum Temperature Correlation

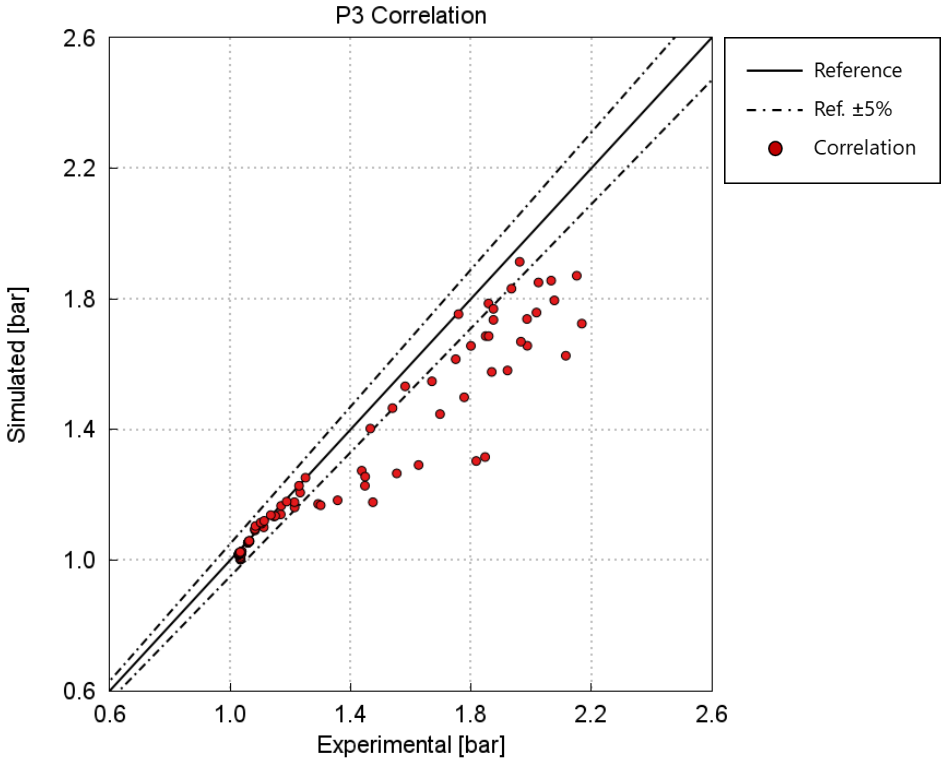

Figure 75 Inlet Turbine Pressure Correlation

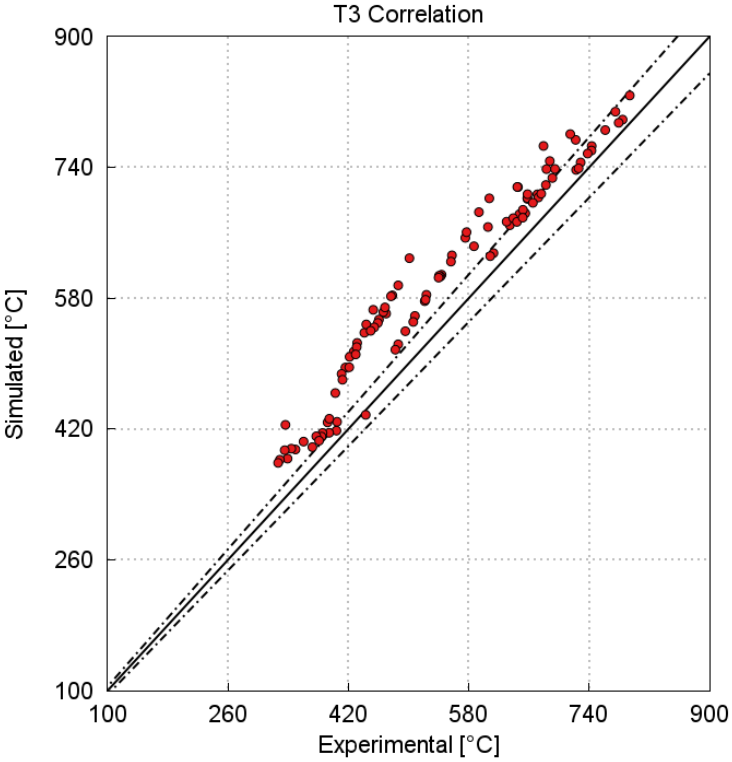

Figure 76 Inlet Turbine Temperature Correlation

Regarding the turbine outlet, an optimal correlation between the model outcome and the experimental data for the pressure (p4) can be assessed. This result is due to the improved pressure drops introduced in the model by fine-tuning the orifice discharge coefficients.

For the temperature at the turbine outlet (T4), however, a clear overestimation is evident. This may be due to the different exhaust line configuration in the complete model - which considers both close-coupled and underfloor solutions - compared to the IFPEN setup, which implemented a flap to simulate the entire exhaust line. Therefore, while the pressure drops can be adjusted, some differences in temperature are expected.

The final consideration for the turbo group concerns its speed, as presented in Figure 79. Some engine points lack experimental acquisition; therefore, these points appear on the left side of the chart, corresponding to an experimental value of 0. For engine points operating at low speeds, the controller's failure is visible, likely due to the turbo maps not covering corrected speeds below 6000 RPM, which affects the speed interpolation. At high-speed conditions, an underestimation is present, mainly caused by the underestimation of p5.

Finally, regarding mean effective pressure, the correlation plot of the Gross IMEP is illustrated in Figure 80, showing that an optimal correlation is achieved for all cases.

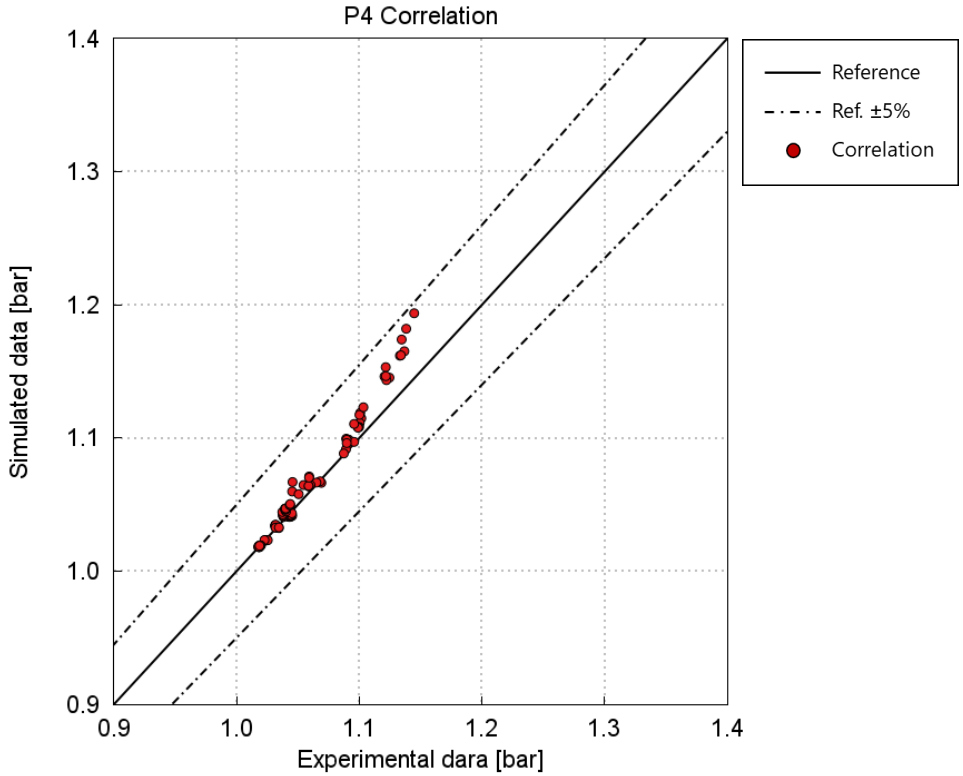

Figure 77 Turbine Outlet Pressure Correlation

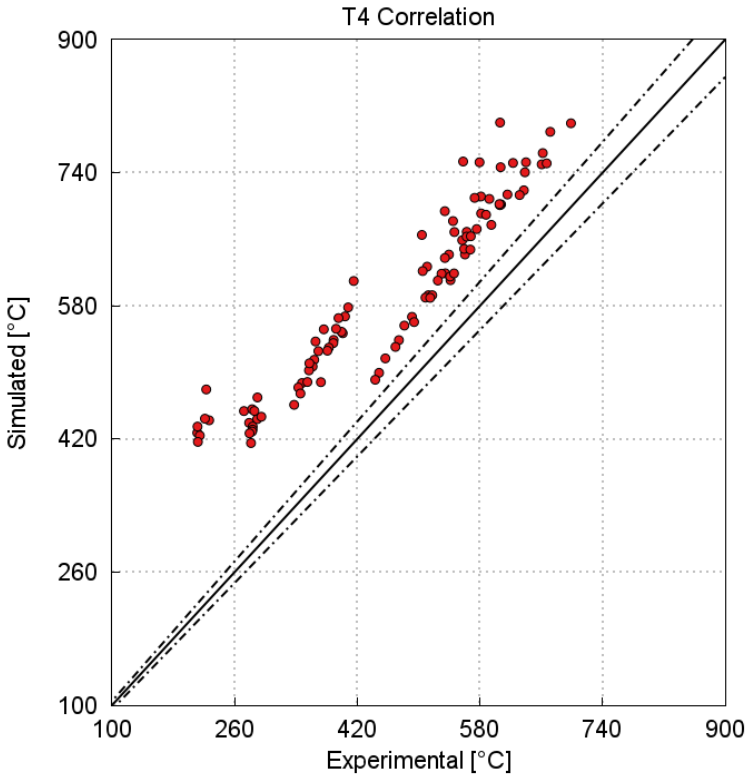

Figure 78 Turbine Outlet Temperature Correlation

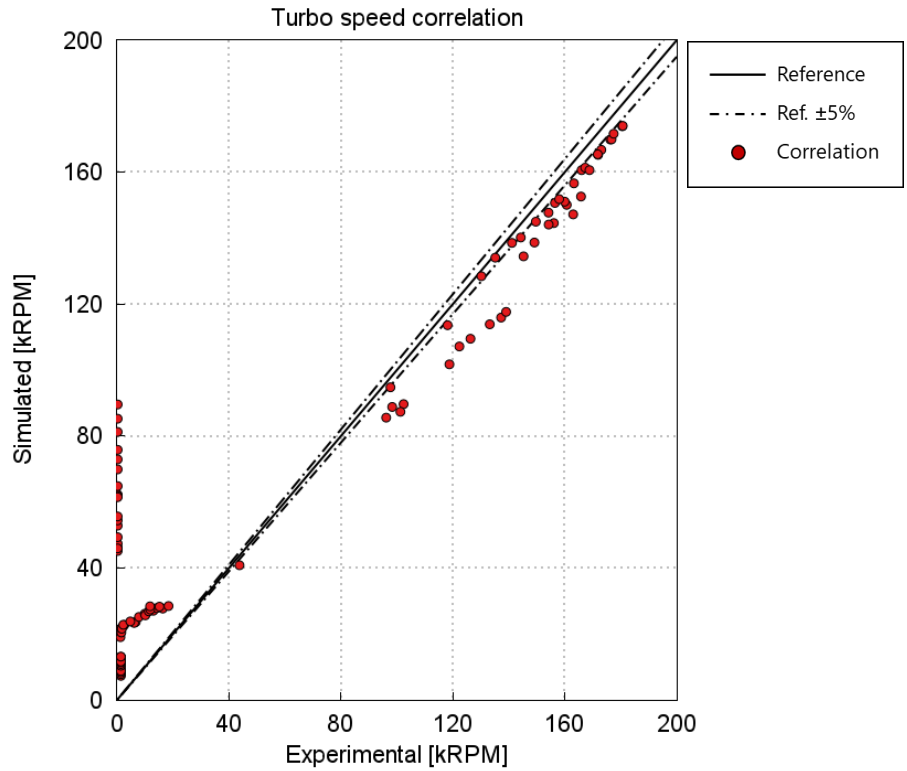

Figure 79 Turbocharger Speed Correlation

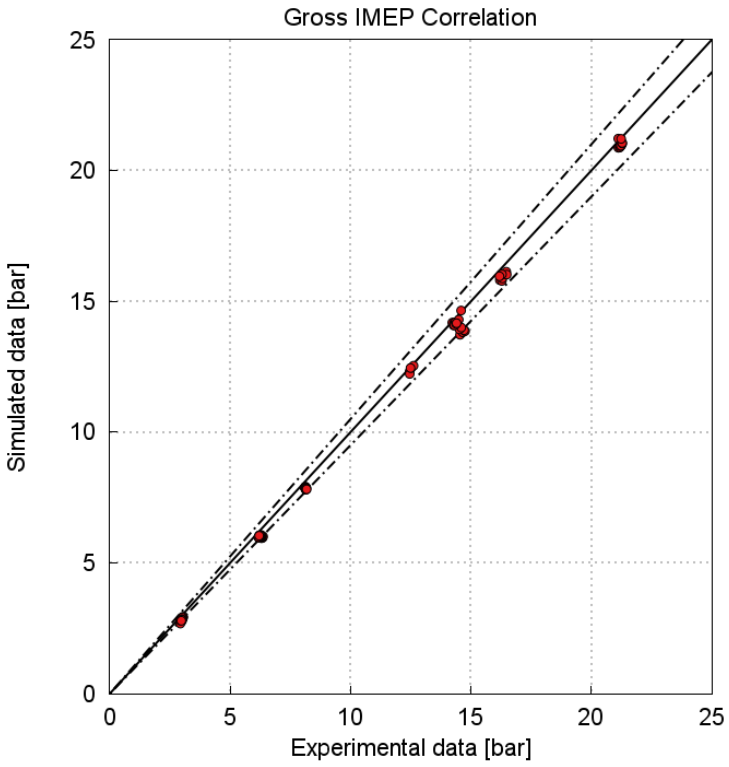

Figure 80 Gross IMEP Correlation

To better inspecting the quality of the correlation procedure, some pressure cycles are reported. In particular, the operating engine points at 3000 RPM and 7 bar of BMEP is examined, as it represents the most interesting test case. In fact, at this specific load, the transition between naturally aspirated and boosted operation is performed.

Figure 81 and Figure 82 show the outcomes of the correlation procedure for different values of air-fuel ratio at a fixed EGR rate, equal to 5%. It is notable that the imposed burn rate, together with the imposed air flow rate, positively influences the pressure cycles simulation. This positive result is enhanced with the increase of λ, since a larger amount of trapped air implies lower heat transfer, resulting in a recovery of the expansion line. However, an overestimation of the pressure before the intake valve closure (IVC) is visible throughout the pressure cycles, possibly due to the interpolation errors in the valve lift subassembly. This error affects the subsequent compression line, where a clear overestimation is visible compared to the experimental cycles.

Similar conclusions can be drawn when considering a variation in EGR at a fixed air-fuel ratio. Figure 83 depicts an example of the engine operation at 3000 RPM and 7 bar of BMEP with $\lambda = 1$ and two possible EGR rates, 0 and 20,6%, respectively. Again, the heat transfer reduces as the EGR rate increases, resulting in a recovery of the expansion line. The computational error regarding the IVC remains present.

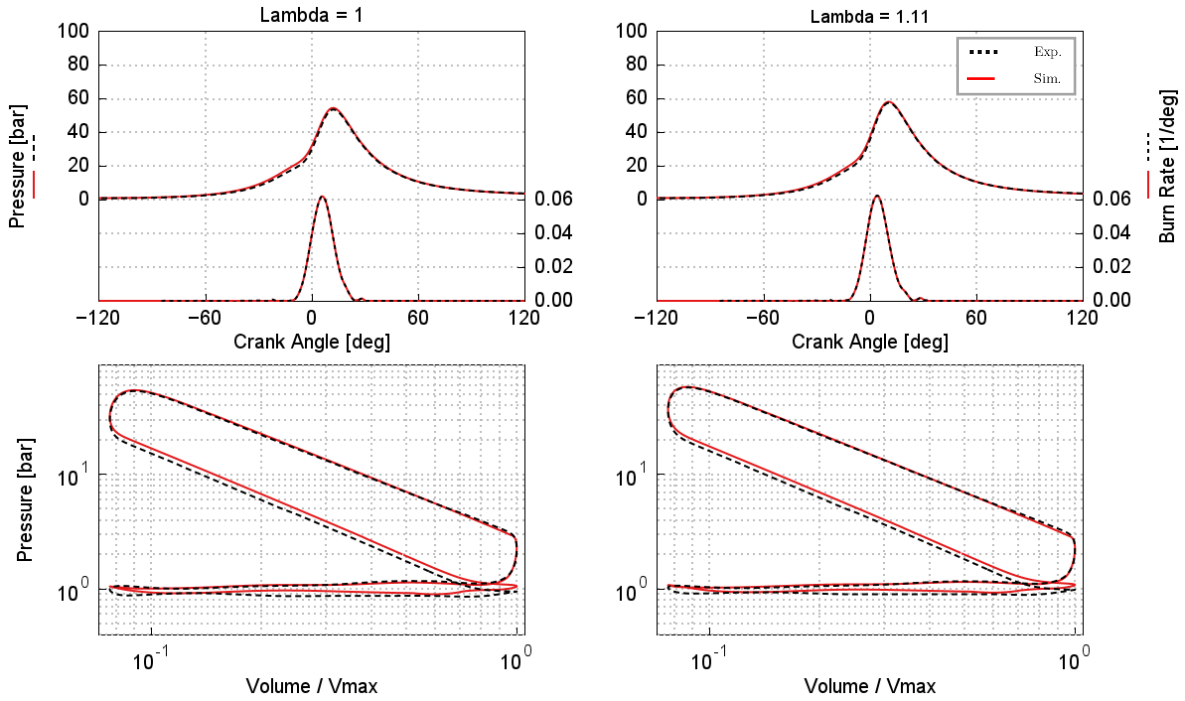

Figure 81 Pressure Cycles and Burn Rate for λ = 1 and λ = 1,11

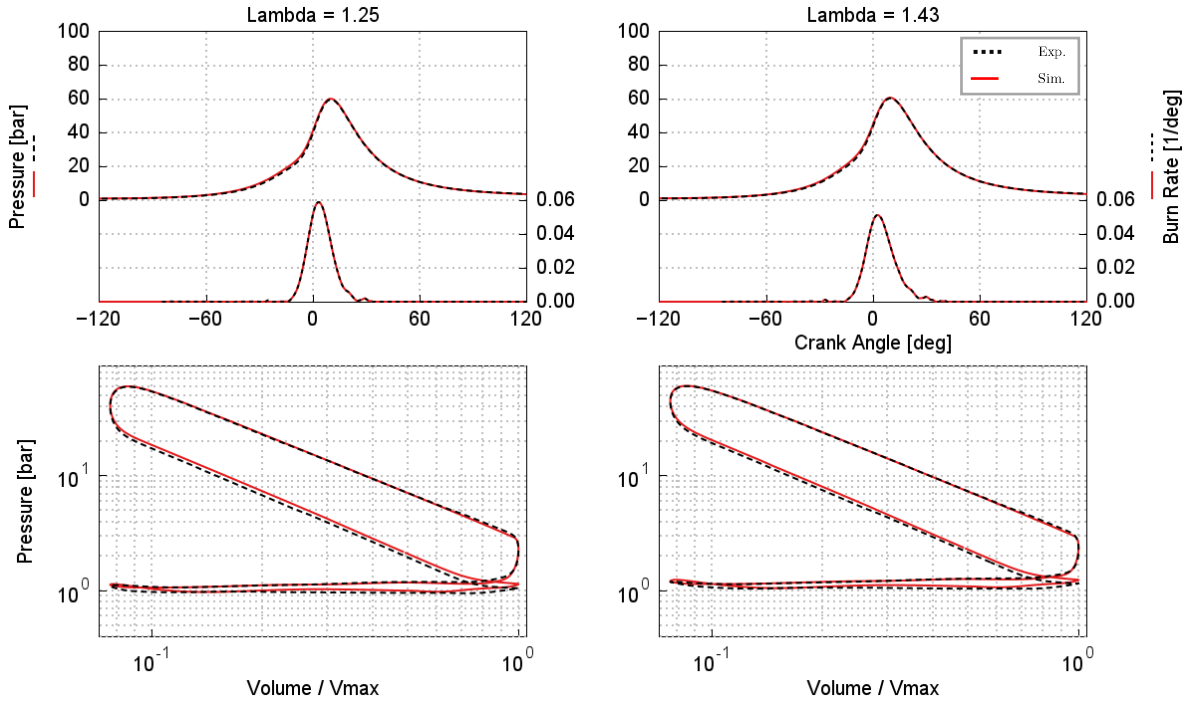

Figure 82 Pressure Cycles and Burn Rate for λ = 1,25 and λ = 1,43

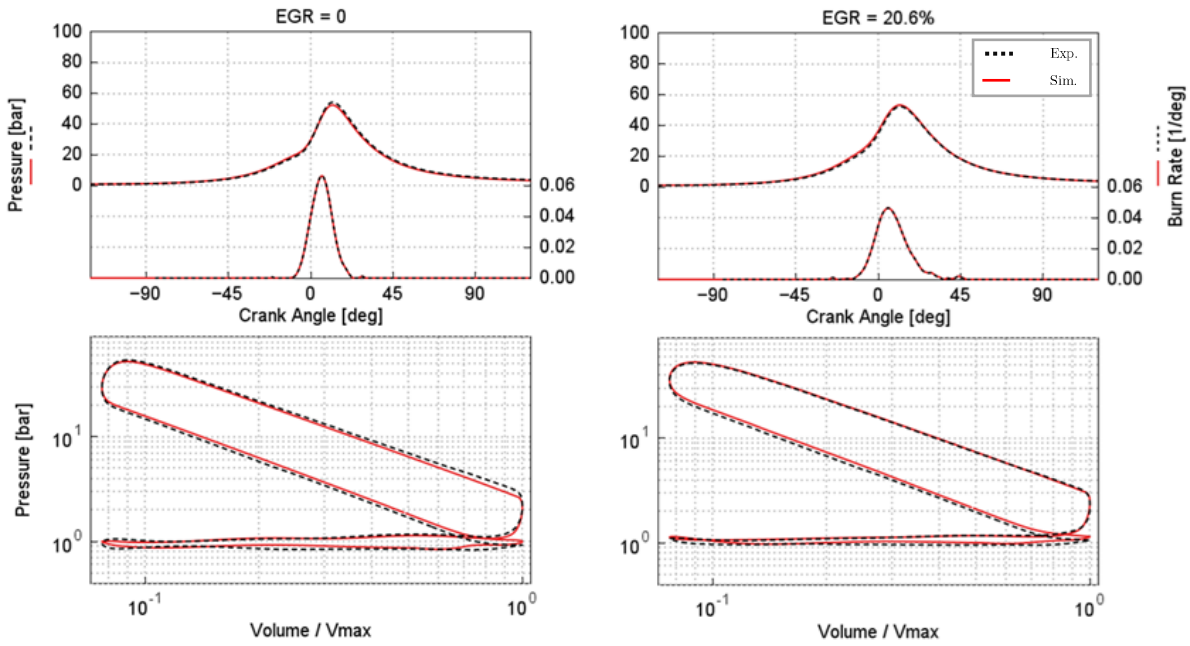

Figure 83 Pressure Cycles and Burn Rate for EGR = 0 and EGR = 20,6%

5.3.2 Predictive Combustion Model Validation

Regarding the implementation of the predictive combustion model, this section presents the results of the validation process. It is important to note that these results stem from a calibration process aimed at determining the optimal parameters influencing the combustion process, followed by the identification of an interpolating surface that enables the calculation of these parameters across the entire experimental dataset.

Before starting with the validation results, the outcomes of the TPA turbulence model must be discussed. It is important to recall that the experimental data for the turbulence model are represented by a 3D CFD cold-flow analysis, which examines the Swumble™ in-cylinder motion at fixed speed of 2000 RPM, without fuel injection or combustion. The objective of the TPA model is the evaluation of the turbulence parameters, with a particular focus on Turbulent Kinetic Energy, Turbulent Length Scale and Mean Flow Strength. The results of this model are presented in Figure 84 and Figure 85, from which the accuracy of the turbulence model can be clearly assessed.

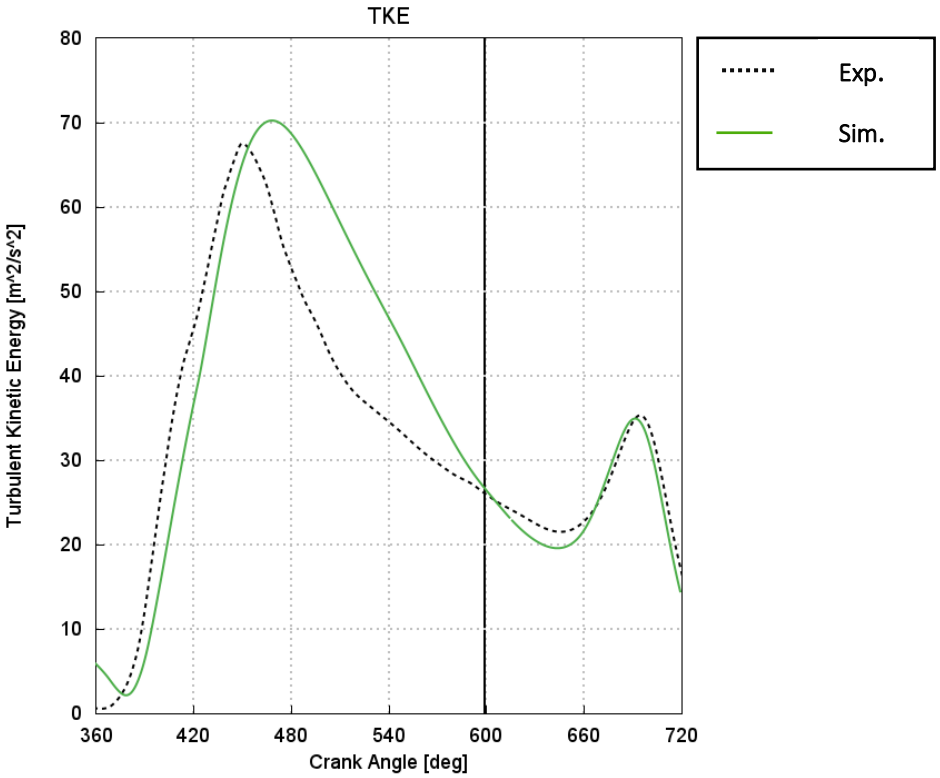

Figure 84 Turbulent Kinetic Energy

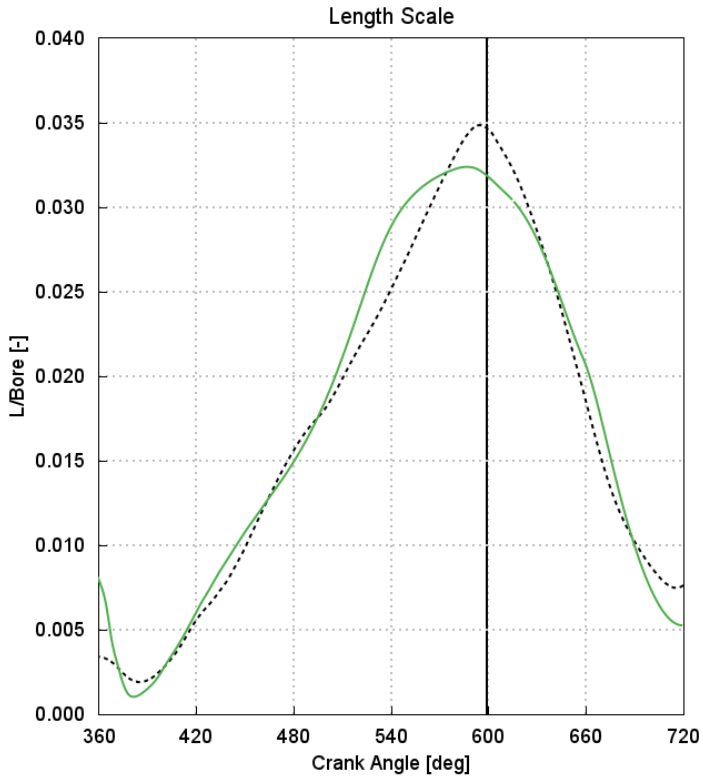

Figure 85 Turbulent Length Scale

The first key index to examine the outcomes of the predictive combustion model is the barycentre of combustion (MFB50), shown in Figure 86 as a correlation plot. It can be observed that the combustion model accurately predicts the MFB50 for most tested conditions. However, under low-speed, low-load engine operating conditions the correlation is not optimal. This issue arises due to difficulty in estimating the dilution effect multiplier. Specifically, for these operating conditions the aggressive LIVC Miller cycle and the possible boot-lift effect negatively impact the amount of residual gasses trapped inside the cylinder. Consequently, the interpolation method fails to correctly estimate the value of DEM associated with these engine operating conditions.

The combustion duration is presented in Figure 87 as burn duration 10-90. It is evident that the predictive model does not accurately predict the burn duration. This result is primarily influenced by the MFB90, which deviates from the experimental data in most cases. Further refinements and improvements of the calibration procedure are necessary to enhance the accuracy of the combustion duration simulation.

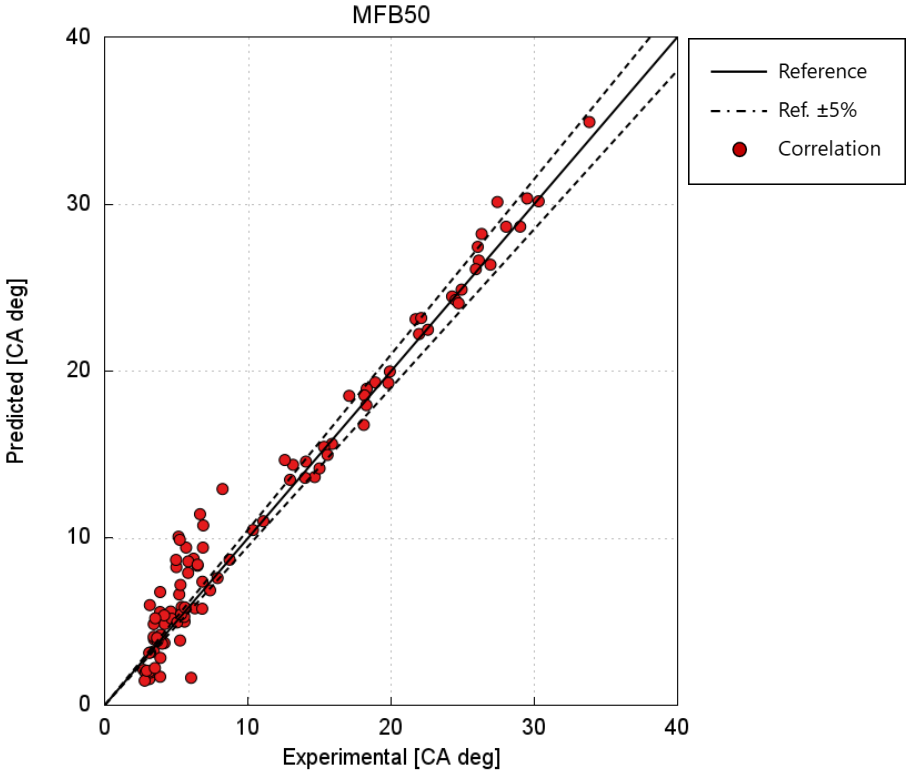

Figure 86 Predictive Combustion Model MFB50 Correlation

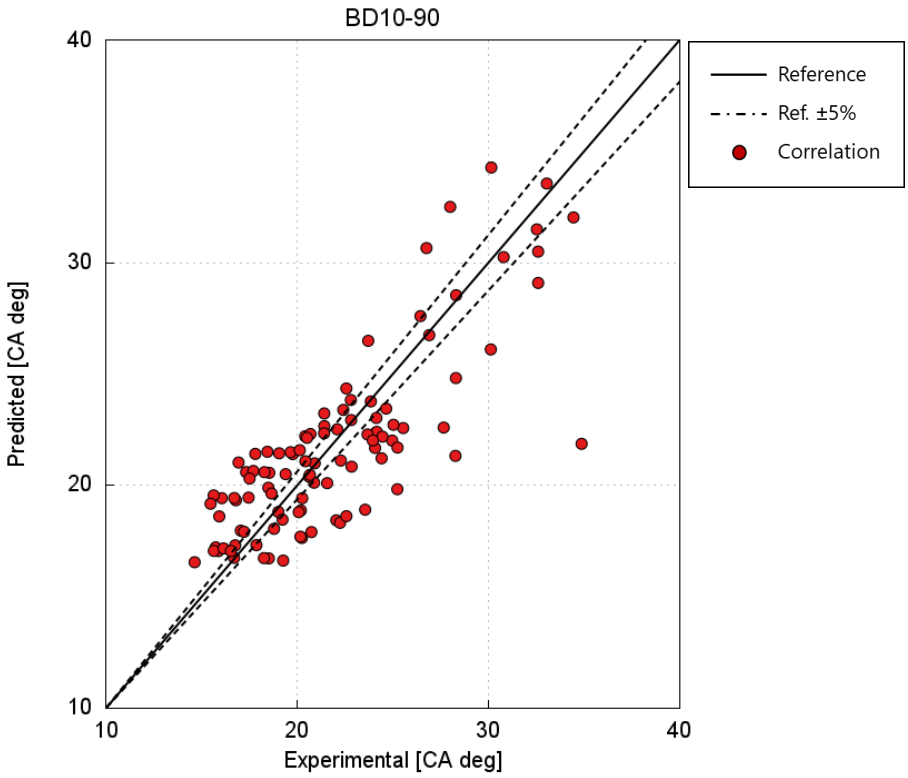

Figure 87 Predictive Combustion Model Burn Duration 10-90

Another parameter used to assess the combustion process is the in-cylinder maximum pressure, presented in Figure 88. The predictive combustion model accurately calculates the maximum pressure within the cycle, with most tested points falling within the error margin of ±5% relative to the reference values.

Figure 89 illustrates the crank angle at which the in-cylinder maximum pressure occurs. The correlation results optima for most of the tested points; however, an overestimation is observed in operating conditions where the interpolating surface underestimates the DEM calculation.

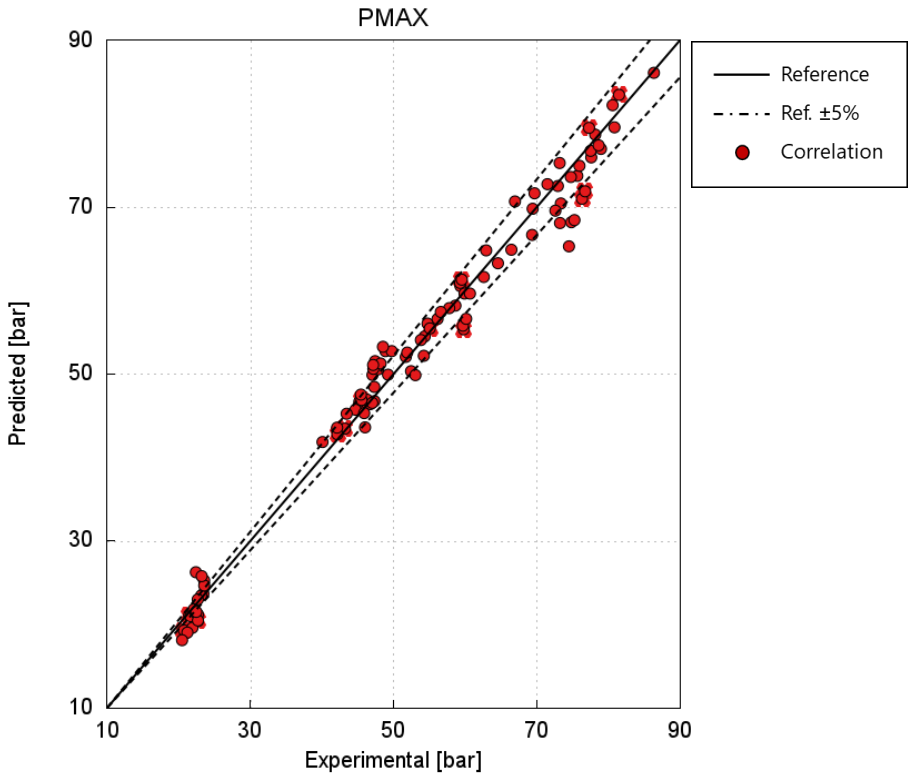

Figure 88 Predictive Combustion Model In-cylinder Maximum Pressure

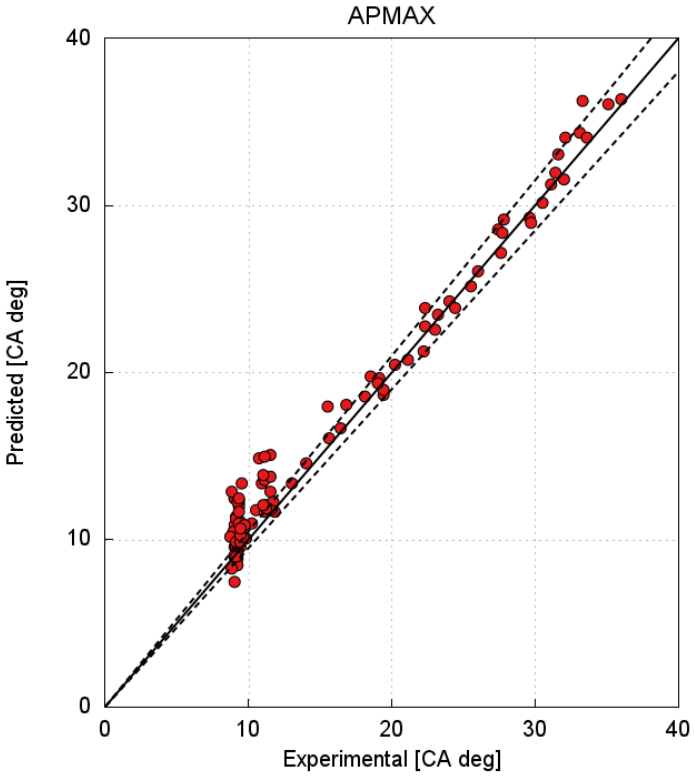

Figure 89 Predictive Combustion Model Maximum Pressure Crank Angle

To evaluate the accuracy of the implementation of the predictive combustion model, some pressure cycles and burn rates are reported. As in the assessment of the complete model correlation, the presented charts result from simulations conducted at the most relevant operating point: 3000 RPM and 7 bar of BMEP.

Three different combinations of EGR and air-fuel ratio are analysed, to verify the model's predictive accuracy under varying conditions of the dual dilution approach. Specifically, the reported cases correspond to $\lambda = 1{,}00$ and EGR $= 21{,}5\%$, $\lambda = 1{,}11$ and EGR $= 14{,}4\%$ and $\lambda = 1{,}43$ and EGR $= 0$.

For all tested conditions, as shown in Figure 90, Figure 91 and Figure 92, the predictive combustion model accurately estimates burn rates and pressure cycles with minor errors, demonstrating its reliable integration within the complete engine model.

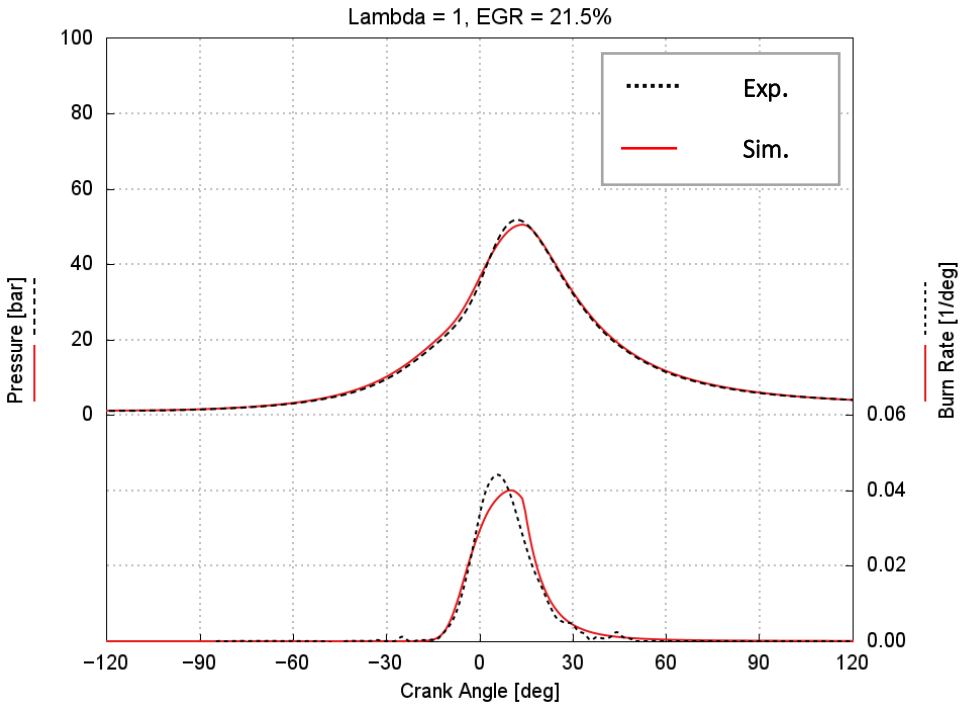

Figure 90 Predictive Combustion Model Pressure Cycles and Burn Rate Case 1

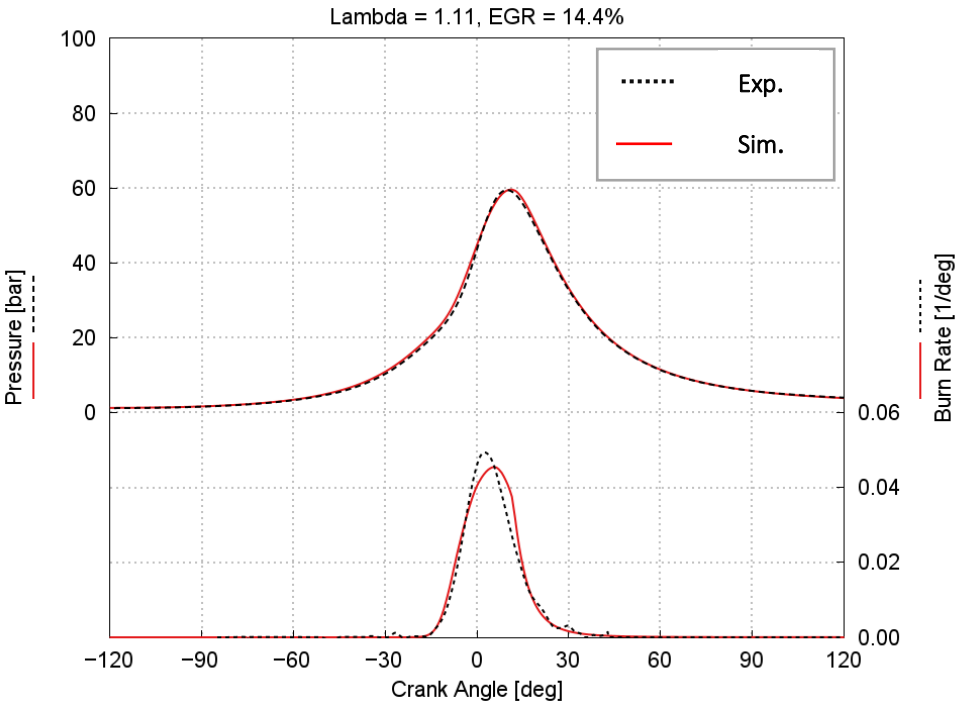

Figure 91 Predictive Combustion Model Pressure Cycles and Burn Rate Case 2

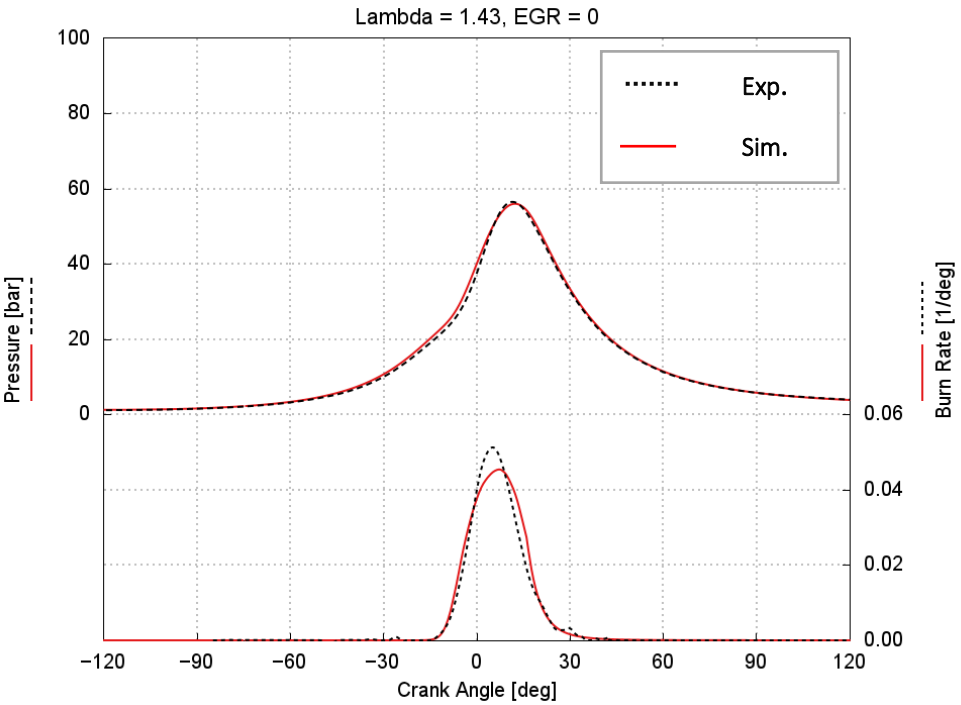

Figure 92 Predictive Combustion Model Pressure Cycles and Burn Rate Case 3

5.4 Conclusions

This chapter was dedicated to the development of the engine digital twin, a reliable simulation platform capable of extending the experimental research activities.

The first step in this development was represented by the correlation procedure applied to the complete engine model. This procedure was based on the IFPEN experimental acquired data and involved the tuning of several subassembly parameters of the entire model.

The satisfactory results achieved during the correlation procedure allowed to proceed to the next step, represented by the implementation of a predictive combustion model. This step was further divided into two phases: calibration and validation. The calibration process aimed to determine the optimal tuning of the combustion key parameters, while the validation procedure ensured the correctness of the model's implementation.

The final results confirmed the high level of accuracy achieved by the complete model, in which the predictive combustion model was implemented. This validation establishes the engine model as a reliable digital twin of the testbench prototype engine.

6 PHOENICE Features Split Analysis

6.1 Introduction

The scope of the different implementations introduced in the PHOENICE project is to enhance the baseline engine efficiency to achieve the target of 47% Indicated Thermal Efficiency.

In this chapter, a brief analysis of the impact on the ITE of the various features of the project is illustrated. The evaluation of the project implementations does not rely on Brake Thermal Efficiency, as it is influenced by accessory-related efficiency. To account for frictionless considerations and focus solely on the influence on engine performance, Indicated Thermal Efficiency is used in the analysis.

Starting with the results from the engine model built in GT-Suite, the contributions of the technological implementations are gradually removed to analyse their impact on the overall engine efficiency.

The final objective aims to assess the improvements obtained through the project's innovative technological implementations, paving the way for future research into potential solutions.

6.2 Methodology

To evaluate the impact of the technological solutions, the results of the complete engine model are considered.

The analysis of the benefits provided by the features introduced on the PHOENICE prototype engine begins by considering the ITE derived from the dual dilution combustion approach, the higher compression ratio compared to the baseline engine and the optimized VVA strategy.

Subsequently, the features are individually removed, and the resulting variation of ITE is examined. First, the ultra-lean combustion – main feature of the project – is removed, leaving only the dilution provided by the EGR. Next, this dilution is removed, retaining only the larger compression ratio and the optimized VVA

strategy. Finally, the engine is returned to baseline conditions, represented by a compression ratio of 10,5 and a waste-gate type turbocharger.

This analysis is repeated for two specific engine points: 1500 RPM at 5,5 bar BMEP and 3000 RPM at 13 bar BMEP. These operating conditions are selected as they represent two contrasting modes of engine operation.

A critical aspect of the final analysis, concerning the reduction of the compression ratio from 13,6 to 10,5, is the control of knock. In fact, at the baseline compression ratio, the appropriate spark advance value is not known for the two operating conditions under investigation, causing the engine model to experience knock. To determine the correct SA, the knock controller is activated. This controller, by using the average burn duration 0-50 and the average MFB50 as inputs, adjusts the SA to ensure an incipient knock condition during the simulated cycles.

6.3 Results

The initial values of Indicated Thermal Efficiency of the PHOENICE prototype engine are shown in Figure 93. For both engine points, the results were obtained assuming an EGR rate of 10% and an air-fuel ratio of 1,11. It is evident how the ITE increases passing to higher speed and load. Furthermore, the engine performance are consistently more efficient compared to standard gasoline engines under typical operating conditions. This higher efficiency is due to the combination of a high compression ratio, an aggressive Miller cycle, dual dilution combustion, and the enhanced performance of the VNT E-Turbo.

When the possibility of the mixture enleanment is removed, the engine ITE consequently decreases. Figure 94 illustrates this trend, considering for the two engine's operating point a stoichiometric mixture with EGR rate equal to 10%. The lower air flow rate adversely affects the pumping losses at low engine speed, resulting in a lower throttle angle. Conversely, at high engine speed the heat losses become larger, reducing the respective ITE.

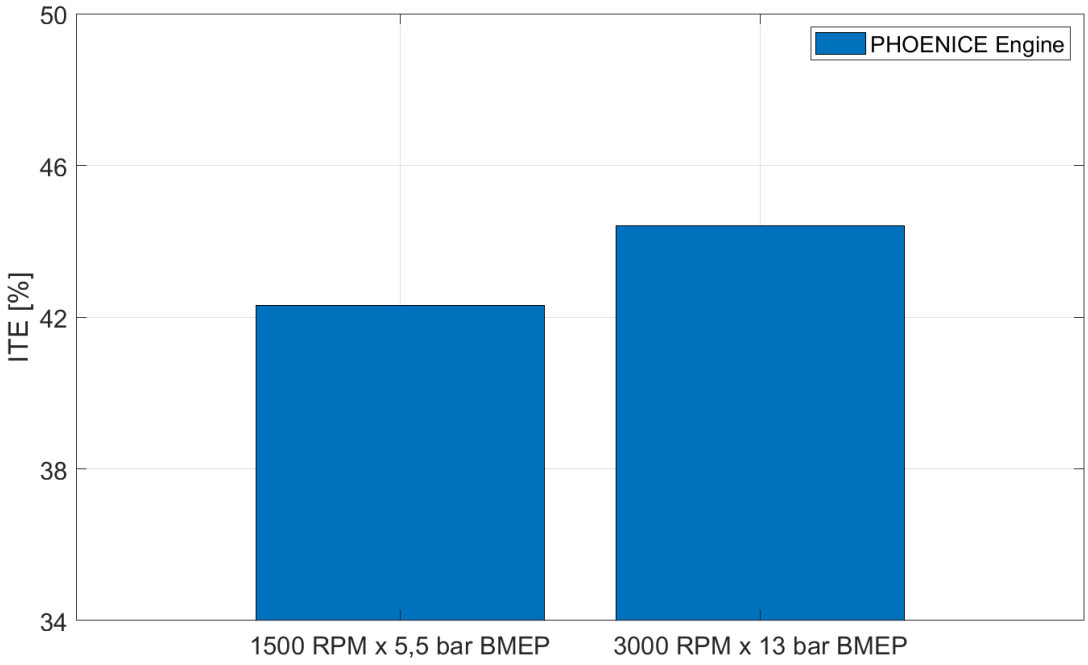

Figure 93 PHOENICE Engine ITE

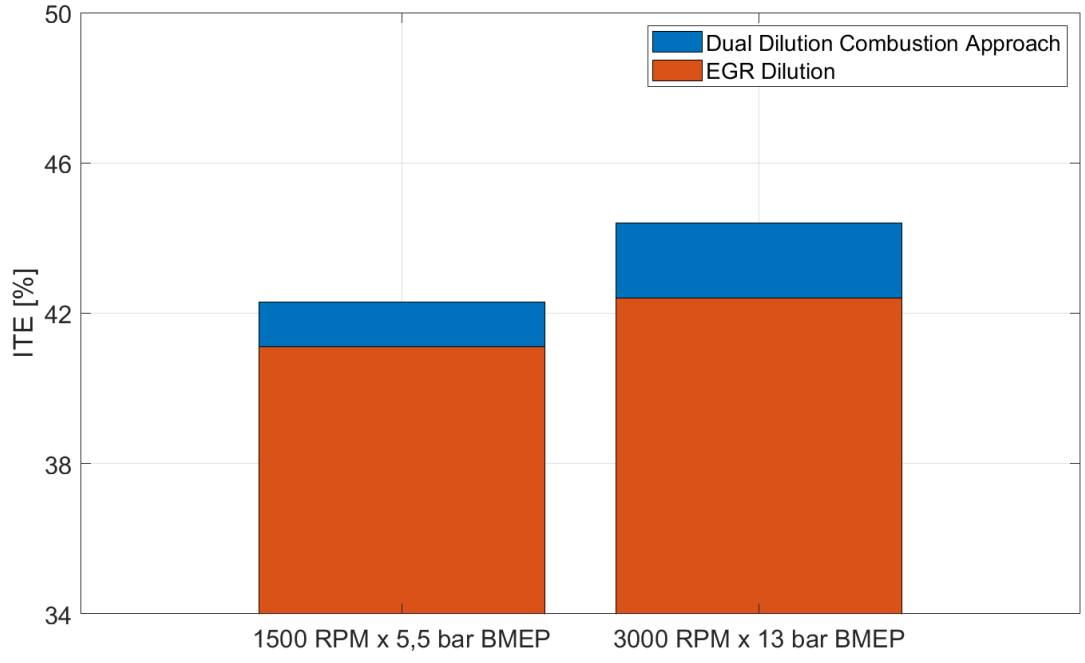

Figure 94 Effect of the Dilution on the ITE

Continuing with the analysis, the next step is to remove the contribution of the EGR dilution. This corresponds to operating the engine solely with a higher compression ratio, optimized VVA, and E-Turbo. The outcome is shown in Figure 95. For the operating point at high load, a decrease in efficiency of about 2% is recorded, while the reduction is of about 7%. Again, this result is due to increased pumping work at low-load, low-speed engine points - caused by a lower mass of air entrained at the intake - and higher heat losses during high-speed operations, as the in-cylinder temperature is higher.

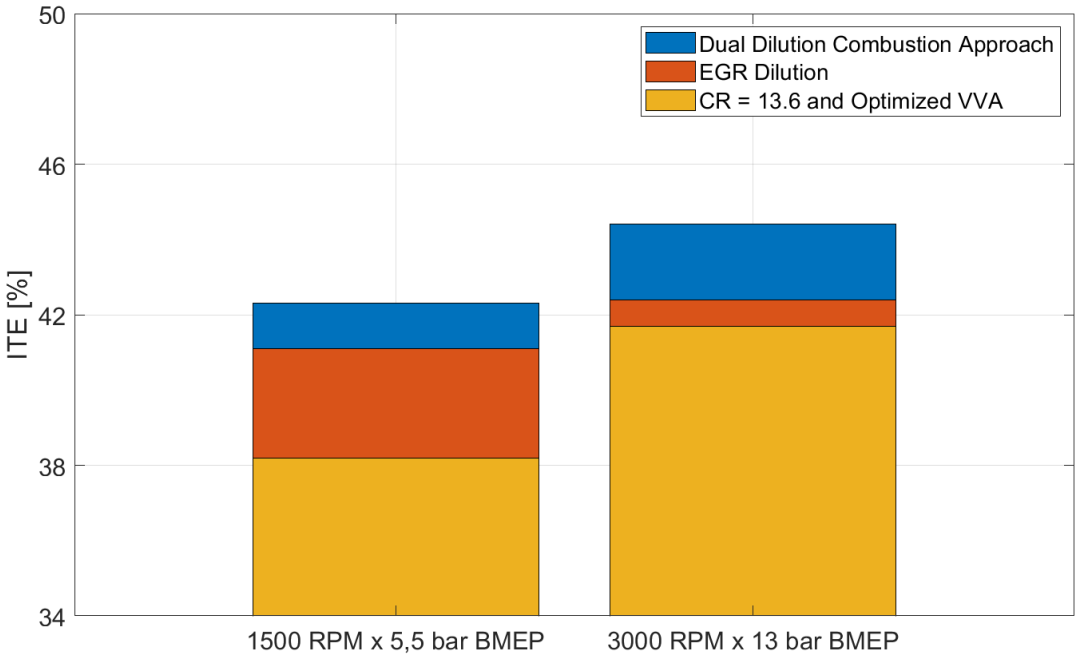

Figure 95 Effect of the CR = 13,6 and Optimized VVA on ITE

Finally, the engine is returned to the original functioning conditions, with a CR of 10,5 and a waste-gate turbocharger. For high load working conditions, a reduction in ITE of about 6% is visible in Figure 96. This difference in ITE can be attributed to the optimized VVA strategy, which, in conjunction with the larger CR and E-turbo, allows a stronger de-throttling. At low speeds, the ITE decrement is less pronounced because the effect of the VVA strategy is less aggressive. Moreover, at low speeds, operating with a larger CR requires a more retarded spark advance to avoid an increased tendency for knocking.

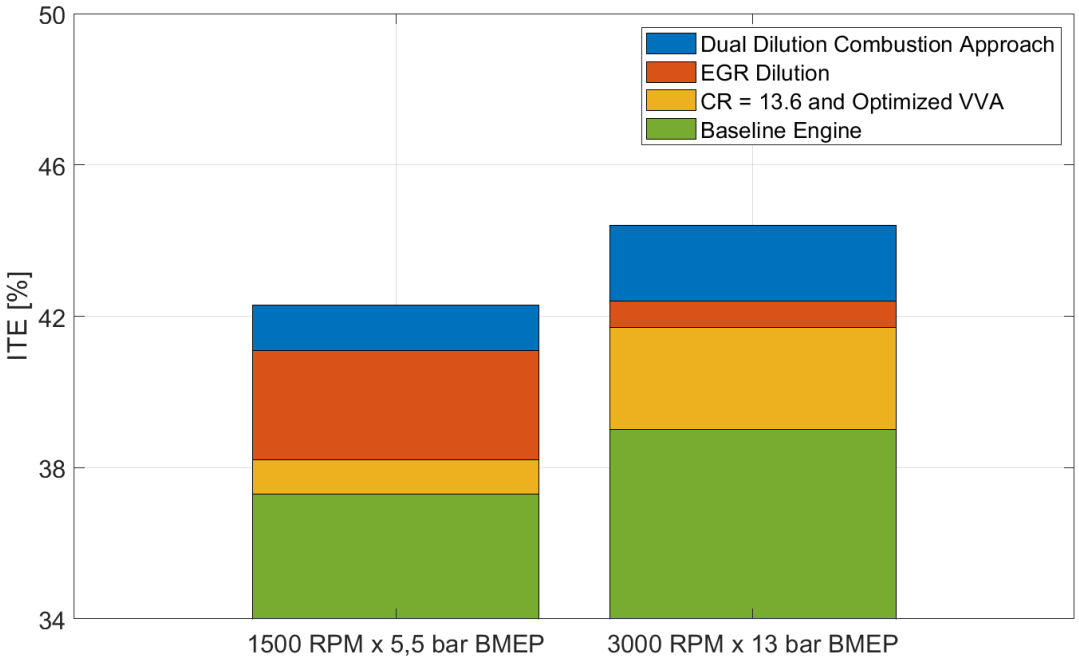

Figure 96 Baseline Engine ITE

Therefore, transitioning from the baseline engine to the PHOENICE prototype with all the innovative technological solutions implemented results in an ITE increase of about 14%.

It would be incomplete to consider only the enhancement in thermal efficiency without also discussing the impact that the different solutions have on application costs. In fact, the use of the E-Turbocharger significantly affects a possible market price, as this component was specifically built for this research and is not suitable for mass production. On the other hand, implementing a higher compression ratio combined with an optimized VVA strategy has a lower cost impact. This makes it a scalable solution that still offers a substantial ITE improvement.

Therefore, this research study aims to highlight the various contributions for a long-term perspective, exploiting the potential of different implementations, not only as experimental results but as viable options for production, thanks to the many possible combinations of study parameters.

6.4 Conclusions

The aim of this chapter was to examine the benefits of the various PHOENICE technological implementations on the Indicated Thermal Efficiency (ITE).

The analysis procedure involved assessing the impact on ITE by isolating the contributions of the different innovative solutions. Starting from the PHOENICE prototype engine's ITE, the contributions of the dual dilution combustion, higher compression ratio, VVA strategy, and E-Turbo were sequentially removed, returning the engine to its baseline configuration.

An increase of about 14% in ITE was observed when comparing the baseline engine to the PHOENICE prototype. Additionally, a brief discussion was provided regarding the potential real-world applications of this project.

Conclusions

The aim of this thesis was to support the experimental development of the PHOENICE project prototype engine. The project is based on the concept of a new lean-burn spark ignition engine, developed using a state-of-the-art 1.3L gasoline engine. Several innovative technologies were integrated into the prototype to enable a dual dilution combustion approach and maximize synergy with the plug-in hybrid demonstrator vehicle.

This research was founded on experimental data acquired during the IFPEN and PoliTo steady-state calibration tests. The first part of the thesis focused on analysing these experimental data, assessing the potential of various implementations introduced in the prototype engine, which led to an increase in ITE of about 47%.

To support the calibration activity at the PoliTo test cell, a simulation of the WLTC cycle was performed. This simulation was based on fuel consumption and engine-out emissions maps obtained during stationary tests and aimed to determine the ideal fuel consumption and emissions that the engine could achieve under real driving conditions. In particular, different engine operating conditions were tested, demonstrating that a reduction in fuel consumption of about 5% could be achieved. This analysis was followed by an optimization of the gearshift strategy, which continued to target ambitious reductions in fuel consumption and CO emissions.

Another key aspect of this research was the creation of a digital twin of the engine. The engine model was calibrated using the IFPEN experimental data, ensuring a reliable simulation platform that extended the experimental study. The successful results from the correlation process led to the introduction of a predictive combustion model. The calibration and subsequent validation of this model provided a trustworthy tool for evaluating the dual dilution combustion approach.

Finally, the thesis concluded with a split analysis of the various features introduced in the PHOENICE prototype engine. This study assessed the benefits of the dual dilution approach, increased CR, E-Turbo, and VVA strategy, revealing an increase in ITE of about 14% for the prototype engine compared to the baseline engine.

Overall, this thesis aimed to highlight future trends in the production of low-emission, high-efficiency engines by exploiting the potential of different innovative solutions and their possible integration, not only from an experimental perspective but also as a viable option for mass production.

Bibliography

[1] European Parliament Press Release, 14 February 2023. [Online]. Available: https://www.europarl.europa.eu/news/en/press-room/20230210IPR74715/fit-for-55-zero-co2-emissions-for-new-cars-and-vans-in-2035. [Accessed March 2025].

[2] M. Ovaere and S. Proost, "Cost-effective reduction of fossil energy use in the European transport sector: An assessment of the Fit for 55 Package," *Energy Policy,* p. 168, 2022.

[3] Z. Samaras, A. Kontes, A. Dimaratos, D. Kontes and et al., "A European Regulatory Perspective towards a Euro 7 Proposal," *SAE Int. J. Adv. & Curr. Prac. in Mobility 5(3),* pp. 998 - 1011, 2023.

[4] The European Parliament and the Council of the European Union, "Regulation (EU) 2024/1257 of the European Parliament and of the Council of 24 April 2024 on type-approval of motor vehicles and engines and of systems, components and separate technical units intended for such vehicles," August 2024. [Online]. Available: http://data.europa.eu/eli/reg/2024/1257/oj. [Accessed March 2025].

[5] J. Dornoff and F. Rodriguez, "Euro 7: The new emission standard for light- and heavy- duty vehicles in the European Union," International Council on Celan Transportation, 2024.

[6] A. Ihlemann and N. Nitz, "Cylinder deactivation: A technology with a future or a niche application?," in *10th Schaeffler Symposium*, 2014.

[7] E. Nakai and et al., "Mazda SkyActiv-X 2.0 L Gasoline Engine," in *Aachen Kolloquia*, 2019.

[8] Y. He, J. Liu and B. Zhu, "Development of an aggressive Miller cycle engine with extended Late-Intake-Valve-Closing and a two-stage turbocharger," *Proceedings of the Institution of Mechanical Engineers, Part D: Journal of Automobile Engineering,* vol. 233(2), pp. 413-426, 2019.

[9] R. Osborne, A. Lane, N. Turnern, J. Geddes and et al., "A New Generation Lean Gasoline Engine for Premium Vehicle CO2 Reduction," SAE Technical Paper 2021-01-0637, 2021.

[10] S. D. Boggio, A. Irimescu, S. Merola, P. Lacava and P. Curto, "Flame Front Propagation in an Optical GDI Engine under Stoichiometric and Lean Burn Conditions," Energies, 2017.

[11] C. Tornatore, F. Bozza, V. De Bellis, L. Teodosio, G. Valentino and L. Marchetto, "Experimental and numerical study on the influence of cooled EGR on knock tendency, performance and emissions of a downsized spark-ignition engine," *Energy,* pp. 968-976, 2019.

[12] X. Gautrot, M. Bardi , T. Leroy, P. Luca, L. Nowak and B. Reveille , "Swumble In-Cylinder Fluid Motion for High Efficiency Gasoline SI Engines: Development of the second generation," in *SIA Powertrain and Electronics*, Rouen, France, 2020.

[13] C. De Marino, G. Maiorana, P. Pallotti, S. Quinto and et al., "The Global Small Engine 3 and 4 Cylinder Turbo: The New FCA's Family of Small High-Tech Gasoline Engines," in *39th International Vienna Motor Symposium*, Vienna, 26-27 April 2018.

[14] L. Bernard, A. Ferrari, D. Micelli and et al., "Electro-hydraulic valve control with multiair technology," MTZ Worlwide, 2009.

[15] J. S. Castellanos, N. Bontemps, M. André and L. Rolando, "Project PHOENICE and the role of E-Turbo in a high-efficiency PHEV," in *ATK*, Dresden, Germany, 26th September 2023.

[16] T. Tahtouh, F. Millo, L. Rolando, G. Castellano and et al., "A Synergic Use of Innovative Technologies for the Next Generation of High Efficiency Internal Combustion Engines for PHEVs: The PHOENICE Project," *SAE Technical Paper 2023-01-0224,* 2023.